IMAGE ANALYSIS OF EPIPHYTE-SEAGRASS DYNAMICS ON *Thalassia testudinum* FROM DIFFERENT ENVIRONMENTAL CONDITIONS

A Thesis

by

CHI HUANG

BS, Ocean University of China, P. R China, 2018

Submitted in Partial Fulfillment of the Requirements for the Degree of

MASTER OF SCIENCE

in

MARINE BIOLOGY

Texas A&M University-Corpus Christi
Corpus Christi, Texas

December 2020

December 2020

IMAGE ANALYSIS OF EPIPHYTE-SEAGRASS DYNAMICS ON *Thalassia testudinum* FROM DIFFERENT ENVIRONMENTAL CONDITIONS.

A Thesis

by

CHI HUANG

This thesis meets the standards for scope and quality of
Texas A&M University-Corpus Christi and is hereby approved.

Kirk Cammarata, PhD
Chair

Ruby Mehrubeoglu, PhD
Committee Member

Ed Proffitt, PhD
Committee Member

Patrick Larkin, PhD
Committee Member

December 2020

ABSTRACT

Seagrasses are globally threatened due to increasing environmental stressors in coastal ecosystems. Excessive accumulation of algal epiphytes is suggested to be harmful to seagrass. The biomass and morphological measures widely used in understanding seagrass-epiphyte relationships provide limited insight into the dynamics of epiphyte colonization relative to leaf growth and senescence. Color scanning and image analysis methods were developed to characterize epiphyte accumulation with seagrass growth. *Thalassia testudinum* collected monthly or bimonthly from July 2019 to April 2020 near Redfish Bay, Texas, was analyzed through traditional and image-based measures. Spectral Angle Mapper (SAM) algorithms within ENVI Program distinguished the pixels of epiphyte-free leaf blades from many epiphytes. Unclassifiable pixels averaged < 5%. Classification accuracy was also evaluated by correlation of traditional biomass and morphology metrics *vs.* image-based metrics for seagrass (n = 2052) and epiphyte (n = 1822) collected across different seasons and environmental conditions. Image-derived leaf area strongly correlated with leaf biomass (R^2 = 0.98, P < 0.0001) but linear regressions of epiphyte biomass *vs.* epiphyte area (pixels) (R^2 = 0.61, P < 0.0001) and biomass ratio of epiphyte to seagrass *vs.* epiphyte coverage (epiphyte pixels/leaf pixels) ($R2$ = 0.51, P < 0.0001) were weaker. However, correlations greatly improved (R^2 = 0.52 ~ 0.98, P < 0.0001), and the epiphyte accumulation presented linear or exponential patterns when parsed by season and environmentally different sites. The observation from both traditional and image-based metrics indicated that the seagrass-epiphyte relationship changed significantly across environmental context (P < 0.05). The observation that the mean epiphyte coverage stayed relatively constant (maximum range of variation was about 15%) across seasons, but differed by

site, suggests that leaf growth may be regulated to maintain the proportion of uncolonized leaf surface. The epiphyte accumulation relative to seagrass was greatest at low temperatures and at sites with elevated N:P ratio in sediment porewater. Image analysis may be insightful as an indicator of environmental change and suggests that epiphyte accumulation combines linear and exponential processes representing its colonization and growth. Future work will involve optimizing the spectral libraries to improve algal group classification to include diverse epiphytic community components.

Key word: Epiphyte, Image analysis, Biomass, Seagrass, Environmental conditions

DEDICATION

To those who read it and support me

ACKNOWLEDGEMENTS

This study was financially supported by the Texas A&M University-Corpus Christi (TAMU-CC) Research & Innovation Awards (to Chi Huang; to Mohammed Ahmed), TAMU-CC Research Enhancement Award (to Kirk Cammarata), TAMU-CC general international scholarship (to Chi Huang), TAMU-CC President's International Excellence Award (to Chi Huang) and Millicent Quammen Memorial Research Award (to Chi Huang). We would like to thank the Department of Life Science, TAMU-CC, and ICW RV Park for their support of this project; numerous people who assisted with field and laboratory work to collect seagrass samples and provide kayaks, in particular Carissa Pinon, Dr. Kirk Cammarata (TAMU-CC), and Robert Duke (TAMU-CC Center for Coastal Studies); Dr. Blair Sterbaboatwright (TAMU-CC) and Dr. Ed Proffitt (TAMU-CC) for their assistance with statistical analysis and model building, Dr. Hua Zhang (TAMU-CC) for his maps of sampling field, Dr. Ruby Mehrubeoglu for her assistance with overlap analysis, Dr. Simon Geist (TAMU-CC), Dr. John Scarp (TAMU-CC), and Dr. Ed Proffitt for their support of sample process facilities (e.g., microbalance, beakers, and oven). Thanks to Dr. Kirk Cammarata, Dr. Patrick Larkin (TAMU-CC), Dr. Ed Proffitt, and Dr. Ruby Mehrubeoglu, who helped review and improve the earlier research proposal and this thesis. Grateful thanks to Dr. Kirk Cammarata for supporting my Master's education at TAMU-CC.

TABLE OF CONTENTS

LIST OF FIGURES

FIGURES PAGE

LIST OF TABLES

TABLES PAGE

CHAPTER I: INTRODUCTION AND LITERATURE REVIEW

Seagrasses are important marine plants providing multiple ecological services to coastal ecosystems. Investigation of global ecosystem services (Costanza et al. 1997) ranked coastal ecosystem seagrasses highest in nutrient cycling ability, and second for area of coverage and global economic value in the coastal areas. Seagrass beds enhance biodiversity and provide ideal habitat for marine organisms in different life stages, including commercially important species (Wolaver et al. 1980, Heck et al. 1997, Orth et al. 2006a, Katwijk et al. 2016). As major primary producers (Moncreiff et al. 1992, Duarte & Chiscano 1999), seagrasses supply organic carbon and food resources for marine organisms inhabiting tropical and temperate areas (Suchanek et al. 1985). Increased benthic species richness resulted from revegetation of bare sediment with the introduced seagrass *Zostera Japonic*a (Posey 1988). Seagrass restoration in the Delmarva Coastal Bays demonstrated habitat improvement and fisheries recoveries (Orth et al. 2006b). Seagrass plays a significant role in filtering nutrients flowing into coastal ecosystems, and they stabilize sediments to store blue carbon derived from leaves and rhizomes (Hemminga & Duarte 2000, Greiner et al. 2013). Water quality improvement and seagrass reintroduction has been shown to enhance ecosystem function world-wide (Bell et al. 2008, 2014, Greening et al. 2011, Katwijk et al. 2016).

However, seagrasses are experiencing global losses from a variety of anthropogenic or environmental stressors, including eutrophic risk, dredging, and invasive species, and changing or extreme climatic events (Posey 1988, Orth et al. 2006a, Burkholder et al. 2007, Waycott et al. 2009, Mateu-Vicens et al. 2010). The impact of global warming and ocean acidification due to increasing anthropogenic CO_2 emissions strongly increases the potential loss of biodiversity in

the ocean ecosystems which play major economic and food security roles in many countries (Martin et al. 2008, Koch et al. 2013, Nagelkerken & Connell 2015). Invasive tropical fish range expansions due to warming trends might reduce the complexity of seagrass meadow habitat in the Gulf of Mexico and indirectly decrease the nursery role and food resources for native temperate fish populations (Claydon et al. 2012). Gut content analysis in lab studies suggested that invasive parrotfish consumed fourfold more seagrasses than native pinfish and filefish (Heck et al. 2015).

Another important contribution to seagrass decline is the trophic cascade caused by overfishing, an effect apparently mediated through phytoplankton and epiphyte abundance increases (Heck & Valentine 2006). Conclusion from reviewed studies (Orth & Van Montfrans 1984, Heck & Valentine 2007, Jaschinski & Sommer 2008) on the interactions between herbivory and algal epiphytes have suggested that fish herbivores and mesograzers are primary controllers of seagrass and associate epiphytes. A conceptual model (Figure 1) explained that overharvesting of larger predator fish increases the abundance of intermediate consumers which decrease the mesograzers that control epiphyte accumulation. This loss of top-down control would increase epiphyte abundance and reduce light required for seagrass growth.

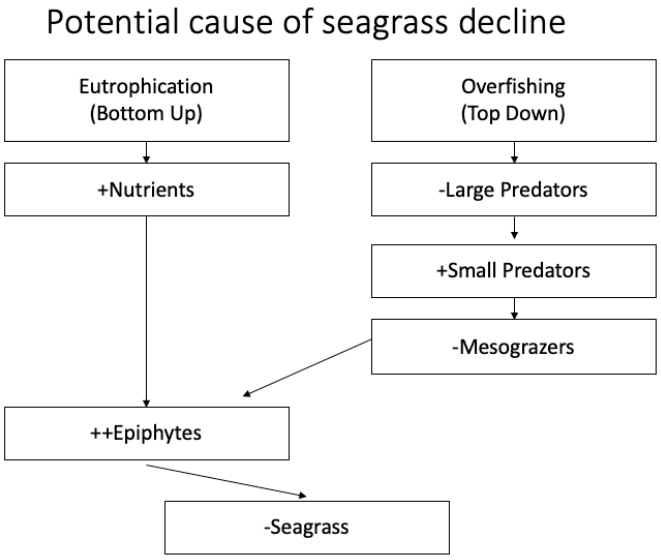

Figure 1. Conceptual model of how bottom-up and top-down both lead to seagrass decline (adapted from Heck & Valentine 2006)

Eutrophication and excessive sedimentation, in combination with top predator overharvesting, are considered to be the main environmental causes of seagrass disappearance (Duarte 2002, Orth et al. 2006b, Burkholder et al. 2007,). Fast-growing micro- and macro-algae thrive in high nutrient conditions, but the slower-growing seagrass is more competitive only at low nutrient levels (Duarte, 1995). These stressors act by reducing light availability, which diminishes seagrass productivity through adverse effects on photosynthesis (Sand-Jensen 1977, Dennison & Alberte 1982, Bulthuis & Woelkerling 1983, Lee & Dunton, 1997, Ralph et al. 2007, Ow et al. 2020), nutrient uptake processes (Dennison & Alberte 1985, McGlathery 2001, Armitage et al. 2005) and species diversity in seagrass meadows (Moore & Wetzel, 2000, Peterson et al. 2007). Nutrient enrichment increases phytoplankton and algal epiphyte growth (Fong & Harwell 1994, Duarte 1995, Frankovich & Fourqurean 1997, Lee & Dunton 2000, Armitage et al. 2005, Hays 2005) which, together with suspended particulate matter, reduce the light available to seagrass.

Light attenuation is the major driver to limit seagrass growth by decreasing its photosynthesis (Abal et al. 1994, Grice et al. 1996, Ralph et al. 2007). The ensuing decrease in oxygen diffusion into the root zone may lead to sulfide intrusion and toxicity to seagrass (Abal et al. 1994, Dunton 1994, Lee & Dunton 2000, Koch & Erskine 2001). In a low-light environment, the reduced carbon balance restricts the carbon storage capacity and respiration of the root/rhizome system, resulting in less sediment oxidation, which in turn increases levels of toxic ammonium and sulfide (Dunton 1994, Lee & Dunton 1997, Hemminga 1998). Seagrasses are considered to be good nutrient indicators because of this sensitivity, but even sublethal levels of Nitrogen (N) loading could be detected in *Zostera marina* based on the C : N ratio in seagrass rhizome tissue (Yang et al. 2018). The interactions of factors contributing to global declines of seagrasses are complex, but human impacts are undoubtedly the major factor to cause a crisis of estuarine ecosystems and change species and habitats associated with seagrass meadows (Lotze et al. 2006, Orth et al. 2006a, Waycott et al. 2009). These combined issues underscore the need for seagrass system monitoring that can detect changes early, and an awareness of what constitutes critical tipping points. Efforts are underway to monitor (McKenna et al. 2007, Dunton et al. 2010, Neckles et al. 2012, Hobson & Whisenant, 2018) and map (Pasqualini et al. 2005, Baumstark et al. 2013, Sherwood et al. 2017) seagrass distribution, composition and abundance, including characterization of their biological condition and habitat quality.

1.1 Seagrass morphological responses to changed environmental conditions

Understanding seagrass responses to environmental change requires accurate assessment of morphological impacts as a first level of response. For example, interspecific competition for resources among the ramets, the basic unit of seagrass patches, alters seagrass clonal growth

patterns which can be regarded as a type of observation to understand morphological change to nutrient variability (Kendrick et al. 2005). Seagrass leaf growth and shoot production are variable in different environmental conditions, and there is an underlying genetic component to these responses. Numerous efforts established linkage between genetic diversity, intraspecific competition and resilience (Hughes & Stachowicz 2004, Larkin et al. 2017) and concur on the benefits of genetic diversity. A variety of methods are used to examine such responses. Biomass, leaf length and leaf width are common indicators used for seagrass condition assessments in large scale monitoring projects (McKenna et al. 2007, Neckles et al. 2012, Hobson & Whisenant 2018,). However, out of necessity, these measures are typically made once per year at peak biomass time, or seasonally at best. Such studies are missing valuable information represented by the dynamic nature of seagrass growth responses, which requires study by measures capable of greater spatial and temporal resolution.

Seagrass leaf growth and shoot production have been studied through a rhizome tagging method (Abal et al. 1994), which delineated newly-produced *Zostera* tissues to calculate shoot production rates. Leaf growth and morphology can also be measured by clip and re-growth or by a hole punching leaf-marking technique (Grice et al. 1996, Kowalski et al. 2009) which determines the productivity of each leaf and shoot based on the length the hole created by leaf growth from the initial location near the ligule. Alternatively, on a different scale, photosynthetic performance can be measured with photosynthesis-irradiance (P-I) curves (Olesen et al. 2002), and photosynthetic efficiency can be calculated based on chlorophyll *a* fluorescence signal collected from a pulse amplitude-modulated (PAM) fluorometer (Ralph et al. 2005, Enríquez & Borowitzka 2010). Other studies have monitored seagrass leaf respiration rate (Shafer et al.

2011) and concentrations of common ions and free amino acids of seagrass leaves, in response to nitrogen dynamics (Kaldy 2011).

Thalassia testudinum, the subject of this study, is a climax species and one of the three most prevalent seagrass species in the Northern Gulf of Mexico (along with *Syringodium filiforme* and *Halodule wrightii*) (Green et al. 2003, Dunton et al. 2010, Congdon & Dunton 2016). The individual shoot is made up of two to five ribbon-shaped leaves emerging from short shoots connected by horizontal rhizomes buried up to 10 cm deep under sediment. The oldest tissue is found at the top of the leaves, and the oldest leaves are found on the outsides of the bundle and wrap the youngest leaves, which emerge from the center (Hays 2005). Because an individual leaf may persist for months under some conditions, the morphological and physiological states of the leaf provide a temporally-integrated record of the environmental conditions that it was exposed to.

1.2 Epiphyte communities and interactions with seagrass leaves

The relatively long-lived *T. testudinum* leaves provide surfaces to which microorganisms, algae, and invertebrates attach and grow (Humm 1964, Corlett & Jones 2007, Michael et al. 2008, Frankovich et al. 2009). As a major component in seagrass ecosystems, these biofilms, here collectively referred to as epiphytes, contribute high productivity, sometimes exceeding the biomass of the seagrass host (Kitting et al. 1984, Borum 1987, Moncreiff et al. 1992, Jernakoff et al. 1996). Observation of invertebrate feeding behavior and isotope tracking indicated that epiphytic algae can be the primary food resource in seagrass meadows (Nielsen & Lethbridge 1989, Frankovich et al. 2009). Primary production in Mississippi Sound included seagrass,

epiphytic algae, sand microflora and phytoplankton, with the dominant producer being epiphyte algae (Moncreiff et al. 1992).

In a successional pattern, diatoms and other microorganisms attach directly to the seagrass leaves, followed by a variety of red, green and brown algae, some filamentous and some coralline (Corlett & Jones 2007). These epiphytes provide additional surfaces which can be utilized by diatoms and other algae for secondary colonization. Invertebrates, some of which consume the primary producers and some which just take advantage of the substrate, are also attached or attracted. Some algae preferentially attach to the edges of the *Thalassia* leaves (Humm 1964). Humm (1964) found 113 species of algal epiphytes on *T. testudinum* in Florida.

These complex epiphyte communities are spatiotemporally dynamic. Epiphyte community structure on *Thalassia testudinum* from Grand Cayman (Corlett & Jones 2007) was different compared to that from Florida Bay (Frankovich et al. 2009). Two most common epiphytes were found on every leaf in Great Cayman, including *Hydrolithon farinosum* and an indeterminate coralline alga (Corlett & Jones 2007). Seven species of macroscopic red algae, mainly *Melobesia* and *Fosliella*, and 11 faunal phyla, such as *Spirorbis* (most ubiquitous), were identified on the same seagrass species in Florida (Frankovich & Fourqurean 1997). Additional variation with seasons and with environmental conditions have been noted for epiphytic algae (Borum 1985, Armitage et al. 2005, Hasegawa et al. 2007) and invertebrates (Novak 1982, Peterson et al. 2007a, Whalen et al. 2013)

The seagrasses are not only just simple substrata for epiphytes (Pinckney & Micheli 1998), the epiphytes may select suitable seagrass leaves because of positive or negative interactions. Recent work (Crump et al. 2018) has greatly illuminated our understanding of the complex biochemical interactions between epiphytes and their hosts that were previously demonstrated (Harlin 1973, 1975, Buschmann & Gómez 1993, Callaway et al. 2002). The seasonal changes of seagrass hosts and their associated epiphytic algae communities could change dramatically (Borum 1987, Hall & Bell, 1988; Jernakoff et al. 1996) and were affected by nutrient levels (Armitage et al. 2005; Hasegawa et al. 2007). Since light availability is the main factor driving seagrass status (Ralph et al. 2007), changes of epiphyte accumulation and the intensity of competition between seagrass and epiphytes for light and nutrients may influence seagrass condition (Borum 1985). Hence the epiphyte-seagrass dynamics are determined by multiple environmental and biological factors.

However, excessive accumulations of algal epiphytes can be detrimental to seagrass, or even the whole coastal ecosystem. Seagrass plant morphology can be affected as a response to competition for light and nutrients (Frankovich & Fourqurean 1997, Brush & Nixo 2002, Nelson 2017a, Whalen et al. 2013, Ow et al. 2020). For example, as *Zostera* (eelgrass) grows, the accumulation pattern of epiphyte biomass on leaves occurs in two different phases. New leaves are continuously produced interior to older leaves to replace the older epiphyte-colonized leaves that are shed to the outside (Sand-Jensen 1975). It is suggested that the epiphyte community biomass on young eelgrass leaves increases exponentially, but epiphytes on older leaves may be in a “stable” status (Borum 1985). That means that total epiphyte biomass accumulation on old seagrass leaves plateaus, because the accumulation is counterbalanced by loss of the oldest parts of seagrass leaves due to death of these portions of leaves and their resultant breakage. It should

be noted that this is distinct from senescence and shedding of the entire leaf. Rather, the oldest, dead parts of leaves successively break off until senescence of the remainder occurs when virtually all of the leaf is dead. This mechanism explains in part why excessive epiphyte growth is one of the factors to drive seagrass decline.

It is widely acknowledged that epiphytes can be top-down controlled by grazers, which in turn are controlled by higher trophic levels (Figure. 1) (Heck & Valentine 2006). But this relationship can be complicated by simultaneous bottom-up effects of nutrients (Burkholder et al. 2007, Peterson et al. 2007a, Whalen et al. 2013) as well as feeding preferences associated with the nutrition content or algal chemical deterrents to grazing (Landsberg et al. 2009, Nielsen & Lethbridge 1989, Crump et al. 2018). Due to eutrophication, fast-growing epiphytes may reduce the light penetration to the leaf by intercepting the light (Duarte 1995, Ruiz & Romero 2001, Armitage et al. 2005) to reduce productivity. Higher production and photosynthesis rates were found in control shoots compared to shaded *Thalassia* shoots (Tomasko & Dawes 1989). Understanding the negative consequences of eutrophication and overharvesting requires knowledge of these complex interactions and will be important to improve water quality and achieve seagrass restoration.

Under conditions of eutrophication-induced phytoplankton blooms, turbidity from sediment disturbance, and/or overgrowth of epiphytes, light availability reduced below the approximate threshold of 4-36% surface irradiance can limit seagrass photosynthesis (Dunton 1994, Ralph et al. 2007, Nelson 2017b). For this reason, metrics of epiphytes have been regarded as important bio-indicators for nutrient impact on the estuarine ecosystem. However, it has been argued that

epiphyte composition is limited in predicting seagrass loss and thus has limited utility as an environmental indicator, probably due to the above-mentioned confounding factors (Worm & Sommer 2000, Fourqurean et al. 2010). Multiple studies of nutrient impacts on seagrass response showed that nutrient levels alone could affect the growth of both seagrass and associated epiphytes, but the effects were highly variable between studies (Frankovich & Fourqurean 1997, Moore & Wetzel 2000, Worm & Sommer 2000, Johnson et al. 2006). A Florida Bay study revealed highly variable epiphyte levels and strongly site-specific nutrient responses (Armitage et al. 2005). More epiphyte biomass and less light availability have been found along a gradient of external N loading in Waquoit Bay (Wright et al. 1995), and epiphytes have been found limited by nitrogen and phosphorus concentration in the northern Gulf of Mexico (Johnson et al. 2006). *Thalassia testudinum,* from different sample sites and with absence of grazers in mesocosms have presented variable epiphyte accumulations (Hays 2005). But other systematic studies manipulating both nutrients and grazers demonstrated clear nutrient effects on epiphyte levels (Peterson et al. 2007, Sweatman, Cuvelier and Cammarata unpublished, Whalen et al. 2013). Moreover, none of these studies teased apart relationships for seagrass leaves in the growth vs. dying phases, and the methods employed were spatiotemporally limited. The extents to which nutrients directly impact mesograzer communities or contribute to increased susceptibility of seagrasses to other stressors are not known.

1.3 Monitoring seagrass and epiphytes

The dominant methods to monitor epiphyte accumulation on marine or land vegetation focus on biomass, including dry weight biomass, ash-free dry weight biomass (Dry organic weight) (Leuven et al. 1985), or chlorophyll *a* and *b* (Porra et al. 1989), and other pigments (Armitage et

al. 2005). Some studies in epiphyte community classification relied on their ecological functions rather than taxonomic discernment (McCune 1993). Compared with characterization of algal epiphytes on seagrass blades, the cryptogamic epiphytes on oak branches were easier to quantify (Holz & Gradstein 2005). Epiphytes on seagrass are typically collected by scraping gently from host plants (Libes 1986, Ray et al. 2014). Some studies removed epiphytes from rooted macrophytes by shaking in bottles with low pH MES buffer (Zimba & Hopson 1997), or preprocessing with dilute acid for removing calcareous epiphytes (Nieuwenhuize et al. 1994), and other mechanical methods including the use of water flow (Hickman 1971), or scraping after lyophilizing on dry ice (Penhale 1977).

While these traditional biomass measures are simple and inexpensive to perform, they are somewhat tedious and all but the pigment studies fail to account for species composition or morphology changes; therefore, these methods provide limited and incomplete information of epiphyte dynamics in response to changing environment and the complex relationship between epiphytes and seagrass. Thus, previous studies with the typical epiphyte and seagrass measurements did not fully capture the dynamic spatiotemporal information on epiphyte biomass distribution on the seagrass leaves (Bulthuis & Woelkerling 1983, Borum 1987, Biber et al. 2004) because of temporally-limited sampling and the inherent limitations of the biomass measures. For example, the epiphyte biomass on a single leaf is the product of accumulation over a period of weeks or longer. Traditional dry weight biomass methods would present the biomass data as single values that represent variable periods exceeding a month. It's necessary to develop other novel technologies and sampling strategies to obtain more information about epiphyte communities.

1.4 Image analysis-based technologies

With the development of advanced digital photography and computer science, image analysis-based methods have been widespread and applied in many plant studies. In the Northern Gulf of Mexico, algal recruitment and a shift in community composition on the rock surface in a newly developed tidal inlet was evaluated by analyzing pictures from a microscope with a digital imaging system (Fikes and Lehman 2008). An image analysis technique was developed to diagnose injured *Zostera* leaves (Boese et al. 2008). The ERMapper program classified healthy vs. diseased leaves based on pigment changes leading to spectral differences. Bacterial aggregation on the bean leaf surface was measured by fluorescence image analysis (Monier & Lindow 2004). The frequency, size and distribution of diverse kinds of bacteria were investigated with their distinguishable spectral information, but the classification was imprecise due to multiple accumulation layers and halos around colonies. Additionally, image analysis estimated shoot biomass of cereal plants with a linear function of shoot area calculated in high-throughput images (Golzarian et al. 2011). Spatial patterns of photosynthetic efficiency were obtained by Imaging-PAM fluorometry (Ralph et al, 2005). Coral researchers calculated coral colonization with Coral Point Count with Excel Extensions (CPCe) software, a visual basic program (Kohler & Gill 2006). However, the CPCe program is limited in that it requires manual classification. In contrast, a machine-learning approach named Pattern Recognition Software was trained with specific features, such as the color, brightness, and texture in the images and subsequently used for feature identification (Shamir et al. 2010). Geographic Information System (GIS) technology has been applied in terrestrial epiphyte ecology research based on image

analysis (Bader et al. 2000). The recent widespread availability of public resources for image-analysis makes these methodologies particularly attractive for seagrass and epiphyte analyses.

Novak (1982) examined the spatial and seasonal distribution of meiofauna on *Posidonia oceanica* through a stereomicroscope. With the pictures of covered area from a camera, they measured the coverage of macro-epiphytes in an automatic area meter. Another study used image-analysis to calculate the proportion of eelgrass leaves infected by wasting disease (Boese et al. 2008). Fluorescence imaging PAM was used to explore the effect of leaf age on photosynthesis in three seagrass species (*Halophila ovalis, Zostera capricorni* and *Posidonia australis*) (Ralph et al. 2005). A novel epiphyte fluorescence measurement (Ray et al. 2014) was used to measure fluorescence of photosynthetic accessory pigments as a proxy for epiphyte abundance. Fluorescence scanning performed similar epiphyte characterization for epiphytes still attached to the seagrass leaves (Contreras et al. 2011), an approach which provides greater spatiotemporal resolution of epiphyte accumulation compared to traditional leaf-scraping methods.

1.5 Aims, hypotheses and objectives

This study aims to develop a color scanning and image analysis-based method to characterize spatiotemporal epiphyte accumulation patterns on seagrass, and to delineate the spatiotemporal shift in seagrass and epiphyte growth. Image analysis methods will be developed to extract the rich information of the images, including metrics related to seagrass morphology, epiphyte coverage pattern, and classification of potential epiphytic groups. The geospatial analytics software, ENVI (L3 Harris Geospatial, Broomfield CO) will be used to process images to train,

distinguish and identify epiphytes vs. uncolonized leaf surfaces. This approach is expected to provide highly informative metrics of epiphyte accumulation profiles, community composition shifts, and seagrass morphological responses to interpret the epiphyte accumulation within growing seagrass leaves under various environmental conditions. Anticipated requirements for interpretation of this information are the description and separate analyses of seagrass leaves at different growth phases, and the effects of changing environmental conditions such as water temperature, salinity, nutrient levels and light availability on seagrass-epiphyte interaction. This is expected to clarify the dynamic short-term relationship between epiphyte accumulation (a composite of colonization and growth) and seagrass growth and morphology changes across environmental context.

Using samples of *T. testudinum* and associated epiphyte from the western Gulf of Mexico, this study focuses on epiphyte-seagrass dynamics with specific objectives of (1) developing the image analysis for seagrass and epiphyte classification; (2) validating the high-resolution information derived from the image-based method, including computing accurately the seagrass leaf morphology, distinguishing diverse epiphytes and seagrass, and estimating epiphyte accumulation pattern; (3) delineating spatial and temporal variability of seagrass growth and epiphyte accumulation through traditional epiphyte biomass measurement and image-based measurement for further validation; (4) simulating the epiphyte colonization driven by *T. testudinum* growth phases (recruitment and senescence) under changing environments through biomass metrics to examine the contribution of variable environmental factors, including water temperature, salinity, depth, and nutrient levels of sediment porewater, to epiphyte-seagrass dynamics. This study provides a new method to assess the seagrass-epiphyte relationship within

changing environments and estimate accumulation patterns of epiphytes with growing seagrass leaves quantitively. This information about the epiphyte effect on seagrass health will lead to more informed management decisions in seagrass protection and recovery.

Research hypothesis and objective 1: The first hypothesis to test is that *Thalassia testudinum* can be imaged and analyzed to derive new metrics, such as leaf area and epiphyte cover, which correlate with the traditional biomass and morphological measure of seagrass and epiphytes. High-resolution information on epiphyte coverage area of seagrass from image analysis will characterize epiphyte accumulation and allow tests of correlation between epiphyte biomass and epiphyte coverage metrics to compare the measurements.

Research hypothesis and objective 2: The second hypothesis is that the sampling and image-analysis methodology will capture spatiotemporal shift in both seagrass morphology and epiphyte communities. Traditional epiphyte biomass measurements of total epiphytes are commonly expressed relative to total seagrass biomass and obtained only in limited annual or seasonal sampling. More frequent sampling (at least bimonthly) using image analysis techniques should provide sufficient data to delineate short-term spatiotemporal variability of epiphyte-seagrass dynamics to capture the morphological response of seagrass in relation to accumulation patterns of epiphytes.

Research hypothesis and objective 3: The third hypothesis that various internal and external factors alter seagrass-epiphyte interactions (Harlin 1980, Fong & Harwell 1994, Biber 2004, Nelson 2017) at the plant level, will be tested by producing a multiple linear regression model.

Affirmation of the hypothesis would suggest that epiphyte accumulation with seagrass growth (recruitment and senescence) might serve as indicators of environmental conditions. The sampling strategy design will allow investigation of the effects of environmental factors, such as nutrient levels in sediment porewater, depth, temperature, and salinity. The study attempts to clarify the contribution of any accessible factors to seagrass-epiphyte interaction.

CHAPTER II: MATERIALS AND METHODS

2.1 Study Location

The study location is adjacent to the Intracoastal Waterway (ICWW) and Redfish Bay in Aransas Pass, Texas (Figure 1; GPS coordinates in Table I). Redfish Bay encompasses an area of approximately 90 km^2 with average depth ranging from 0.75m to 2m (Su & Huang 2019), and average annual inflow of about 19.34 million cubic meters (Asquith et al. 1997). The mean winter inflow was significantly higher than in other seasons. Within a semiarid and subtropical climate, water temperature in Redfish Bay varies from 0℃ in winter to 40℃ in summer (Kornicker 1964). The water temperature generally follows the air temperature, but it occasionally rises or drops quickly due to fluctuating weather conditions (Asquith et al. 1997). *Halodule wrightii*, *Thalassia testudinum*, and *Cymodocea filiformis* are the co-dominant seagrass species in Redfish Bay (Fry & Parker 1979, Congdon & Dunton 2016).

The study location is near the Redfish Bay State Scientific Area (to the northeast), where seagrasses are protected by law. It is bounded by the City of Aransas Pass Wastewater Treatment Plant on the northwest, and the ICWW to the east, and centered around the ICW RV Park (Figures 1&2). Preliminary scouting revealed what appear to be different epiphyte communities in two areas on the north and south sides of the RV Park "peninsula", which provides both access and a physical barrier to water flow between two areas (Figure 2). Redfish Bay had a high epiphytic loading according to previous research (Su & Huang 2019). The study areas can be easily accessed by wading or kayaking from the ICW RV Park, and access permission has been granted from the owner. The Wastewater Treatment Plant is adjacent to the RV park and

permitted to discharge treated effluent at two sites (marked on Figure 1; as per discharge permit) with potential impacts on the study area (Figure 2).

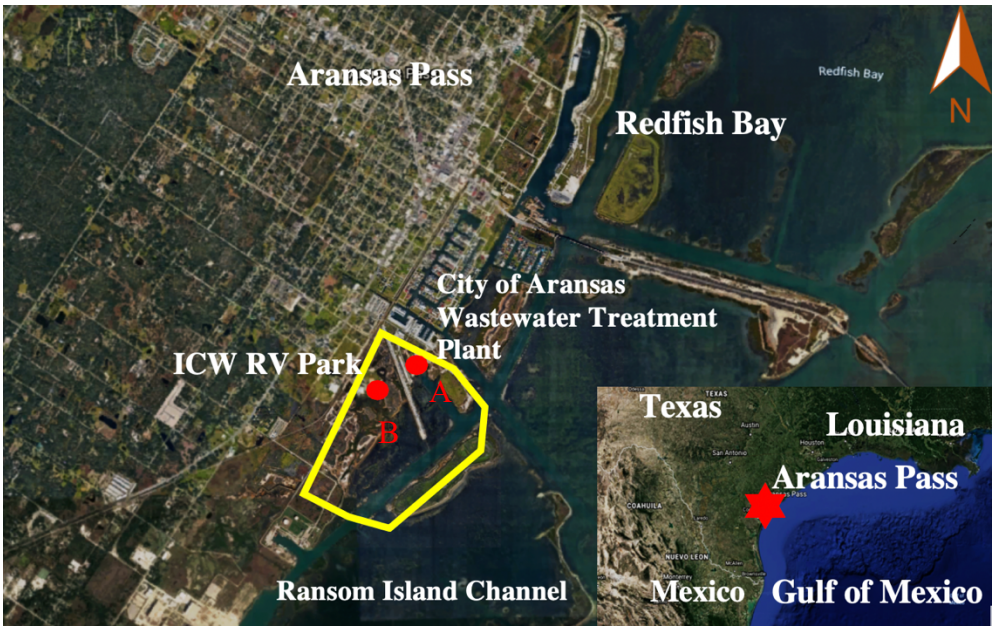

Figure 2. Map of the Texas Coastal Bend (right bottom) and the Aransas Pass-Redfish bay sampling area (Yellow boundary area). The maps are from Google Earth. Dots represent two permitted WWTP discharge sites. A, B, refer to WWTP and Control areas, respectively.

Sampling areas on the north (A) and south (B) sides of the RV Park, respectively, are designated as the "Wastewater Treatment Plant" (WWTP) and "Control" areas, respectively. The "WWTP" area is presumed to receive a direct discharge of treated wastewater, whereas the "Control" area may receive indirect impacts from an alternative wastewater discharge site, but such discharge, in the latter case, would receive additional mitigation by filtering through a wetland system before encountering the seagrass. The "WWTP" area potentially receives other nutrient-related impacts from a fish-cleaning station which attracts abundant birdlife. These two areas are otherwise in close geographic proximity and mostly similar in fetch. "WWTP" has somewhat

more exposure to northeast winds while the "Control" area has somewhat more exposure to southeast winds. These two areas have observable differences in the appearance of their epiphyte communities (Figures 3 and 4) which is further supported by a preliminary 18s rRNA comparison of epiphytes. The seagrasses are primarily monotypic patches of *T. testudinum* or *C. filiformis*, with mixed communities in between. Small scattered clumps of oysters are found throughout the seagrass in both areas. It is expected that different environmental conditions, such as nutrient level and grazing density, exist at the two areas due to the observation of variable epiphyte communities (Frankovich & Fourqurean 1997, Heck & Valentine 2006, Johnson et al. 2006, Frankovich et al. 2009, Nelson 2017b). We sampled seagrass and epiphytes from 5 sites distributed in the "Control" and the "WWTP" areas, across a depth gradient. A site on the extreme southeast of the "Control" area, named Control ICWW (CI) (Figure 2), showing the highest epiphyte loading and shallowest depth compared to all other sites, was also sampled for seagrass and epiphytes (Table 1). This CI site is within approximately 5 m of the ICWW and a shallow subtidal oyster reef. All sampling stations are primarily mud sediment with sand, except at CI site, where there is also an abundance of embedded oyster shell.

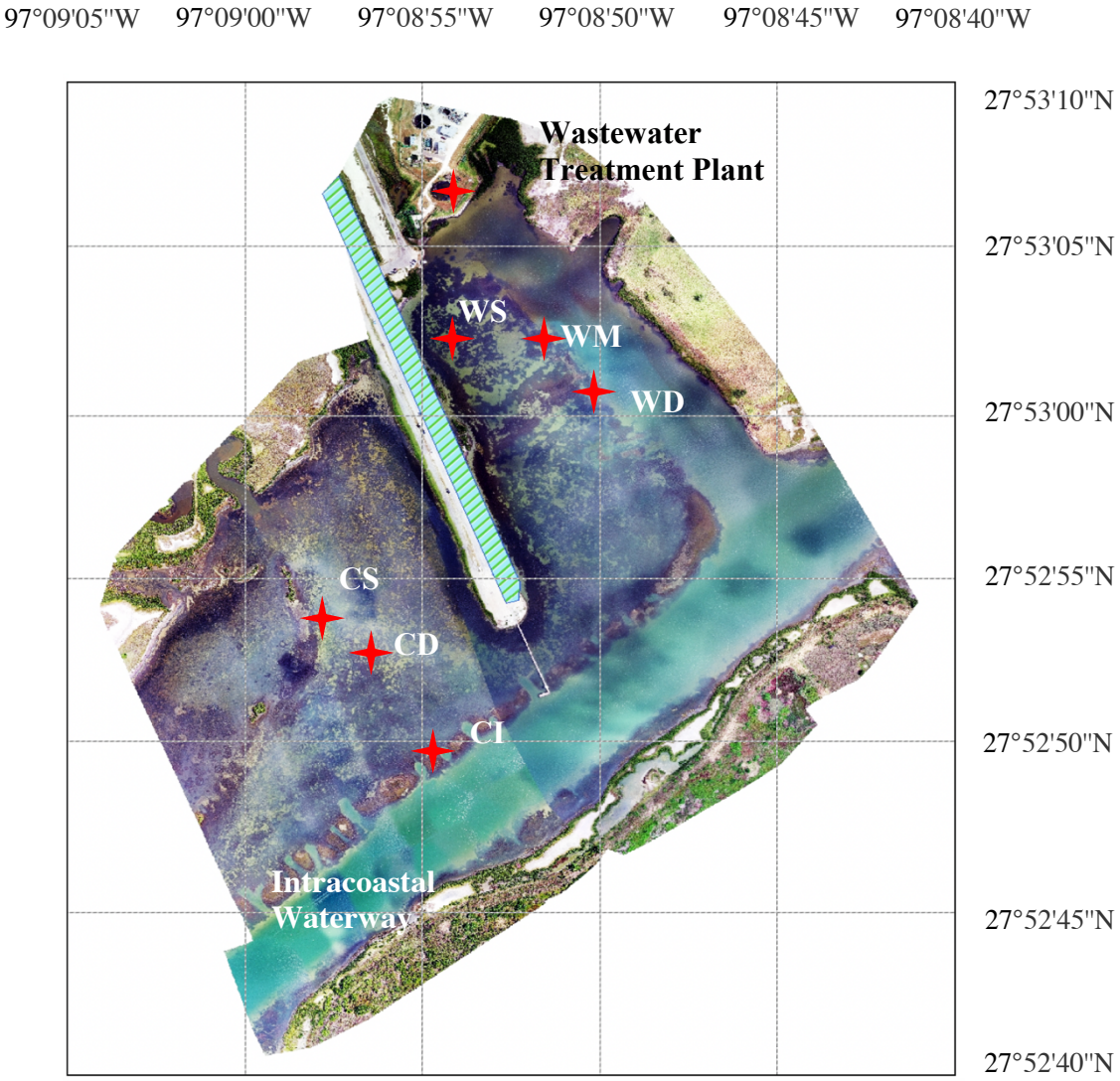

Figure 3. Drone imagery of study area courtesy of Dr. Hua Zhang at TX A&M University-Corpus Christi. The "Control" site is at the south of the RV park, comprising shallow (CS) and deep sites (CD). The "WWTP" area is at the north of RV park, comprising shallow (WS), medium (WM) and deep (WD) sites. The Control ICWW (CI) site showing the highest epiphyte loading is also located.

2.2 Seagrass and epiphyte sampling

Five sampling sites were selected in two areas ("Control" and "WWTP") (Figure 2) (Table 1). Three sampling sites were chosen in the "WWTP" area so that measurement occurred across a gradient of depth to examine the effect of light attenuation. We also compared a shallow and a

deep site in the "Control" area. Seagrass samples from CI site were collected simultaneously when we were in the "Control" area (Figure 2). Each sample collection site is at least 30 meters from the next one. Sites generally differed in depth by about 10-15 cm compared to neighboring sites, except the CI site, which was shallowest (Table I). From July 31, 2019, to April 30, 2020, shoots of *Thalassia testudinum* were collected monthly or bi-monthly. The volume and time requirements of sample processing work necessitated that visits to the south and north ICW RV Park be staggered at approximately three week intervals.

Table 1. Depth and GPS coordinates for 6 sampling sites in Aransas-Redfish Bay Study area, Texas

Sampling Location	Mean Depth (cm)	Standard Deviation	Minimum Depth (cm)	Maximum Depth (cm)	GPS Coordinate
Control Shallow (CS)	58.0	13.0	45.0	88.0	W 027.88053 N 097.15044
Control Deep (CD)	83.3	13.4	65	107	W 027.88021 N 097.15002
Control ICWW (CI)	47.2	11.9	35	73	W 027.88053 N 097.15044
WWTP Shallow (WS)	67.2	17.8	29	95	W 027.88485 N 097.14861
WWTP Medium (WM)	79.3	16.6	46	110	W 027.88467 N 097.14790
WWTP Deep (WD)	93.2	16.5	62	125	W 027.88435 N 097.14761

For each sampling, we harvested all seagrass shoots within three haphazardly placed "rings" at each site for triplicate replication. Rings consisted of a thin slice of a 7.6 cm inner diameter PVC pipe, encompassing an area of 4.53×10^{-3} m^2. Seagrass shoots and leaves angled by the current were gently re-positioned so that every leaf, of every shoot that was located within the ring, was contained entirely within the ring. Leaves of shoots anchored outside the ring were excluded from the ring. Then all seagrass shoots anchored inside the ring were harvested by reaching down into the sediment and plucking, keeping all leaves still attached to their shoot. Representation of young shoots was obtained in this manner. This sampling strategy is important

for capturing variation in the different states (ages) of seagrass growth and epiphyte accumulation. Seagrass samples were collected in plastic bottles, placed on ice for transport, and stored at 10℃ in the laboratory.

2.3 Measurement of environmental conditions

Field conditions (depth, salinity, temperature, and general observations of wind, weather, etc.) were recorded at each visit to each sampling site to provide contextual information on factors that affect seagrass condition and epiphyte growth in variable ways across the growing season. Depth was measured with a calibrated PVC pole. Salinity measurements were made using a refractometer (VEE GEE, STX-3), in the laboratory, on 50 mL water samples collected at seagrass canopy depth, without headspace. Field water temperatures vary over a wide range and can exceed 30°C in summer. Laboratory salinity measurement avoided the potential error caused by high temperatures since most refractometers do not temperature compensate above 30°C. The temperature of the water column near the seagrass canopy height was measured with a calibrated thermometer.

2.4 Porewater collection and nutrient analysis

Sediment was collected on May 15, 2020, from the 6 sampling sites (Figure 2), in triplicate, using a 10 cm inner diameter PVC corer inserted to a sediment depth of 15-20 cm. The water column seawater was drained, and the sediment was gently extruded into a semi-cylindrical PVC pipe (10 cm inner diameter). The upper 5cm of sediment was discarded and the succeeding 10 cm of sediment core, representing the 5-15 cm root zone, was transferred into a plastic storage

bag. Sediment samples were kept cold (4°C) during transport and at the laboratory. All sediment samples were processed within two days.

Porewater was collected using centrifuge extraction. Collected sediments were mixed in the storage bag and portioned (80-100g) into 50ml centrifuge tubes with a plastic spoon. Sediment tubes were centrifuged at 5000 × g for 20 minutes at 4°C. After centrifugation, the supernatants were collected into new 50 mL tubes and kept on ice before filtration. Supernatants were filtered through VWR glass microfiber filters, grade 696 (particle retention: 1.2µm). The filtrates were stored at -25°C and shipped frozen for nutrient analyses at the University of California-Davis Analytical Lab (UC Davis). Nutrient analyses of the porewater were conducted for nitrate and ammonium using Method 847 (Cadmium Reduction Flow Injection Method & Flow Injection Analysis), and for orthophosphate by Method 865 (Flow Injection Analysis for Orthophosphate) (Clesceri et al. 1988). For the following analyses, the nutrient levels of sediment porewater measured at this single time were considered to be a long-term indicator of relative sediment porewater nutrient level across our sampling periods. Nitrate levels were generally very low and below the routine detection limit of 0.05 mg/L. In some of these cases, there were measurements of less than 0.05 mg/L that would have had higher levels of uncertainty. These values were used, where available. In other cases, there was no measured value, in which case there was no value available for statistical analysis, necessitating the use of the “Shaffer" procedure for multiple comparisons of unbalanced data (Shaffer, 1986; Bretz er al., 2016).

2.5 Sample processing, seagrass and epiphyte imaging, and biomass determinations

The epiphyte-seagrass dynamics were quantified by both traditional biomass measurements and image-based metrics, which were evaluated herein. Initial sample processing in the laboratory was completed within 72 hours of harvest. Seagrass samples were gently soaked for 2-3 minutes in deionized water to remove salt and loose non-specifically associated material (e.g. sand). Leaves were removed from a single whole shoot at the ligule, measured for morphometrics (leaf length and width), and then arranged on a fluid mount scanning tray for the Epson Perfection V-750 Pro color flatbed scanner (Epson, Carson, CA). To avoid air bubbles and reflective effects, the seagrass leaves were flooded with deionized water and weighted down with clear glass microscope slides. Leaf images were obtained using 24-bit color scanning at 1200 dpi resolution and then saved as .tiff files (Figures 3 and 4). Leaves longer than 23 cm were cut diagonally with a razor blade to fit onto the scanning tray. The upper leaf portion was offset to indicate it was part of the adjacent leaf, and the diagonal cut assures that the same leaf surface is imaged for both parts.

Figure 4. Scanning picture of one *Thalassia testudinum* shoot from "WWTP" area (Lightened by 35%)

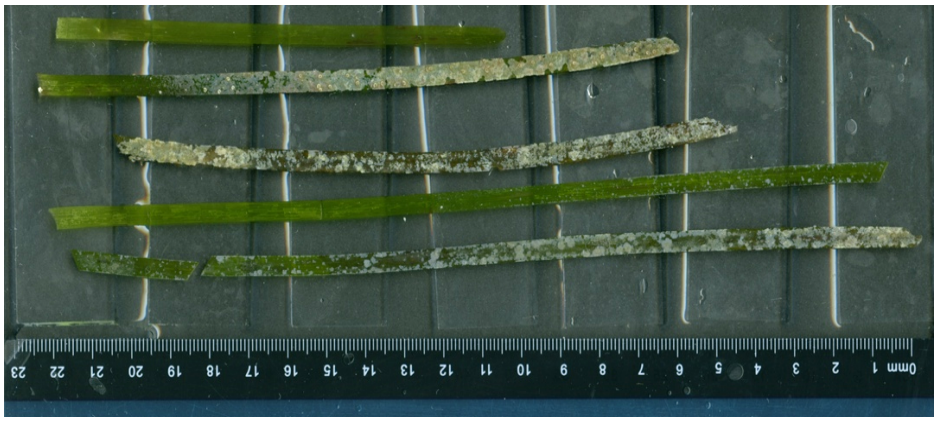

Figure 5. Scanning picture of one *Thalassia testudinum* shoot from "Control" area (Lightened by 15%)

The biomass measurement was performed individually for each leaf of each shoot to explore the epiphyte accumulation on leaves of different growth states or ages. After scanning, epiphytes were removed from seagrass blades by scraping with a microscope slide into a small volume (<10 mL) of deionized water in a flat-bottomed plastic tray. The removed epiphytes were quantitatively transferred to a graduated tube for volume measurement and withdrawal of a 1 mL aliquot for further analyses. Remaining epiphytes were transferred to a pre-weighed empty tin, and the stripped seagrass blades were transferred to a pre-weighed beaker. The epiphytes and the epiphyte-free leaves were dried to constant weight at 60°C for biomass measurement (Aloi 1990). The dry biomass of the epiphyte fraction was proportionally adjusted upwards to compensate for the removal of the 1 mL aliquots.

2.6 Image analysis

Image-based measurements to quantify seagrass and epiphytes based on their spectral information were developed using ENVI 5.0 program (L3 Harris Technologies, Niles, Ohio).

ENVI is widely used for earth science, construction, and vegetation research, including some seagrass mapping studies (Canty 2014). Here, it was applied on a micro-level to analyze epiphyte accumulation on the leaves. The area of each seagrass leaf and associated epiphyte were recorded by counting the pixels of the uncovered and covered areas of the leaf, respectively. The proportional coverage of the seagrass leaf by epiphyte was considered to be an indicator of epiphyte recruitment and growth relative to seagrass growth.

Spectral angle mapper (SAM) algorithm, implemented in ENVI as a classification method for comparing image spectra directly, was applied in this image analysis project to distinguish between uncolonized seagrass leaf and areas covered by epiphytes (Kruse et al. 1993). In a true-color image, the standard creation of different colors in each pixel is produced by combining three hues of the light spectrum, including red, green, and blue. Each pixel on the image is stored as a red-by-green-by-blue three data array, and these three bands are considered to be three spectra in ENVI. By considering each pixel with three spectra as a vector, spectral information of each pixel can be transformed into a vector (R, G, B) in a three-dimensional cartesian coordinate system (X, Y, Z) (Figure. 5). The SAM algorithm can quantify the similarity (difference) between two spectra by the magnitude of a spectral angle θ calculated by the following equation:

$$Cos\theta = \frac{\sum_{i=1}^{n} t_i r_i}{\sqrt{\sum_{i=1}^{n} t_i^2} \times \sqrt{\sum_{i=1}^{n} t_i^2}}$$

where, n is the number of bands in an image, t is the pixel spectrum, r is the reference spectrum, and θ is the spectral angle.

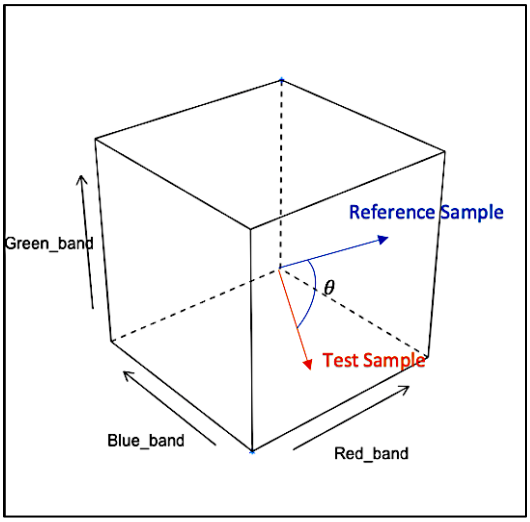

Figure 6. Spectral angle θ between two spectral vectors in a 3-dimensional coordinate system

Classifications of seagrass and epiphytic coverage were estimated by evaluating the degrees of the spectral angles between the pre-established reference spectra and the test spectra. The reference spectra were selected by the minimum, mean (±SD), and maximum of spectra in multiple manually captured areas (1000~5000 pixels), which were visually classified as seagrass or epiphytes, from approximately 200 scanned images. The seagrass leaves for building reference spectra were harvested in the "Control" area in July 2019. A random seagrass blade image was pre-analyzed to further select the applicable reference spectra. Through visual inspection, spectra that misidentified seagrass and epiphyte pixels were eliminated from the spectral reference libraries. Remaining spectra were combined respectively to produce a seagrass spectral library and an epiphyte spectral library. The seagrass spectral library contained 482 reference spectra, which included the uncolonized area of seagrass blades which had different colors due to variable growth status. The epiphyte spectral library contained 843 reference spectra from a mixed group of diverse epiphytic species.

After masking the background and other non-analyzed contents on the images, 2,061 scanned images of seagrass blades were analyzed by ENVI 5.0 program, sequentially using the seagrass and epiphyte spectral libraries. The background was excluded by creating an outline around each seagrass blade using polygon. The threshold of spectral angle identification was set on 0.04 angle radian (≈2.3°). The pixels were identified as seagrass, epiphyte, or unclassified content by calculating their spectra's similarity to the corresponding reference spectra through ENVI program.

2.7 Validation

In the validation stage, the classification output accuracy was assessed using different validation methods to demonstrate if the identification via the SAM algorithm is reliable and reproducible for investigating the seagrass-epiphyte relationship. Two types of validation methods, including "Intrinsic Validation" and "Extrinsic Validation", were used to calculate the accuracy of identified seagrass and epiphyte pixels. By comparing pixels identified from seagrass and epiphyte spectral libraries with each other and to ground-truth pixels, the "Intrinsic Validation" revealed the proportion of correctly identified pixels. From another approach, the process of "Extrinsic Validation" compared the imaging-derived metrics and the traditional biomass metrics to observe the correlation between the two types of indicators. The image-based measurement is considered to be valid if the error from "Intrinsic Validation" is sufficiently small, and if there is a goodness of fit between the classification out and biomass measurements in "Extrinsic Validation".

2.7.1 Intrinsic validation

The “Intrinsic Validation” was used to evaluate the accuracy of identification by comparing the difference between the outputs from seagrass-classified images (from seagrass spectral library) and epiphyte-classified images (from epiphyte spectral library). The “Intrinsic Validation” methods included the comparison of epiphyte coverage determined by seagrass-classification (*SG*) of images and epiphyte-classification (*Epi*) of the same images (Figure 6) and the overlap in identification by the two complementary approaches. This validation procedure quantified pixels that could not be accurately identified.

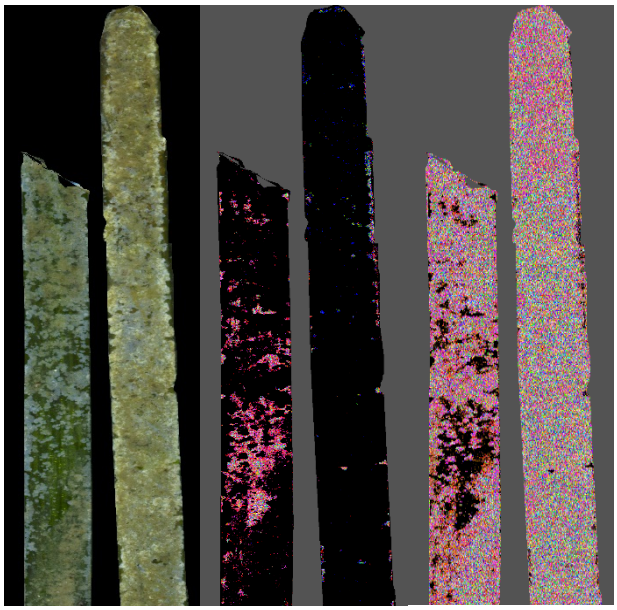

Figure 7. An example of seagrass blade color scans and ENVI classification of seagrass and epiphyte collected at the CS site in July 31, 2019. The black areas are the unclassified pixels. (A) scanned blade; (B) original Seagrass Classified Image (ENVI); (C) original epiphyte classified image (ENVI). Images lightened by 15%.

To validate the image analysis for seagrass-epiphyte study in the ENVI program, we compared the epiphyte coverage of each leaf between their *SG*- and *Epi*-classified images. This validation procedure was expected to demonstrate that the difference of epiphyte coverage between *SG*

images and *Epi* images was as less as possible. The difference between two types of epiphyte coverage was used to show how many percent of the area in the classified images were classified incorrectly. The percent cover of epiphyte in *SG*- and *Epi*-classified images were calculated as follows:

Unclassified Area *(SG)*
= (pixels of unclassified area) / (pixels of total leaf area)×100% (Eq. 1)

where, the pixels which could not be identified as seagrass by the seagrass spectral library were counted as epiphytes.

Epiphyte Coverage (*Epi*)
= (pixels of identified epiphytes) / (pixels of total leaf area)×100% (Eq. 2)

The number of unclassified pixels, identified epiphyte pixels, and total leaf area pixels were tallied by the ENVI program. The difference in epiphyte coverage was calculated as:

Difference of epiphyte coverage
= Epiphyte Coverage (*Epi*) - Unclassified Area (*SG*) (Eq. 3)

The identification of epiphytes and seagrass was considered to be valid if the unclassified area in *SG* images matched the epiphyte coverage in the *Epi* images.

The overlap analysis compared the *SG*- and *Epi*- classified images by calculating what percent of pixels were identified correctly in each image. By overlapping the *Epi* images over the *SG* images, the output of overlap validation created three kinds of pixels, including correctly paired pixels, "overlapping" pixels, and "unaccounted" pixels. The paired pixels were the pixels that were uniquely identified by either the seagrass or the epiphyte spectral libraries. If the pixels were identified as both seagrass and epiphytes by the two spectral libraries simultaneously, they were regarded as "overlapping" pixels. Pixels that could not be identified by either seagrass or

epiphyte libraries were regarded as "unaccounted" pixels. This overlap analysis thus revealed the proportion of indeterminate pixels, those not uniquely identified.

Overlap analysis was conducted by Dr. Ruby Mehrubeoglu at Texas A&M University–Corpus Christi (TAMUCC). Four hundred and seventy-nine *SG*-classified images were selected to compare with corresponding *Epi*-classified images for the overlap analysis. To decrease bias from variance in sites and seasons, images of two seagrass shoots from each sampling time at each site were used for overlap analysis. The selected images were converted to grayscale in MATLAB. Pixels were presented as grayscale with values from 0 to 255. The manually determined background value was converted to white color (255) and then excluded from the analyses. The values of ENVI-based non-classified pixels in both *SG* and *Epi* images were kept black color (0) as original (Figures. 7B and 7C), and the ENVI-based identified pixels, which either identified as seagrass or as epiphytes, were all converted to a single middle value "A" between 0 and 255. This value "A" was selected arbitrarily in each image for overlapping analysis. The overlapping and unaccounted pixels were located by adding the converted *SG* and *Epi* images. The grey value of paired pixels would stay at the value "A". However, the overlapping and unaccounted pixels would produce a double "A" value and zero value, respectively (Figure 8). The percent of overlapping pixels and unaccounted pixels were computed as:

% Overlapping Pixels

= (total number of overlapping pixels) / (pixels of total leaf area) ×100% (Eq. 4)

% Unaccounted Pixels

= (total number of unaccounted pixels) / (pixels of total leaf area) ×100% (Eq. 5)

where, the number of overlapping pixels, unaccounted pixels, and total leaf area pixels were tallied by the MATLAB. The percent of indeterminate pixels was calculated as:

% Indeterminate Pixels

= (total number of overlapping pixels + total number of unaccounted pixels) / (pixels of total leaf area) ×100% (Eq. 6)

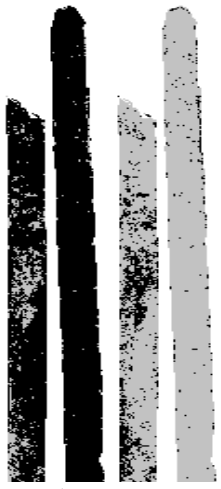

Figure 8. "A" value converted images of Figures 7B and 7C. (A) blade area (black), background (white), and seagrass-segmentation (single gray); (B) blade area (black), background (white), and epiphyte segmentation (single gray). Images lightened by 15%

2.7.2 Extrinsic validation

In the "Extrinsic Validation", the epiphyte and seagrass classification output from imaging analyses were compared to biomass or morphometrics measures. Correlations were drawn from the entire dataset, as well as separately for samples from differing environmental contexts or seasons. Detection of differences between locations or seasons is an attribute of useful

environmental indicators. The dominant methods to monitor epiphyte accumulation on marine or land vegetation determine biomass (dry weight biomass or ash-free dry weight biomass) (Leuven et al. 1985), or chlorophyll a and b (Porra et al. 1989), or other pigments (Armitage et al. 2005). These are expressed relative to host plant morphology (such as biomass, length, width, or leaf area). This validation was primarily determined by evaluating correlations between the dried biomass measures, such as epiphyte biomass, seagrass biomass and epiphyte load (epiphyte biomass/ seagrass biomass) and the image-derived metrics for seagrass leaf area (number of leaf pixels), epiphyte covered area (number of epiphyte pixels) and epiphyte coverage of leaves (number of epiphyte pixels/number of leaf pixels). The data for correlation analyses were collected from each seagrass blade individually. Scatter plots of traditional biomass and morphology metrics *vs*. image-based metrics for seagrass (n = 2052) and epiphyte (n = 1822) measures were created to find the best-fitting regression models. The best-fit relationship between traditional and image-based metrics was acquired through regression analysis using R studio and assessed by the R^2 value. "Extrinsic validation" of image-based metrics was also evaluated by comparing their site- and seasonal- patterns to those of the biomass-based indicators.

2.8 Statistical analysis

Comparisons of the epiphyte-seagrass dynamics across environmental context from July 2019 to April 2020 were analyzed using two-way analysis of variance (ANOVA) followed by a Tukey's honest significant difference with false discovery probability of p=0.05. Both traditional biomass and image-based metrics were used to explore the seagrass growth condition and epiphyte accumulation on location-season variables. Seagrass growth response was determined by the

changes in seagrass leaf biomass and seagrass leaf area, and the epiphyte accumulation was demonstrated by epiphyte load (Fong & Harwell 1994) and epiphyte coverage per leaf (%). The epiphyte load was calculated by dividing the epiphytic dried biomass by the dried biomass of stripped seagrass leaf. A one-way ANOVA was performed to evaluate the significance of differences (p=0.05) for epiphyte-seagrass dynamics among sites of different depths in the "Control" and "WWTP" areas, separately.

To further understand the epiphyte accumulation on each seagrass leaf, as affected by environmental difference and seasonal pattern, the relationship between epiphyte biomass and the continuous covariate seagrass biomass were compared using the Moderated Regression (MODREG) approach (Leppink 2018). The MODREG analysis was used to estimate the growth state (age) of seagrass leaf, for which there was a significant difference in epiphyte biomass among environmentally unique sites (Bretz et al. 2016, Leppink 2018). By comparing the linear regression of epiphyte biomass on seagrass biomass among different sites or seasons, significant differences were evaluated by creating simultaneous confidence intervals (p = 0.05) around the differences among linear regressions at different values of seagrass leaf biomass. When the confidence intervals contained 0, there was no significant difference; when they did not contain 0, there was a significant difference (Bretz et al. 2016). All statistical tests were performed in R studio 3.6.2 software.

2.9 Modeling the dynamics of epiphyte accumulation on *Thalassia* blades

A simple mathematical model describing epiphyte growth with seagrass morphological change was developed by multiple linear regression. Following Fong's (1994) seagrass model and

Biber's (2004) epiphyte model, the epiphyte-seagrass dynamics are influenced by a complex combination of environmental factors and biological interactions. The epiphyte biomass is influenced by light, temperature, salinity, and nutrients (water column nutrients) (Kendrick et al. 1988, Frankovich & Fourqurean 1997, Baggett et al. 2010) as well as by grazing invertebrates (Orth & Van Montfrans 1984, Heck and Valentine 2006, Peterson et al. 2007a, Baggett et al. 2010, Whalen et al. 2013). The availability of suitable seagrass substrate also determines the amount of epiphyte biomass. Epiphyte development on young seagrass leaves exhibited an exponential growth phase, but the epiphyte accumulation reached a plateau as seagrass growth diminished from inhibition by excessive epiphytes (Borum 1987, Neckles et al. 1993). Mortality of epiphytes caused by seagrass leaf turnover was normalized by the seagrass shoot biomass, which could estimate seagrass growth states or ages (Duarte & Sand-Jensen 1990, Gallegos et al. 1993).

Seagrass productivity varies from some of the same environmental factors (light, temperature, and salinity), but sediment-porewater nutrients are probably more important than water-column nutrients. On the other hand, seagrass productivity is also impacted by the dynamics of epiphytes, rhizophytes, and drift algae. Epiphytes and drift algae could decrease seagrass growth by attenuating light availability (Fong & Harwell 1994, Irlandi et al. 2004). Due to the negative relationship between depth and seagrass photosynthesis, the site depth served as an indicator of light availability (Campbell et al. 2007).

The multiple linear regression was employed using R studio to relate the fit (R^2) of the accessible physical variables (depth, temperature, salinity, sediment-porewater nutrient) and biotic variables

(seagrass leaf biomass, seagrass shoot biomass) to the dynamics of epiphyte biomass. Before regression analysis, the parameters of seagrass leaf biomass and epiphyte biomass were logarithmically transformed ($Y = \ln(X)$) to obtain normal distributions. Regression coefficients were developed from the data recorded from July 2019 to April 2020, and only the intact seagrass leaves (as opposed to those with broken tips that were likely dying back) were included in the regression. The coefficients were tested to see if they were significantly different from zero.

To assess the predictive power of the regression equation, we compared the observed epiphyte biomass with the predicted epiphyte biomass. 119 seagrass leaves from July 31, 2019, in the "Control" area and August 9, 2019, in the "WWTP" area (not previously included in our analyses) were used to test the model. These samples were collected from two extra sites beyond the above six sampling sites. Depth, water temperature, and salinity were measured simultaneously. The nutrient levels from sediment porewater were represented by the mean levels in "Control" and "WWTP" areas, respectively. The observed epiphyte biomass was compared with the predicted epiphyte biomass from the environmental variables and seagrass variables based on the regression equation to evaluate how well the regression model mimicked the observed epiphyte-seagrass dynamics.

CHAPTER III: RESULTS

3.1 Environmental conditions

Salinity levels differed significantly with seasonal change ($df = 3$, $F = 31.68$, $P < 0.05$), but there was no significant difference in the mean salinity among the "Control" area, CI site, and "WWTP" area (Table 1) (Overall means: "Control": 27.83±1.23‰, CI: 28.17±1.17‰, "WWTP": 28.42±0.79‰). Water column salinities in the three locations were highest in the summer.

Table 2. Average salinity (±SD) in three sampling locations from July 2019 to April 2020. NA = no measurement available.

Sampling Date	"Control" area	CI site	"WWTP" area
07-31-2019	35.00±0.00‰	35.00±0.00‰	34.44±1.73‰
08-09-2019	NA	NA	37.00±0.00‰
08-30-2019	37.00±0.00‰	37.00±0.00‰	NA
09-11-2019	NA	NA	36.00±0.00‰
09-25-2019	34.00±0.00‰	34.00±0.00‰	NA
10-09-2019	NA	NA	29.50±0.00‰
11-20-2019	25.75±0.35‰	26.00±0.00‰	NA
12-18-2019	NA	NA	30.00±0.00‰
01-17-2020	30.00±0.00‰	30.00±0.00‰	NA
02-22-2020	NA	NA	27.50±0.87‰
04-19-2020	NA	NA	26.67±0.58‰
04-30-2020	28.25±0.35‰	28.50±0.00‰	NA

Water temperatures ranged from 16 to 32 ℃ and were stable in summer and early autumn (29.17~32.00 ℃ from July to October). Temperatures dropped in November and fluctuated

through winter with an average temperature of 20.75±1.17℃. In April, the mean temperature warmed up to 24.00±0.56℃ (Table 5).

The average concentrations of nitrate (NO_3^-) and ammonia (NH_4^+) from CI site sediment porewater was nearly two times higher than from "Control" area, but there was no significant difference for nitrate and ammonia concentration among three locations. The average concentration of phosphate (PO_4^{3-}) at the "WWTP" area was more than two times higher than at "Control" and CI ($df = 2$, $F = 5.93$, $P < 0.05$) significantly (Table 3). The difference in total dissolved inorganic nitrogen (DIN = $NH_4^+ + NO_3^-$) (0.83~1.61 mg/L) among the three sampling locations was not significant. However, ratios of DIN:P ($NH_4^+ + NO_3^-$: PO_4^{3-}), varied significantly from low in the "WWTP" area (7.82) to high at the CI site (29.99) ($df = 2$, $F = 7.71$, $P < 0.05$).

Table 3 Average concentration (mg/L) of ammonium, nitrate, total DIN, phosphate, and DIN:P ratio of sediment porewater (±SD) from the "Control" area (n = 6), CI site (n = 3), and "WWTP" area (n = 9).

Location	NH_4^+	NO_3^-	DIN	PO_4^{3-}	DIN : P
"Control"	0.80 (±0.42)	0.035 (±0.005)	0.83 (±0.42)	0.058 (±0.015)	14.83 (±7.76)
CI	1.52 (±0.73)	0.060 (±0.028)	1.63 (±1.05)	0.060 (±0.014)	29.99 (±17.41)
"WWTP"	0.99 (±0.45)	0.044 (±0.015)	1.03 (±0.45)	0.141 (±0.071)	7.82 (±2.43)

3.2 Validation of image-based measurement

"Intrinsic Validation" calculated the accuracy of identified seagrass and epiphyte pixels by comparing the output obtained from seagrass or epiphyte spectral libraries. The "Extrinsic" Validation" evaluated the correlation between the imaging-derived metrics *vs.* the biomass metrics. The image-based measurement is considered to be valid if the error from "Intrinsic Validation" is sufficiently small, and if there is a goodness of fit between the image classification

output and biomass measurements. Further extrinsic validation was assessed by the efficacy of imaging-based metrics to detect differences between samples from different environmental contexts, seasons or stressors.

3.2.1 "Intrinsic validation": Analyses of difference in percent cover of epiphyte

2,001 scanned images of seagrass blades were analyzed by seagrass and epiphyte spectral libraries to derive *SG* and *Epi* images separately. "Intrinsic Validation" found that differences in percent cover of epiphyte between *SG*- and *Epi*-classified images ranged from -27.99% to 27.99% (see Eq. 1, 2, and 3, Materials and Methods). Over 84% of the classification output was within ±5% difference when comparing *SG*- and *Epi*- classified images. A 99% confidence interval of the average difference was from -0.068% to -0.021% (Figure 9). The difference in percent cover of epiphyte between the two kinds of classified images varied significantly between sampling sites ($df = 5$, $F = 3.80$, $P < 0.05$) and sampling times (from July 2019 to April 2020) ($df = 3$, $F = 98.91$, $P < 0.05$). The mean difference ranged from -8.60% (±6.06%) to 0.93% (±3.86%) across the environmental context (Figure 10). The number of epiphyte pixels identified by epiphyte spectral libraries was underestimated in most environmental conditions, except the seagrass samples harvested in the "WWTP" area in August and CI site in January. The percent cover of epiphyte in *Epi* images fitted the unclassified area in *SG* images poorly, probably due to misclassification of green algae. Some green algae pixels were possibly misclassified as seagrass pixels in the ENVI program because of their similar spectra. A noticeable spike in epiphyte under-classification was observed in spring 2020 from all three locations. This was possibly attributed to change of the epiphyte community. Filamentous green algae appeared most abundant in the spring samples. Conversely, the overestimated percent cover of epiphyte for *Epi*

images was attributed mostly to the misclassification of some yellow-brownish seagrass pixels from older leaves, which were incorrectly identified as yellowish or some brownish filamentous *Chlorophyta* groups.

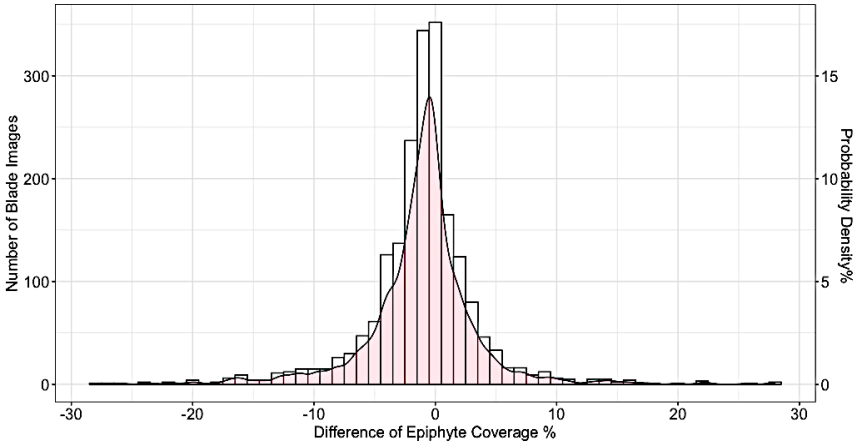

Figure 9. Histogram and probability density plot of difference in epiphyte coverage between *Epi-* and *SG-* images. The white bars are the numbers of analyzed images and the pink shape is the probability density (%) of analyzed images. (n = 2001)

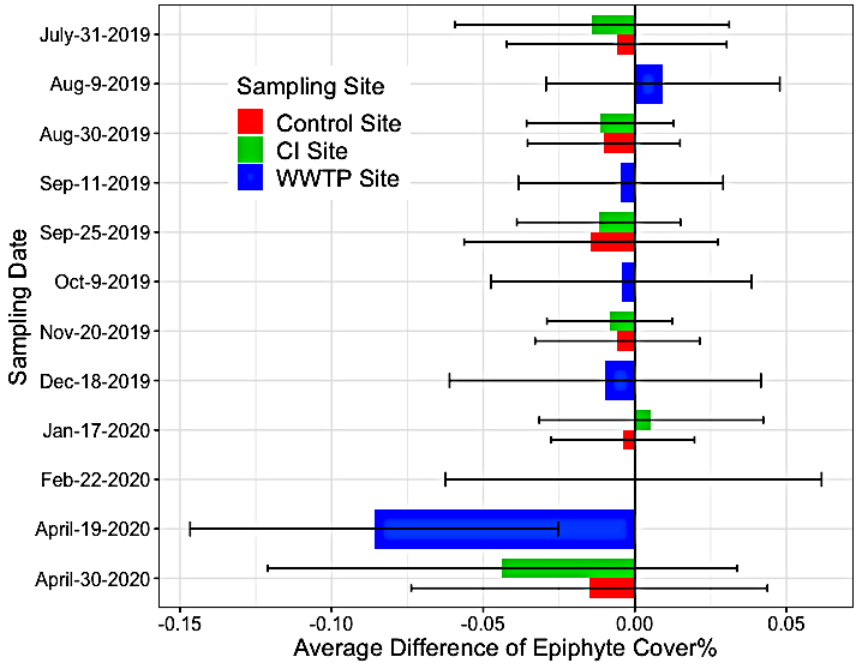

Figure 10. The average difference (±SD) of epiphyte coverage between *Epi-* and *SG-* images from July 2019 to April 2020 at three sampling sites. (n = 2001)

The accuracy level evaluated by the **average** difference in epiphyte coverage did not fully reveal the variability since positive and negative differences could offset each other. Therefore, the differences in the percent cover of epiphyte between (*SG*) images and (*Epi*) images were further assessed by the **absolute difference** analysis. The absolute value of the difference in percent cover of epiphyte between *SG* images and *Epi* images showed < 3.00% absolute difference in 67.02% of the classified output. 83.01% of the output had less than 5.00% absolute difference (Figures 11 and 12). Only 5.55% of the classified images produced more than 10.00% absolute difference.

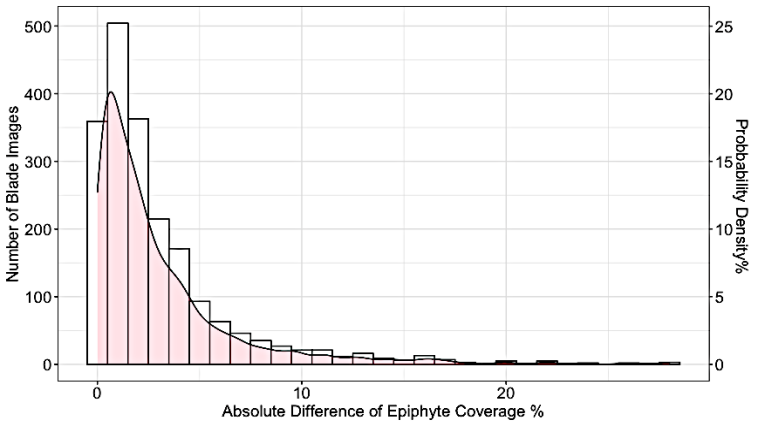

Figure 11. Histogram and probability density plot of absolute difference of epiphyte coverage. The white bars are the numbers of analyzed images and the pink shape is the probability density (%) of analyzed images. (n = 2001)

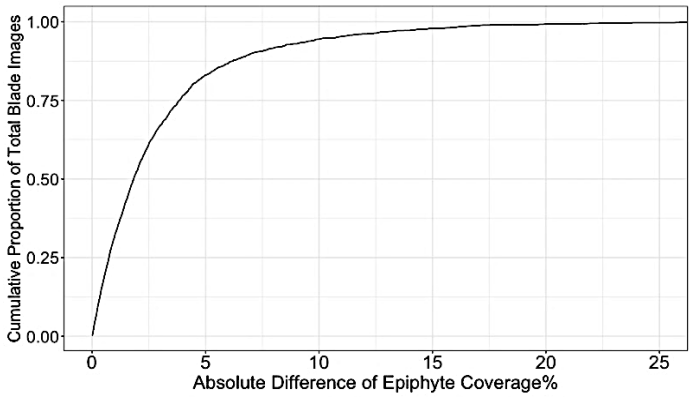

Figure 12. Cumulative distribution of absolute difference of epiphyte coverage. (n = 2001)

The absolute difference in percent cover of epiphyte showed a similar seasonal pattern to the difference of epiphyte coverage among three sites. Although the accuracy of classification outputs varied among sites, there were no distinctions during the same season. In the "Control" area, about 87.19% of blade images produced no more than 5% absolute difference. However, only 76.06% and 78.48% of images revealed a similar accuracy for the "WWTP" area and the CI site, respectively (Figure 13). The average absolute difference was relatively low and stable in summer and autumn, but increased during late winter, and peaked during spring (Figure 14).

There was no significance to the absolute differences that appeared among the three locations from July 31 ("Control" area & CI Sites) to October 9 ("WWTP" area), and the average absolute difference ranged from 1.91% (±1.92%) to 3.05% (±3.07%). However, the absolute difference increased strikingly from December through April in the "WWTP" area ($df = 5$, $F = 58.27$, $P < 0.05$), while the "Control" area ($df = 5$, $F = 10.59$, $P < 0.05$) and CI site ($df = 5$, $F = 24.62$, $P < 0.05$) only showed significantly higher absolute differences in April compared to other months. The maximum mean absolute difference ranged from 4.21% (±4.34%) to 8.68% (±5.95%) in the "WWTP" area. More than 50% of analyzed images from spring had more than a 5% absolute

difference area (Figure 15). This obvious decrease in classification accuracy in the spring was likely seasonal variation in the epiphyte community. Note that the classifications were based on a training image dataset obtained in Summer, so the dramatic deviation in spring suggests a change in the epiphyte community to one with different spectral characteristics.

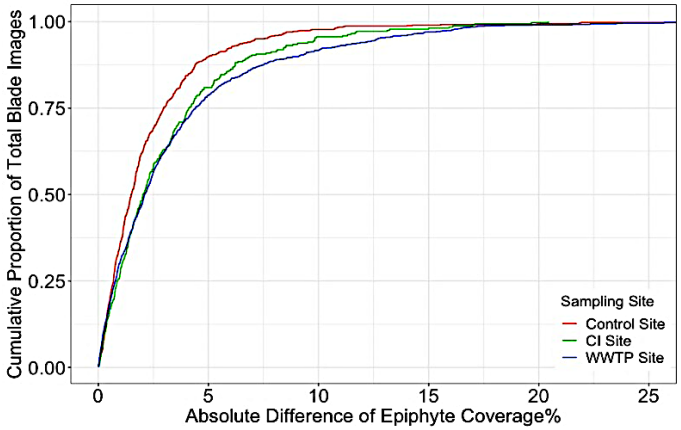

Figure 13. Cumulative distribution of absolute difference of epiphyte coverage at "Control" site (n = 726), CI site (n = 330), and "WWTP" site. (n = 1011)

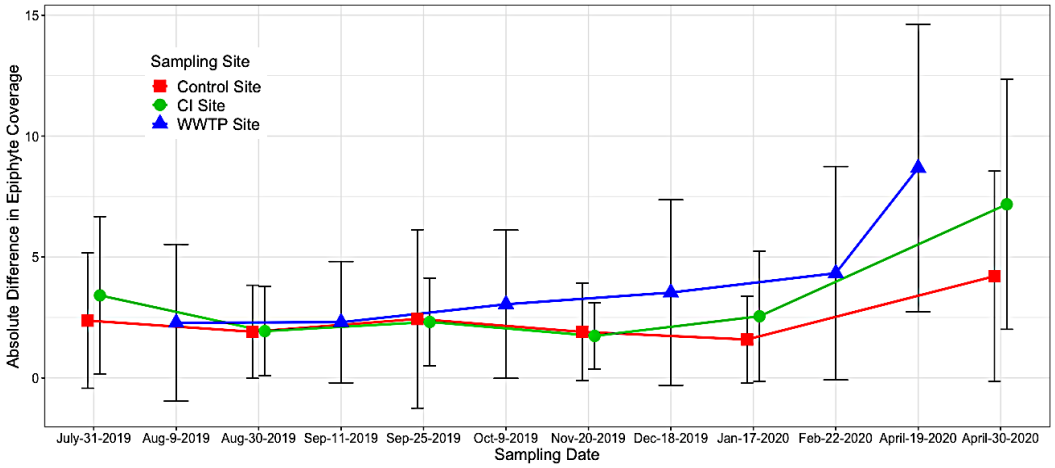

Figure 14. The average absolute difference (±SD) of epiphyte cover between epiphyte and seagrass classification for seagrass leaves from July 2019 to April 2020 at three sampling sites. (n = 2001)

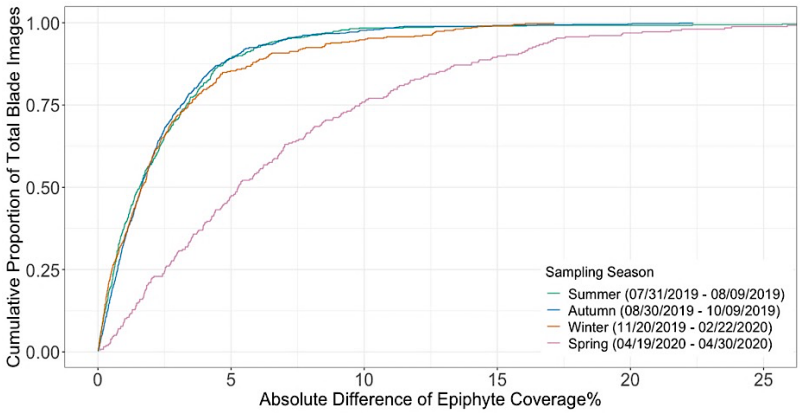

Figure 15. Cumulative distribution of absolute difference of epiphyte Coverage from 2019 Summer (n=509), Autumn (n=828), Winter (n=452), 2020 Spring (n=278). Due to the inconsistent sampling time at three sites, all data were reallocated to four seasons based on the sampling date and average temperature to reveal the variance of absolute difference.

3.2.2 "Intrinsic Validation": Overlap Analysis

The overlap analysis was used to understand indeterminate pixels, which could not be classified uniquely, as a combination of overlapping pixels plus unaccounted pixels. It created three kinds of pixels, including correctly paired pixels (uniquely identified), overlapping pixels (misclassified in one or the other analyses), and unaccounted pixels (not identified in either analysis).

The overlap analysis reported an accuracy of seagrass and epiphyte identification > 90 % in 94.57% of the analyzed images (Figures 16 and 17). The percent of indeterminate pixels fluctuated from 0.21% to 31.50%, but the average percent of indeterminate pixels was only 4.47% ($\pm$3.41%). About 70% of the images had less than 5% indeterminate pixels. These indeterminate pixels include overlapping pixels, which are those identified by both seagrass and epiphyte spectral libraries.

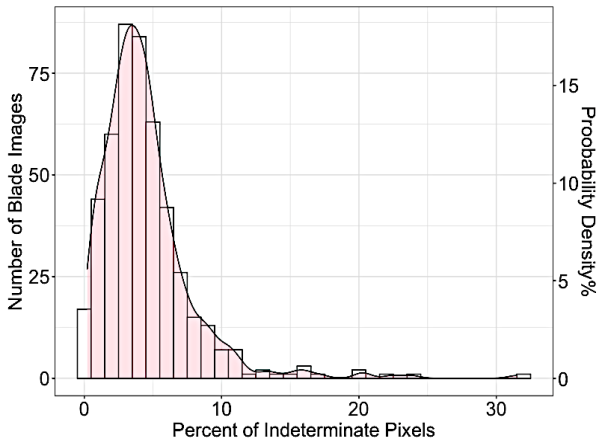

Figure 16. Histogram and probability density plot of Indeterminate Pixels The white bars are the numbers of analyzed images and the pink shape is the probability density of analyzed images. (n = 479)

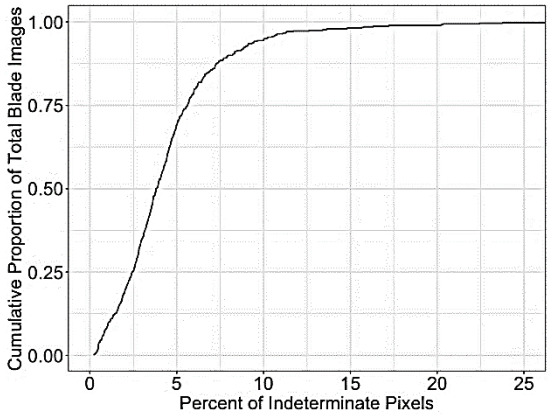

Figure 17. Cumulative distribution of indeterminate pixels. (n = 479)

The percent of overlapping pixels from the two types of independently classified images ranged from 0.01% to 31.50%. The average percent of overlapping pixels was 1.98% (±3.04%). 91.23% of the analyzed images had less than 5% overlapping pixels (Figures 18 and 19).

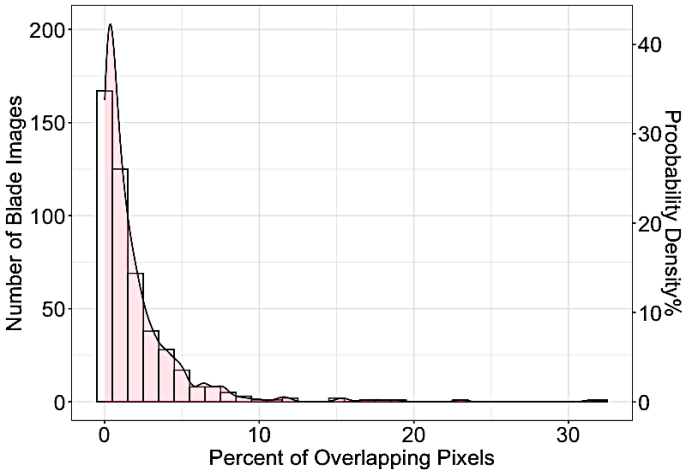

Figure 18. Histogram and probability density plot of overlapping pixels. The white bars are the numbers of analyzed images and the pink shape is the probability density of analyzed images. (n = 479)

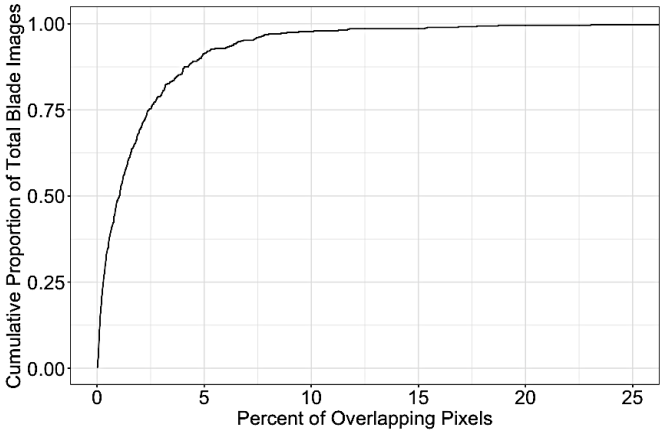

Figure 19. Cumulative distribution of overlapping pixels. (n = 479)

Unaccounted pixels, which were neither identified by seagrass libraries nor epiphyte libraries, also showed a low proportion (< 5%). The percent of unaccounted pixels ranged from 0.00% to 20.12%, and the average percent of unaccounted pixels was 2.48% (±2.24%). 90.81% of the analyzed images had less than 5% of the pixels that were not identified by both seagrass and spectral libraries (Figures 20 and 21).

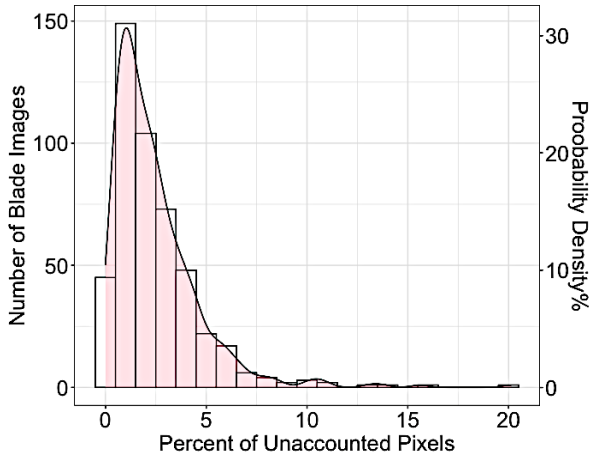

Figure 20. Histogram and probability density plot of unaccounted Pixels The white bars are the numbers of analyzed images and the pink shape is the probability density of analyzed images. (n = 479)

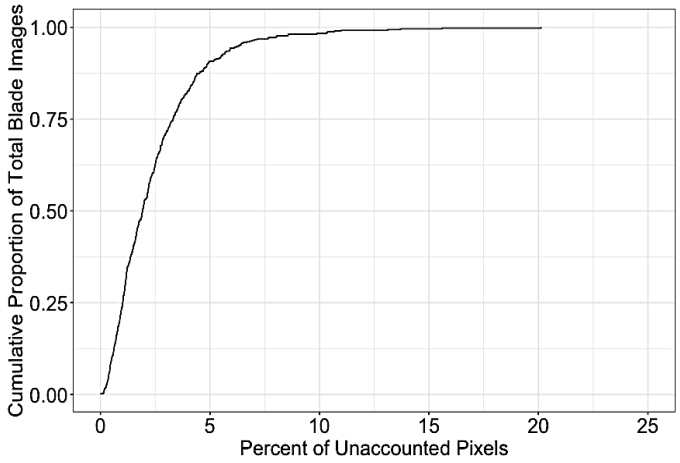

Figure 21. Cumulative distribution of unaccounted pixels. (n = 479)

3.2.3 "Extrinsic validation": Comparative metrics for seagrass

Manually measured leaf length and area, and epiphyte-free leaf biomass were tested for correlation with image-derived seagrass leaf area (total leaf pixels). There were strong linear relationships between the manual measurements and the imaged seagrass leaf area (R^2 = 0.98; Figure 22) and between leaf length and imaged leaf area (R^2 = 0.86; Figure 22). The relationship

between dried leaf biomass and imaged leaf area was also strong (R^2 = 0.88; Figure 22). These strong correlations support use of imaging in seagrass monitoring.

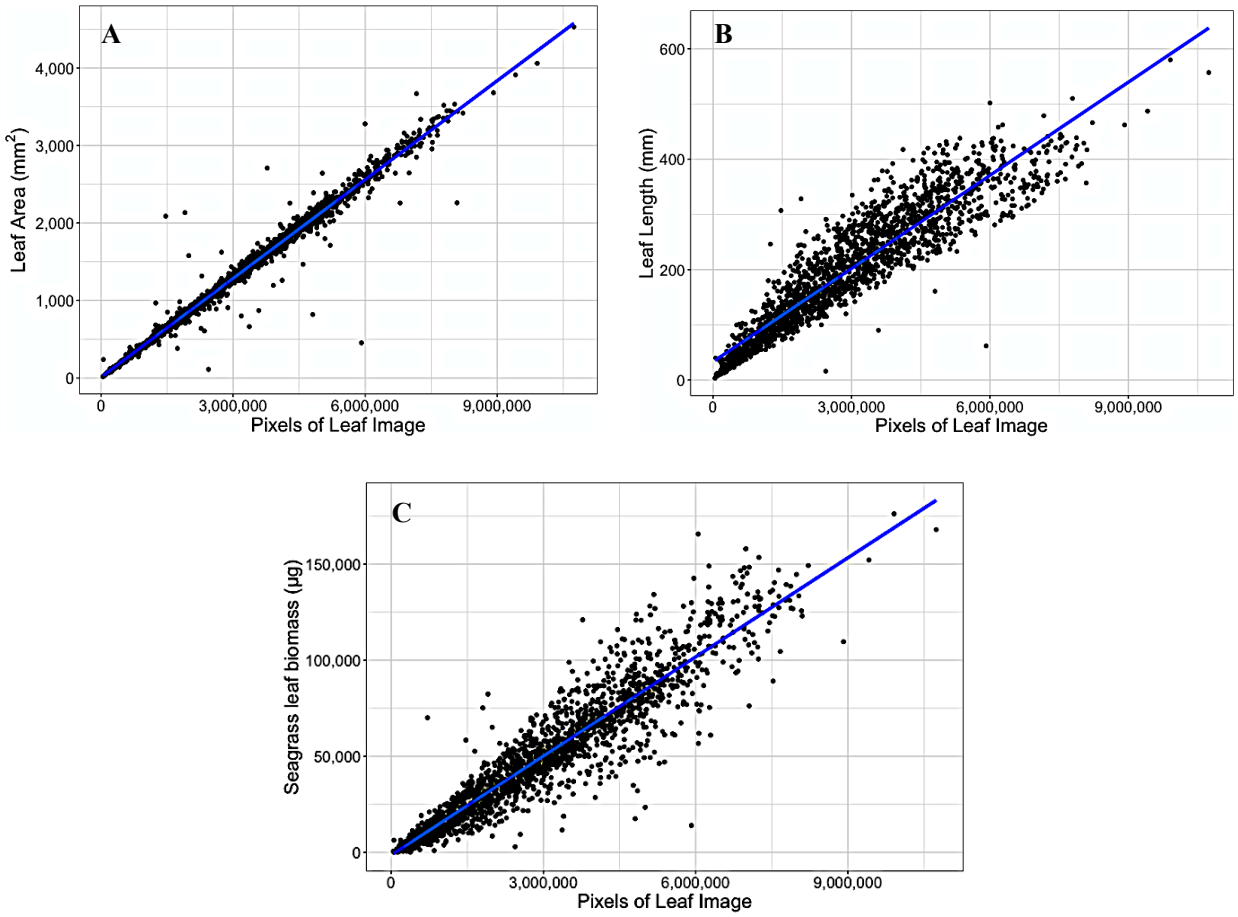

Figure 22. The relationships between manually measured seagrass leaf morphometrics and the number of leaf-image pixels: A) the manual leaf area and leaf-image pixels, the best fit regression: Manual leaf area = 0.42 × 10^{-3} Total number of image pixels + 11.8 (R^2 = 0.98, P < 0.0001, n = 2052); B) the manual length of seagrass leaf and leaf-image pixels, the best fit regression: Leaf length = 5.63 ×10^{-3} Total number of image pixels + 33.21 (R^2 = 0.86, P < 0.0001, n = 2053); and C) leaf biomass and leaf-image pixels, the best fit regression: Leaf biomass = 17.20 × 10^{-3} Total number of image pixels – 1449 (R^2 = 0.88, P < 0.0001, n = 2048).

3.2.4 "Extrinsic validation": Comparative metrics for epiphyte accumulation

The dried biomass of epiphyte per seagrass leaf was correlated with image-derived epiphyte identification by epiphyte spectral libraries. The correlation of epiphyte biomass to the total number of identified epiphyte pixels was moderate (R^2 = 0.61; Figure 23). However, analysis of

the data by environmental context (sampling locations and seasons) improved the correlations markedly (Table 3) and revealed unique **patterns** of accumulation. The proportion of variation explained by linear regression ranged from 0.67 to 0.94, but there was a marked and consistent increase in the slope of the regression line, from all sampling areas (environmental contexts), with seasonal progression from summer through winter (Table 3). This slope provides an indicator of the seasonally changing relationship between epiphyte biomass and epiphyte coverage of the leaf. As an example, linear regression of the data from the "Control" area, July 31, 2019, had an R^2 of 0.81 and a slope of 0.017, representing that there was 0.017 µg epiphyte biomass per identified epiphyte pixel. Epiphyte accumulation gradually increased to 0.0559 µg per epiphyte pixel through winter into spring (Table 3). Similarly, epiphyte accumulation in the "WWTP" area increased from 0.014 µg to 0.033 µg over the same period (but with a peak at 0.0675 µg in February), and at CI epiphytes increased from 0.024 µg to 0.0434 µg over the same period (but with a peak at 0.0709 µg in February). These observations are indicative of an increased "thickness" and/or density of the epiphyte biofilm, and a seasonal pattern that could result from changes in the community composition and/or growth rate of the epiphytes, as previously observed (Corlett & Jones 2007, Giovannetti et al. 2010).

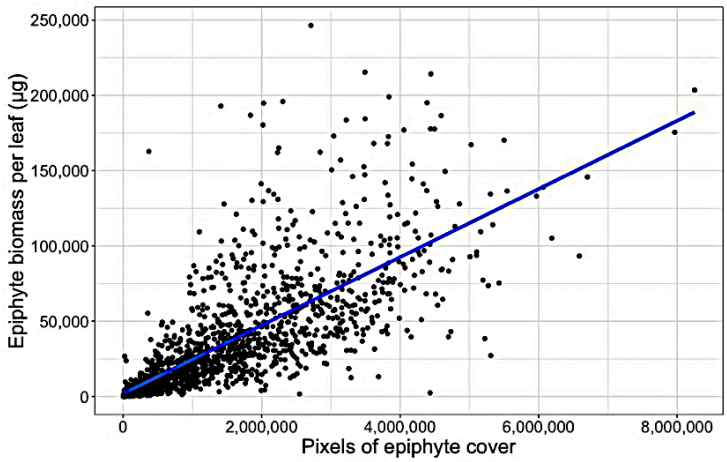

Figure 23. The relationship between epiphyte biomass per leaf (µg) and the epiphyte covered area counted by the number of identified epiphyte pixels. The best fit regression: Epiphyte biomass per leaf = 22.70 × 10^{-3} Pixels of epiphyte cover +1902 (R^2 = 0.61, P < 0.0001, n = 1915).

Table 4. Slope of regression of epiphyte accumulation on epiphyte covered area for "Control" area, "WWTP" area, and CI site. The epiphyte biomass per identified epiphyte pixel was determined by the slope of linear regression. R^2 for the linear regressions are given in parentheses

Sampling Date	"Control" area	CI Site	"WWTP" area
07-31-2019	0.0170 (R^2 = 0.81)	0.0240 (R^2 = 0.70)	
08-09-2019			0.0140 (R^2 = 0.73)
08-30-2019	0.0253 (R^2 = 0.87)	0.0259 (R^2 = 0.86)	
09-11-2019			0.0178 (R^2 = 0.76)
09-25-2019	0.0242 (R^2 = 0.91)	0.0378 (R^2 = 0.87)	
10-09-2019			0.01534 (R^2 = 0.86)
11-20-2019	0.0275 (R^2 = 0.88)	0.0437 (R^2 = 0.95)	
12-18-2019			0.0311 (R^2 = 0.73)
01-17-2020	0.0318 (R^2 = 0.68)	0.0709 (R^2 = 0.86)	
02-22-2020			0.0675 (R^2 = 0.87)
04-19-2020			0.0332 (R^2 = 0.71)
04-30-2020	0.0559 (R^2 = 0.67)	0.0434 (R^2 = 0.84)	

3.2.5 "Extrinsic validation": Comparative metrics for seagrass-epiphyte correlations

Expression of epiphyte metrics relative to the host seagrass leaves is another approach to represent the epiphyte-seagrass dynamic relationship. The epiphyte load (epiphyte biomass/ seagrass biomass) (Fong & Harwell 1994) and the image-derived % cover of leaf by epiphyte

(epiphyte coverage; see Eq.2, Materials and Methods) were correlated and revealed seasonal changes in the seagrass-epiphyte relationship. Regression analyses, including the linear model, quadratic model, power law model, and the exponential model, were used to quantify this relationship based on the scatter plot of epiphyte load (epiphyte biomass / leaf biomass) *vs.* epiphyte coverage (Figure 24). The best model was then selected, given the goodness of fit and the intrinsic biological meaning (Johnson & Omland 2004). Based on the Akaike Information Criterion correction (AICc), there was no significant difference in these four models. The simplest linear model, therefore, was selected to describe the relationship for the overall data.

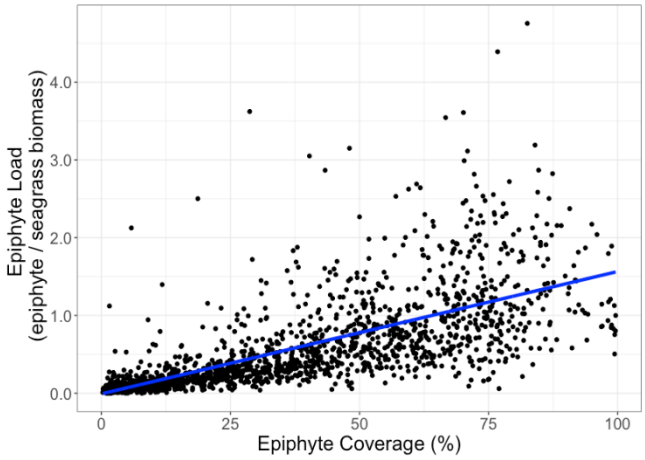

Figure 24. The relationship between epiphyte load and epiphyte coverage (%) classified by epiphyte spectral library. Epiphyte load is calculated by dividing the epiphyte dry biomass by seagrass leaf biomass. The best regression equation: Epiphyte load = 15.70×10^{-3} Epiphyte coverage (%) – 0.07 *(*R^2 = 0.52*,* $P < 0.0001$*,* n = 1817).

Epiphyte load was moderately correlated with epiphyte coverage (R^2 = 0.52, $P < 0.0001$, n = 1817). The high degree of variance in epiphyte measures may be due to environmental factors changing the relationship between the two measures. The potential regression models above were applied for the "Control", "WWTP", and CI sampling locations across six sampling times. Two scenarios emerged to describe the relationship between epiphyte load (Y) and epiphyte

coverage (X) after separating the data. For example, the analyses of this relationship in the "WWTP" area showed a strong linear regression from August through December. However, the exponential-rise model was the best-fitted model in February and April 2020 based on the AICc (Figure 25). The fitted exponential model indicates a strong and significant tendency for the accumulation of epiphyte biomass to increase much faster than the expansion of epiphyte coverage in the "WWTP" area during winter and spring. The change in the nature of the relationship between epiphyte load and epiphyte coverage are attributed to two types of epiphyte-seagrass dynamics under different seasonal conditions. As leaves grow, primary colonization by epiphytes gradually develop in a linear relationship with the available leaf space. In other work (Bulthuis & Woelkerling 1983, Corlett & Jones 2007, Saha et al. 2019), early epiphytes such as diatoms and coralline red algae species formed the primary colonizing layers and eventually covered most of the blade surfaces. On older leaves where growth has slowed, stopped or even reversed (senescence), epiphytic biomass continues to accumulate via secondary colonization and growth contributed by filamentous algae and epiphytic animals, while the primary coralline algae eventually die (Humm 1964, Borum 1987, Michael et al. 2008). This phase represents the departure from a linear relationship.

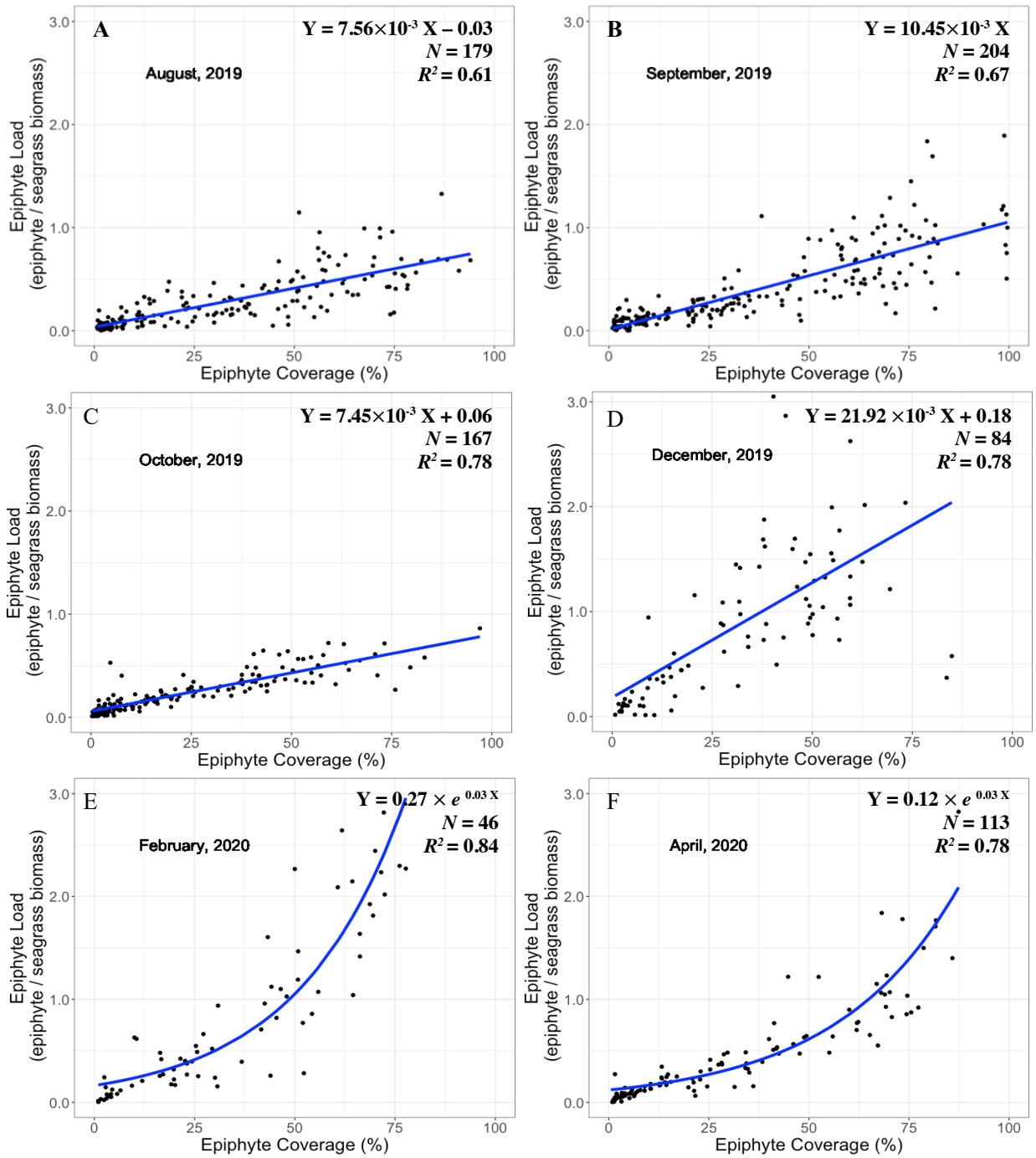

Figure 25. Result from accumulation scenario 1 and 2 in "WWTP" area. Graphs A-F showed the best fitted regression of the relationship between epiphyte load and epiphyte coverage from August 2019 to April 2020.

In the first accumulation scenario (typical of most samples from August – December), the strong linear relationship between epiphyte load and epiphyte coverage implied that primary epiphyte

colonization on the available seagrass leaf surface was dominant due to growth of new leaf surface. This relationship held under most environmental circumstances, except August samplings from “Control” and CI; and April sampling from “WWTP” and CI (Figures 25, 26, and 27). Different slope values revealed different accumulation rates of epiphyte biomass relative to epiphyte coverage. The slopes of this relationship varied from 0.75 to 3.43, with a progressive increase from August to December, and with the highest values observed during winter or spring, when the coolest observed water temperatures prevailed. This increasing accumulation pattern is consistent with the slopes of regression of epiphyte accumulation on epiphyte covered area in Table 3.

The second scenario of accumulation, where epiphyte load increased more rapidly relative to a smaller increase or saturation of epiphyte coverage, was best described by the fitted exponential regression model. In the “Control” area and CI site, the second scenario was generated during August (Figures 26 and 27), and it also presented at the “WWTP” area and CI site during April 2020 (Figures 25 and 27). Although the comparison of epiphyte load and epiphyte coverage revealed two types of epiphyte-seagrass dynamics, the relatively higher degree of identification error could possibly have contributed to the deviation from a linear relationship between epiphyte load and epiphyte coverage of data from April. For example, the misclassification of green algae and seagrass might decrease the estimation of epiphyte coverage so that the corresponding epiphyte load would present a higher relative accumulation than the epiphyte coverage in the scatter plots. The importance of an accurate characterization of the epiphyte community is evident.

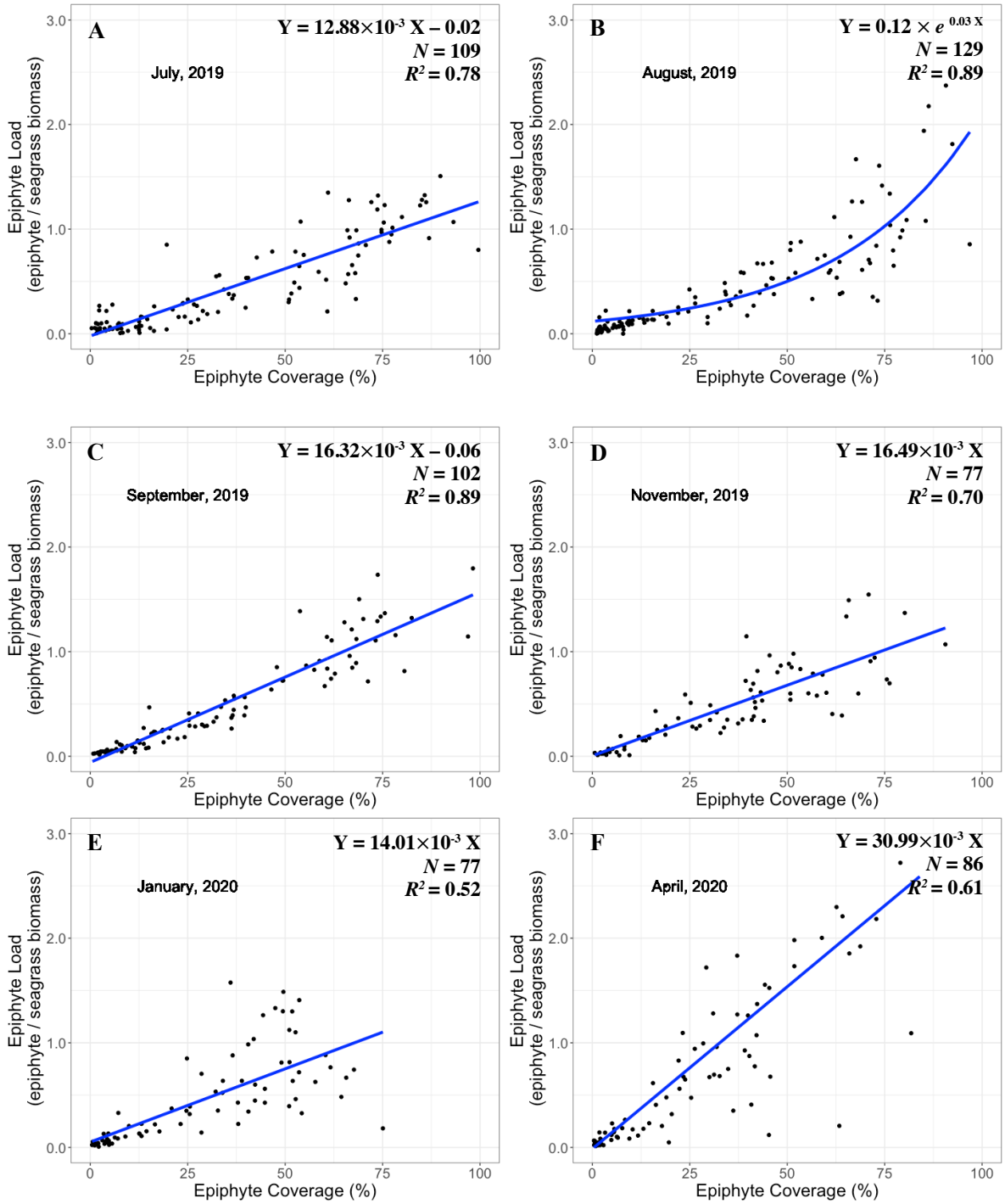

Figure 26. Result from accumulation scenario 1 and 2 in "Control" area. Graphs A-F showed the best fitted regression of the relationship between epiphyte load and epiphyte coverage from July 2019 to April 2020.

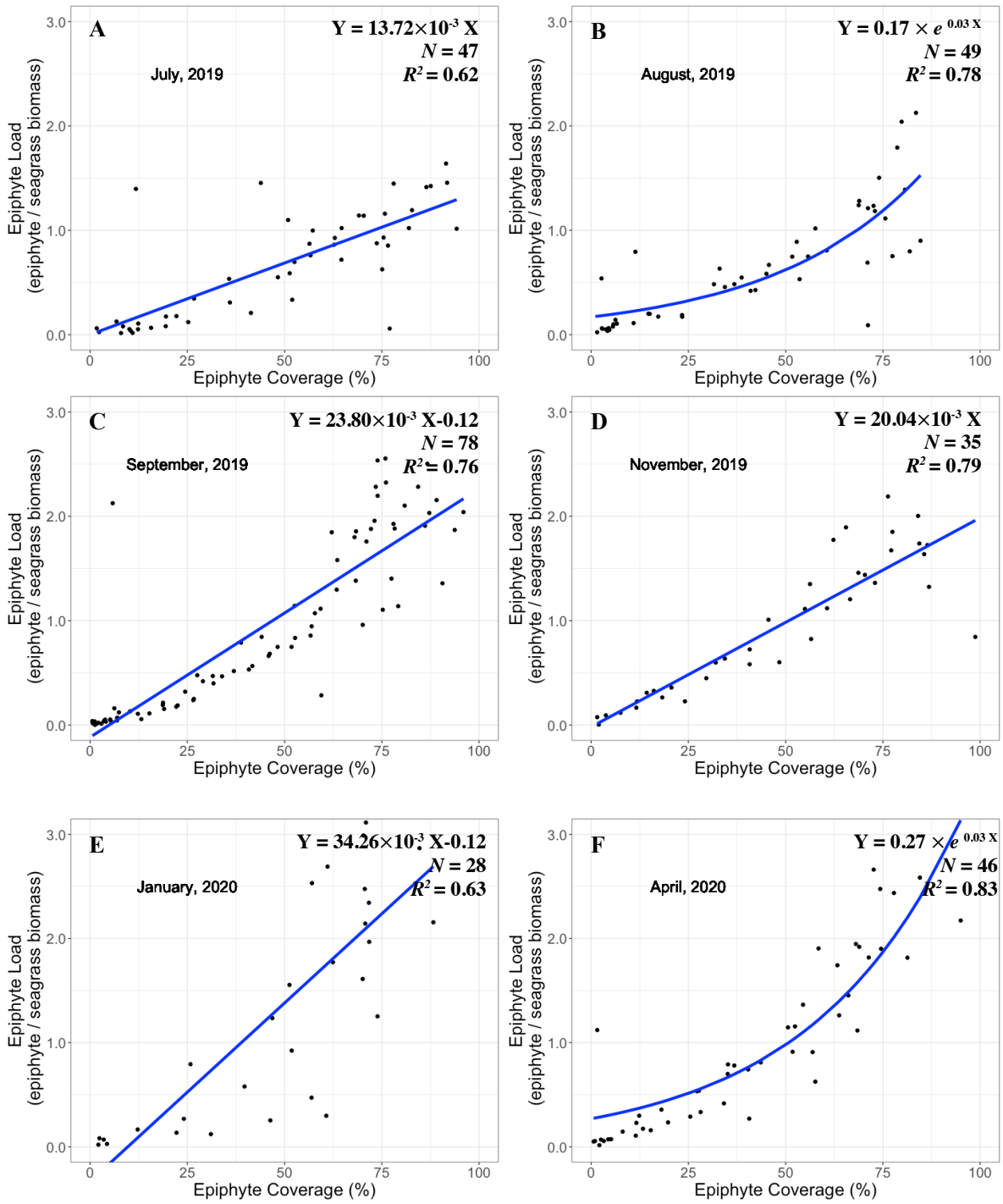

Figure 27. Result from accumulation scenario 1 and 2 at CI site. Graphs A-F showed the best fitted regression of the relationship between epiphyte load and epiphyte coverage from July 2019 to April 2020.

3.3 Spatial and temporal effects on seagrass growth and epiphyte accumulation patterns

As further validation of the utility of imaging-derived metrics, it is important to compare their ability to detect seasonal or environmental patterns of variation in the seagrass community. This section presents spatial-temporal patterns of imaging and biomass metrics used to monitor the seagrass growth and epiphyte accumulation.

Seagrass leaf biomass and imaged seagrass leaf area presented overall similar seasonal patterns in general, where the high levels in summer declined from Autumn through Winter (Figures 28 and 29). However, close inspection shows that the leaf biomass at "Control" increased significantly in September ($df = 5$, $F = 10.34$, $P < 0.05$), but that significant increases were not observed during this period with the imaged leaf area, nor for the other sampling locations. In April, the leaf biomass ($df = 5$, $F = 18.44$, $P < 0.05$) and imaged leaf area ($df = 5$, $F = 18.14$, $P < 0.05$) returned to higher levels in the "WWTP" area only. The leaf biomass did not change significantly relative to the winter month of January in the "Control" area and the CI site.

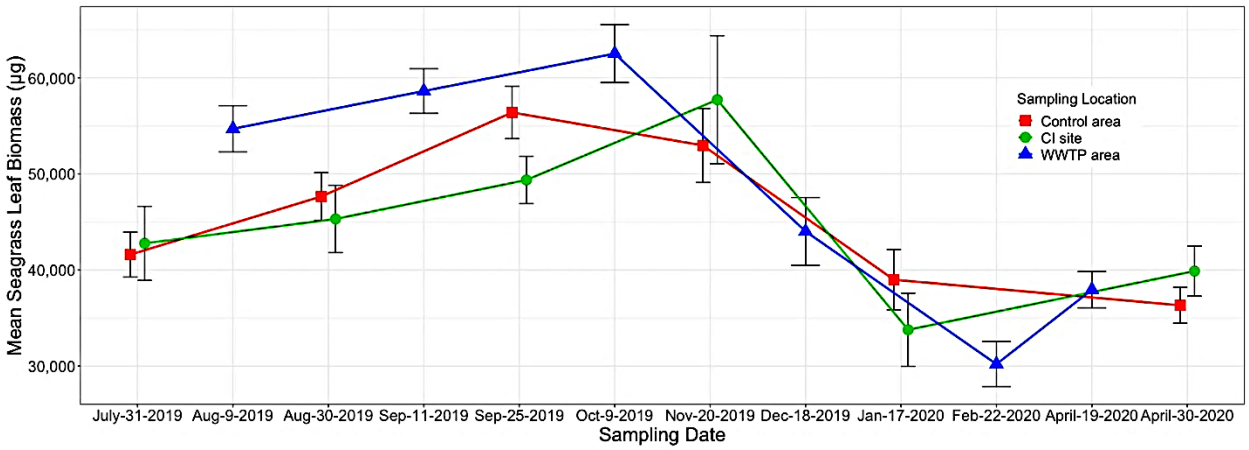

Figure 28. Changes in average seagrass leaf biomass (±SE) in three sampling locations from July 2019 to April 2020. (n = 2062)

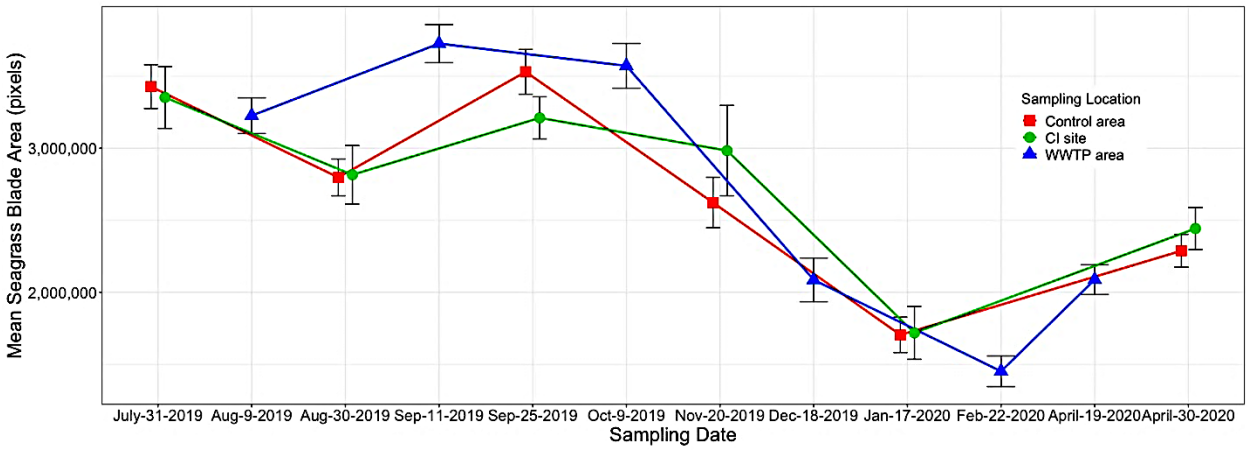

Figure 29. Changes in average seagrass blade area (±SE) in three sampling locations from July 2019 to April 2020. (n = 2055)

Epiphyte loads (epiphyte biomass relative to seagrass biomass) presented an inverse temporal pattern compared to seagrass growth. Epiphyte loads increased significantly from autumn through winter (Figures 30 and 31) for "WWTP" area ($df = 5$, $F = 36.74$, $P < 0.05$) and CI site ($df = 5$, $F = 4.39$, $P < 0.05$), but not for "Control", which only exhibited an increase in the April data. After winter, the epiphyte loads dropped significantly for "WWTP" area and CI site. In contrast to the biomass data, the imaged epiphyte coverage metric did not exhibit the same pronounced seasonal patterns. Epiphyte coverage among the three locations was generally stable across the sampling periods, except for a significant decrease observed only for October in the "WWTP" area. This difference may be informative for understanding the seagrass-epiphyte relationship. However, the biomass and imaged epiphyte coverage indicators both showed that the epiphyte accumulation at the CI site was highest among the three sampling locations. The mean epiphyte loads were 0.63 ~ 1.35 at the CI site and 0.25 ~ 0.75 at the "Control" and "WWTP" areas. The mean epiphyte coverages were 35.38% ~ 46.16% at the CI site and 21.14% ~ 35.01% in the "Control" and "WWTP" areas.

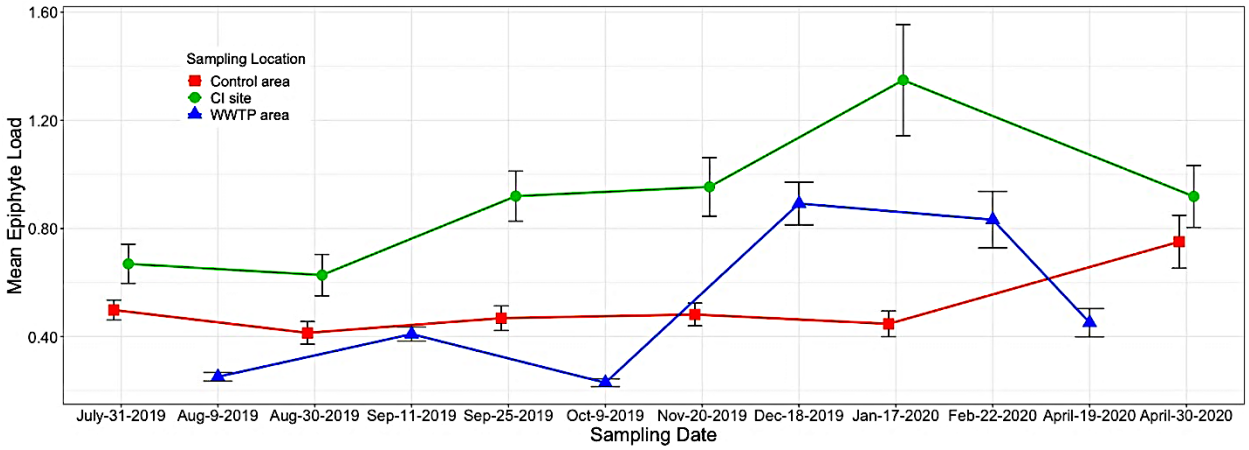

Figure 30. Changes in average epiphyte load (±SE) in three sampling locations from July 2019 to April 2020. (n = 1833)

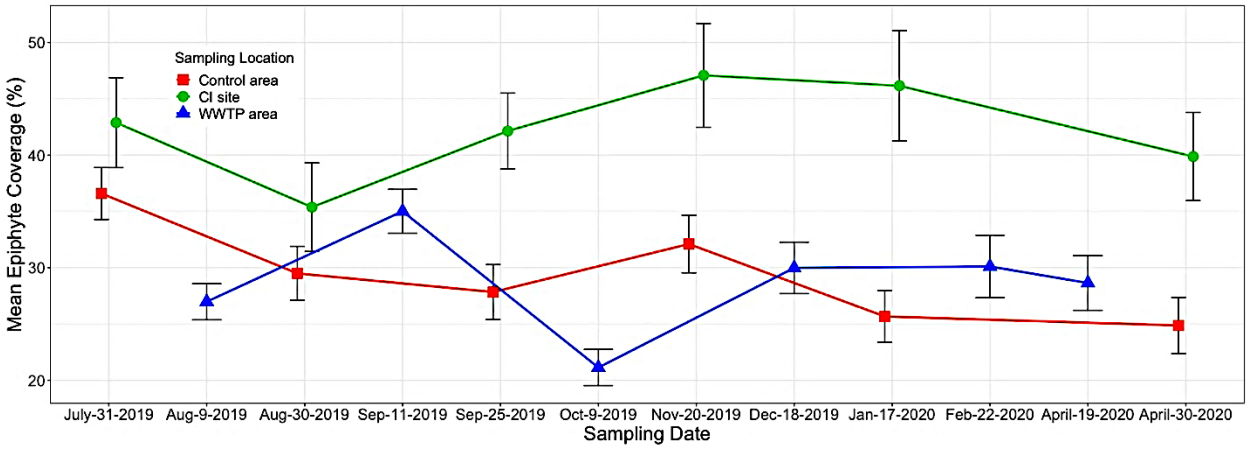

Figure 31. Changes in average epiphyte coverage (±SE) in three sampling locations from July 2019 to April 2020. (n = 2001)

The different sampling times in the "Control" area, "WWTP" area, and CI site precluded the use of ANOVA for statistical comparisons between sampling locations across six sampling times. Instead, data were reallocated to four seasons based on the sampling date and average temperature (Table 5) to facilitate environmental comparisons.

Table 5. Season data for locations-times two-way ANOVA designated by sampling date and corresponding water temperature. Values of water temperature are means (± SE).

Sampling Location	Season	Sampling Date	Mean Water Temperature (℃)
"Control" area and CI site	2019 Summer	2019-07-31	31.47 (± 0.42)
"WWTP" area	2019 Summer	2019-08-09	29.57 (± 0.68)
"Control" area and CI site	2019 Autumn	2019-08-30	30.92 (± 0.68)
"WWTP" area	2019 Autumn	2019-09-11	30.27 (± 0.25)
"Control" area and CI site	2019 Autumn	2019-09-25	31.40 (± 0.50)
"WWTP" area	2019 Autumn	2019-10-09	29.31 (± 0.24)
"Control" area and CI site	2019 Winter	2019-11-20	22.13 (± 0.22)
"WWTP" area	2019 Winter	2019-12-18	16.27 (± 0.44)
"Control" area and CI site	2019 Winter	2020-01-17	23.00 (± 0.00)
"WWTP" area	2019 Winter	2020-02-22	17.57 (± 0.41)
"Control" area and CI site	2020 Spring	2020-04-30	24.37 (± 0.48)
"WWTP" area	2020 Spring	2020-04-19	23.00 (± 0.00)

3.3.1 Seagrass response to variable environments by seasons

There were no significant differences in the seagrass leaf biomass and blade area between the "Control" area and the CI site from summer to spring (Table 6). The mean leaf biomass across the sampling periods was 36.32 ~ 51.54 $\times 10^3$ μg in the "Control" area and 39.88 ~ 47.69 $\times 10^3$ μg at the CI site (Table 6). The leaf biomass in the WWTP area was significantly higher than the "Control" area and the CI site in the summer ($df = 2$, $F = 8.10$, $P < 0.05$) and autumn ($df = 2$, $F = 10.06$, $P < 0.05$), but it decreased strikingly and exhibited significantly lower value than the other two locations in the winter ($df = 2$, $F = 3.40$, $P < 0.05$) (Figure 32). The mean leaf biomass in the "WWTP" area was 38.05 ($\pm$31.75) $\times 10^3$ μg (Table 7). In the spring, there was no significant difference in the leaf biomass among the three locations.

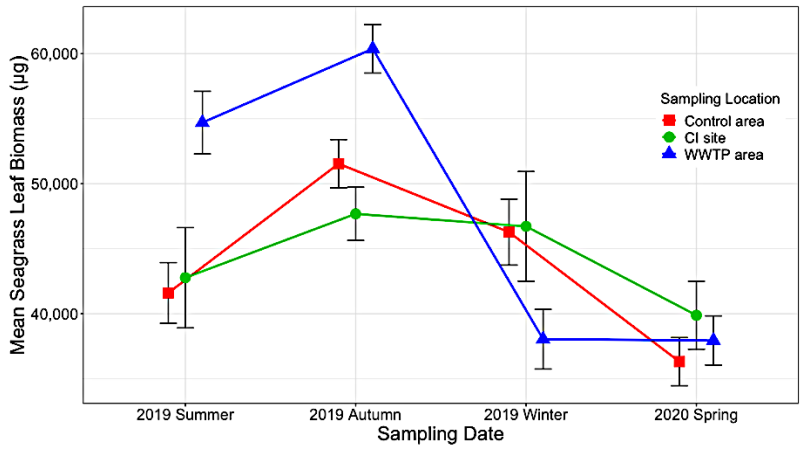

Figure 32. Changes in average seagrass leaf biomass (±SE) between three sampling locations from summer to spring. (n = 2062)

Table 6. Two-way ANOVA for *Thalassia testudin*um leaf biomass (*µ*g) and blade area (pixels), epiphyte load, and epiphyte coverage (%) variables. Independent variables are *T. testudinum* sampling season and sampling locations. *df* = degrees of freedom. Values significant at the 0.05 level are shown in bold.

Source	*df*	*F*	*P*
A. Seagrass leaf biomass			
Location	2	0.16	0.86
Season	3	29.32	**< 0.0001**
Location × Season	6	7.79	**< 0.0001**
B. Seagrass blade area			
Location	2	0.49	0.62
Season	3	86.42	**< 0.0001**
Location × Season	6	5.13	**< 0.0001**
C. Epiphyte load			
Location	2	45.55	**< 0.0001**
Season	3	35.24	**< 0.0001**
Location × Season	6	12.79	**< 0.0001**
D. Epiphyte coverage			
Location	2	23.49	**<.0001**
Season	3	1.45	0.22
Location × Season	6	2.42	**0.02**

The blade area also did not exhibit a significant difference between the "Control" area and the CI site from summer to spring (Table 6). In the "Control" area ($df = 3$, $F = 5.95$, $P < 0.05$) and the CI site ($df = 3$, $F = 16.50$, $P < 0.05$), the blade areas were both significantly higher in the summer and autumn than in the winter and spring (Figure 33). The mean blade areas were $3.044 \times 10^6 \sim 3.428 \times 10^6$ pixels in summer and autumn and $2.176 \times 10^6 \sim 2.443 \times 10^6$ pixels in winter and spring. The blade area from the "WWTP" area was significantly higher than from the "Control" area and the CI site in the autumn ($df = 3$, $F = 11.60$, $P < 0.05$). A decreasing average blade area from the "WWTP" area was observed in the winter, and the blade area was significantly lower than from the other two locations. The blade area in the "WWTP" area increased again in the spring, in which there was no significant difference in the blade area among the three locations. Generally, the seasonal changes of leaf biomass and blade area among three uniquely environmental conditions were similar, with high values in summer and autumn and significantly decreased in winter (Table 7).

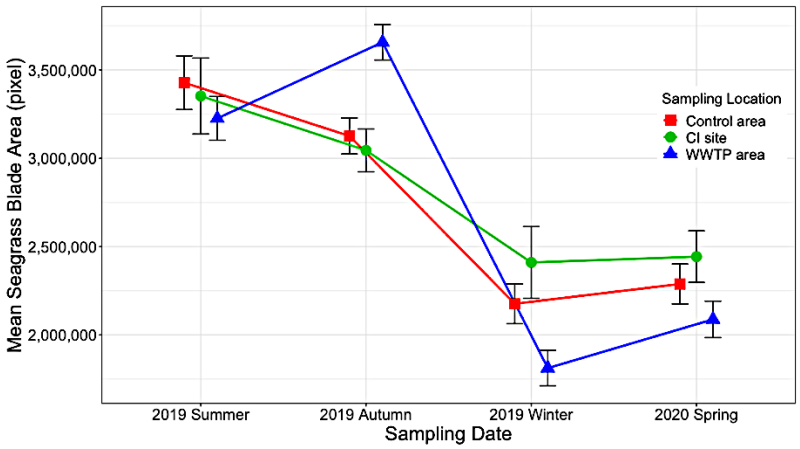

Figure 33. Changes in average seagrass blade area (±SE) between three sampling locations from summer to spring. (n = 2055)

Table 7. Comparison of *Thalassia testudinum* leaf biomass (μg), blade area (pixels), epiphyte load, and epiphyte coverage (%) in the three sampling locations from July to April. Values are means of measurements (± SE) from sites of CS, CD, CI, WS, WM, and WD, respectively.

Location	Season	*n*	Mean Leaf Biomass ($\times 10^3$ μg)	*n*	Mean Blade Area ($\times 10^5$ pixels)	*n*	Mean Epiphyte Load	*n*	Mean Epiphyte Coverage (%)
Control	2019 Summer	169	41.60 (± 2.33)	169	34.28 (± 1.52)	161	0.50 (± 0.04)	173	36.60 (± 2.31)
CI	2019 Summer	57	42.77 (± 3.86)	57	33.52 (± 2.15)	50	0.67 (± 0.07)	57	42.89 (± 3.99)
WWTP	2019 Summer	273	54.70 (± 2.70)	273	32.26 (± 1.24)	240	0.25 (± 0.02)	269	26.98 (± 1.60)
Control	2019 Autumn	271	51.54 (± 1.85)	271	31.26 (± 1.02)	235	0.44 (± 0.03)	266	28.74 (± 1.71)
CI	2019 Autumn	143	47.69 (± 2.04)	143	30.45 (± 1.21)	131	0.81 (± 0.06)	142	39.33 (± 2.57)
WWTP	2019 Autumn	414	60.38 (± 1.87)	414	36.57 (± 1.01)	376	0.33 (± 0.02)	413	28.76 (± 2.31)
Control	2019 Winter	184	46.28 (± 2.54)	184	21.76 (± 1.12)	158	0.46 (± 0.03)	177	28.87 (± 1.73)
CI	2019 Winter	75	46.72 (± 4.22)	75	24.10 (± 2.03)	67	1.13 (± 0.11)	72	42.67 (± 3.34)
WWTP	2019 Winter	192	38.05 (± 2.29)	192	18.12 (± 1.00)	158	0.86 (± 0.06)	175	30.04 (±1.77)
Control	2020 Spring	91	36.32 (± 2.33)	91	22.88 (± 1.13)	89	0.75 (± 0.03)	88	24.87 (± 2.50)
CI	2020 Spring	54	39.89 (± 2.61)	54	24.43 (± 1.46)	49	0.92 (± 0.06)	49	39.87 (± 3.91)
WWTP	2020 Spring	132	37.95 (± 1.89)	132	20.88 (± 1.19)	119	0.45 (± 0.05)	120	38.64 (± 2.42)

3.3.2 Epiphyte accumulation on seagrass leaf by seasons

Observations for seasonally aggregated epiphyte data are consistent with those for monthly data in Figures 30 and 31. There were significant effects of sampling locations on the epiphyte load (mean from the "Control" area = 0.50 (± 0.02); mean from the CI site = 0.87 (± 0.04); mean from the "WWTP" area = 0.42 (± 0.02); Table 6). Epiphyte loads at the CI site were significantly higher than at the "Control" area and "WWTP" area ($df = 2$, $F = 70.64$, $P < 0.05$). Opposite to the seagrass growth pattern, the epiphyte load pattern increased significantly ($df = 2$, $F = 25.89$, $P < 0.05$) in the winter (Figure 34), except for the "Control" area, where epiphyte load

did not change significantly, but was highest in the spring. On the contrary, the epiphyte load in the "WWTP" area decreased and was significantly lower than the other two locations in the spring ($df = 2$, $F = 8.03$, $P < 0.05$). Overall, epiphyte loads exhibited seasonal changes inverse to those of seagrass growth, but CI site always had the greatest, and the "WWTP" area had the lowest epiphyte value except in the winter.

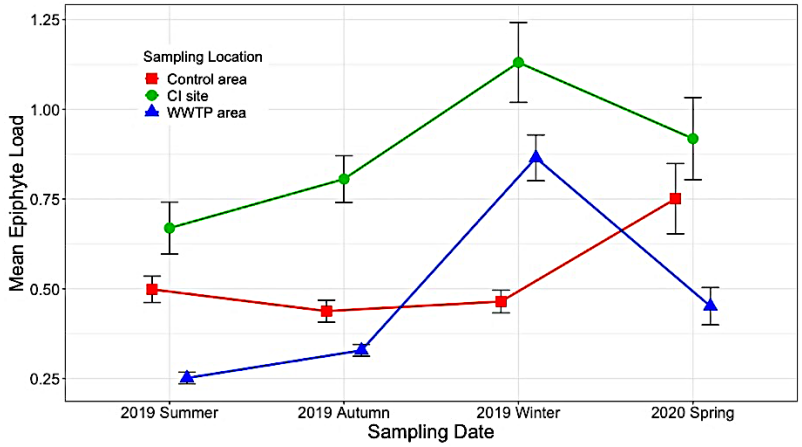

Figure 34. Changes in average epiphyte load (±SE) between three sampling locations from summer to spring. (n = 1833)

Epiphyte coverage did not have a significant seasonal change (Figure 35) but was affected by the environments of the three sampling locations (Table 6). Across sampling periods, epiphyte coverage was highest at the CI site, with mean values at the "Control" area, CI site, and "WWTP" area of 30.22%, 41.70%, and 28.49%. Although the epiphyte coverage in the "Control" area was significantly higher than in the "WWTP" area in the summer ($df = 2$, $F = 10.21$, $P < 0.05$), there was no significant difference in epiphyte coverage from autumn to spring. Even though the seasonal pattern of epiphyte coverage was not similar to that for epiphyte load, these two indicators both ordinated the CI site as highest across all seasons (Figure 35, Table 7).

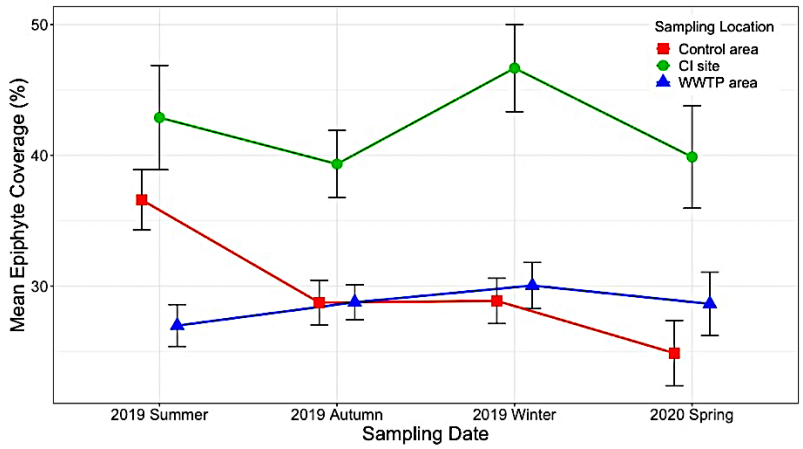

Figure 35. Changes in average epiphyte coverage (±SE) between three sampling locations from 2019 summer to 2020 spring. (n = 2001)

3.3.3 Spatial and temporal effects on epiphyte-seagrass dynamics

In the analysis of MODREG, the influence of environmental conditions at three locations on epiphyte-seagrass dynamics was assessed by comparing the linear regression of epiphyte biomass on associated leaf biomass in the "Control" area, "WWTP" area, and CI site in specific seasons (Table 8). Simultaneous 95% confidence intervals around the differences of potential epiphyte biomass among three sampling locations were calculated at different values of seagrass leaf biomass. Comparisons of the epiphyte biomass derived from the linear regressions in the summer showed no significant difference in epiphyte biomass on young seagrass leaf between different locations. However, MODREG found leaf biomass thresholds, above which epiphyte biomass accumulations would differ significantly, as follows. For summer. the epiphyte biomass at CI site was significantly greater than at "Control" and "WWTP" areas for leaf biomass greater than 50×10^3 μg and 26×10^3 μg, respectively. The "Control" area also had significantly higher epiphyte biomass than the "WWTP" area for leaf biomass > 28×10^3 μg. Similarly, the linear regressions of epiphyte-seagrass dynamics for each sampling season were compared between locations (Table 8). For Autumn, epiphyte biomass on individual seagrass leaves at the CI site

was greater than at the "Control" (> 40×10^3 μg leaf biomass) and "WWTP" areas (> 32×10^3 μg leaf biomass), and the "Control" was also significantly higher than at the "WWTP" area for leaf biomass > 62×10^3 μg. During winter months, the epiphyte biomass accumulation was still highest at the CI site for leaf biomass greater than 26×10^3 μg. There was no significant difference between the "Control" area and the "WWTP" area. However, during the spring, epiphytes at the "Control" area were higher than at the "WWTP" area for leaf biomass > 38×10^3 µg. Across the seasons, analyses of MODREG showed the "estimated" epiphyte accumulation with seagrass growth was generally highest at the CI site and lowest in the "WWTP" area. The accumulation patterns were similar in younger leaves, but they varied in their thresholds at which there would be significant differences among locations.

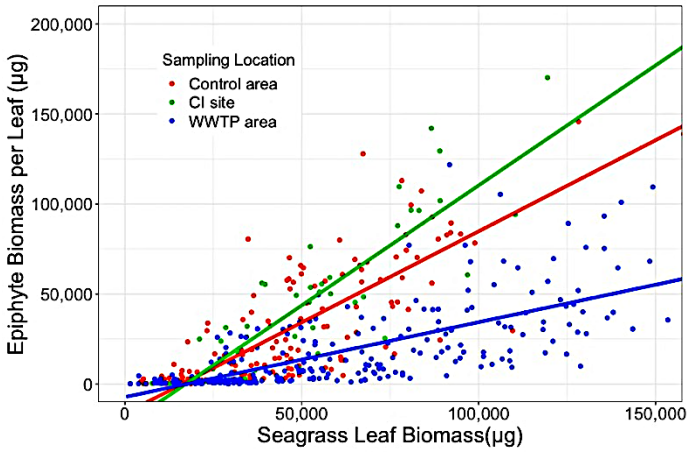

Figure 36. Relationships of epiphyte biomass accumulation on leaves of *Thalassia testudinum* among three sampling locations ("Control" area, CI site, and "WWTP" area) related to seagrass leaf biomass in summer.

Table 8. Analyses of MODREG for epiphyte biomass vs. seagrass leaf biomass. Independent variables are sampling locations ("Control" area, CI site, and "WWTP" area) and sampling seasons. Leaf biomass was a covariate in the analyses. *df* = degrees of freedom. The ranges of leaf biomass for which there were significant differences in epiphyte biomass between locations were calculated by the comparison of linear regressions as illustrated in Figure 36

Main effect and covariate	*df*	*F*	*P*	R^2
A. 2019 summer				0.67
Location	2	95.02	< 0.001	
Leaf biomass	1	540.92	< 0.001	
Location × Leaf biomass	2	81.69	< 0.001	
Comparison of sampling location. The ranges the leaf biomass for which there are significant differences in epiphyte biomass ($p<0.05$) are shown in parentheses:				
CI > "Control"	(> 50×10^3 μg)			
CI > "WWTP"	(> 30×10^3 μg)			
"Control" > "WWTP"	(> 28×10^3 μg)			
				0.34
B. 2019 autumn				
Location	2	55.41	< 0.001	
Leaf biomass	1	219.15	< 0.001	
Location × Leaf biomass	2	25.68	< 0.001	
Comparison of sampling location.				
CI > "Control"	(> 40×10^3 μg)			
CI > "WWTP"	(> 32×10^3 μg)			
"Control" > "WWTP"	(> 62×10^3 μg)			
				0.63
C. 2019 winter				
Location	2	63.66	< 0.001	
Leaf biomass	1	449.95	< 0.001	
Location × Leaf biomass	2	39.17	< 0.001	
Comparison of sampling location.				
CI > "Control"	(> 24×10^3 μg)			
CI > "WWTP"	(> 28×10^3 μg)			
"Control" = "WWTP"	($P > 0.05$)			
				0.27
D. 2020 spring				
Location	2	9.26	< 0.001	
Leaf biomass	1	60.16	< 0.001	
Location × Leaf biomass	2	7.05	0.001	
Comparison of sampling location.				
CI = "Control"	($P > 0.05$)			
CI > "WWTP"	(> 18×10^3 μg)			
"Control" > "WWTP"	(> 38×10^3 μg)			
Regression coefficient (SE)				
Location	2019 summer	2019 autumn	2020 winter	2020 spring
"Control"	1.012 (0.048)	0.567 (0.065)	0.667 (0.069)	1.434 (0.200)
CI	1.333 (0.107)	1.240 (0.127)	1.716 (0.121)	0.968 (0.342)
"WWTP"	0.416 (0.057)	0.414 (0.076)	0.861 (0.101)	0.513 (0.247)

3.3.4 Effect of site depth on seagrass and epiphyte growth

Seagrass leaf biomass and leaf area were compared between samples from different depths at the "Control" and "WWTP" areas (Figures 37). Different patterns with respect to shallow vs deep were observed in the "Control" and "WWTP" areas. Leaf biomass at the CS site was significantly higher than at the CD among sampling times (Figure 37; $df = 1, F = 6.93, P < 0.05$) with a mean difference in leaf biomass of $6.90 \pm 2.67 \times 10^3$ μg. Likewise, CS site also presented a significantly higher blade area than at CD site, with a mean difference of 305650 ± 119161 pixels (Figure 38; $df = 1, F = 4.09, P = 0.05$). Conversely however, there was significantly lower leaf biomass at WS site compared to both WM and the WD sites, with mean differences of 28.78 $\pm 2.75 \times 10^3$ μg and 21.86 $\pm 2.68 \times 10^3$ μg, respectively (Figure 37; $df = 2, F = 49.49, P < 0.05$). Leaf biomass at the WM site and the WD site did not show a significant difference. Spatiotemporal variation of the imaged blade area at "WWTP" area was generally similar to leaf biomass observations, being highest in summer and lowest in winter, and lowest for WS but highest for WM, which was significantly higher than for WD site (Figure 38; $df = 2, F = 44.19, P = 0.05$).

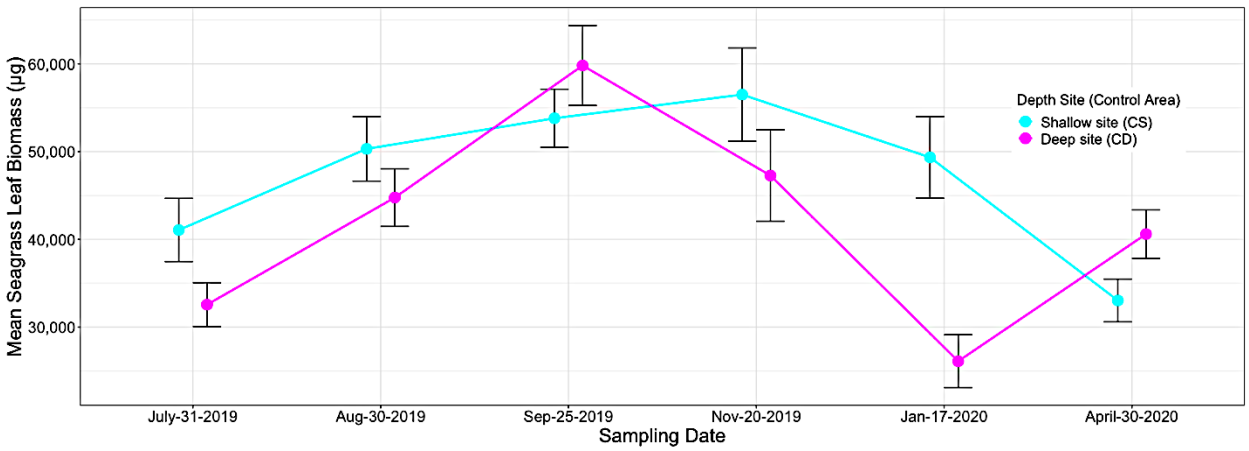

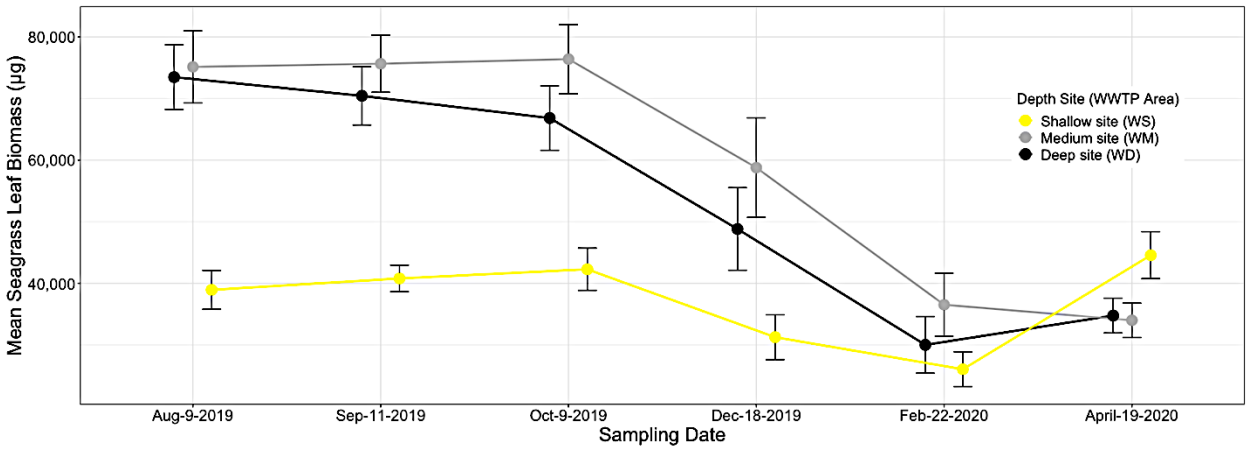

Figure 37. Changes in average seagrass leaf biomass (±SE) among depth sites from the "Control" area (first panel, n = 675) and the "WWTP" area (second panel, n = 932) from July to April.

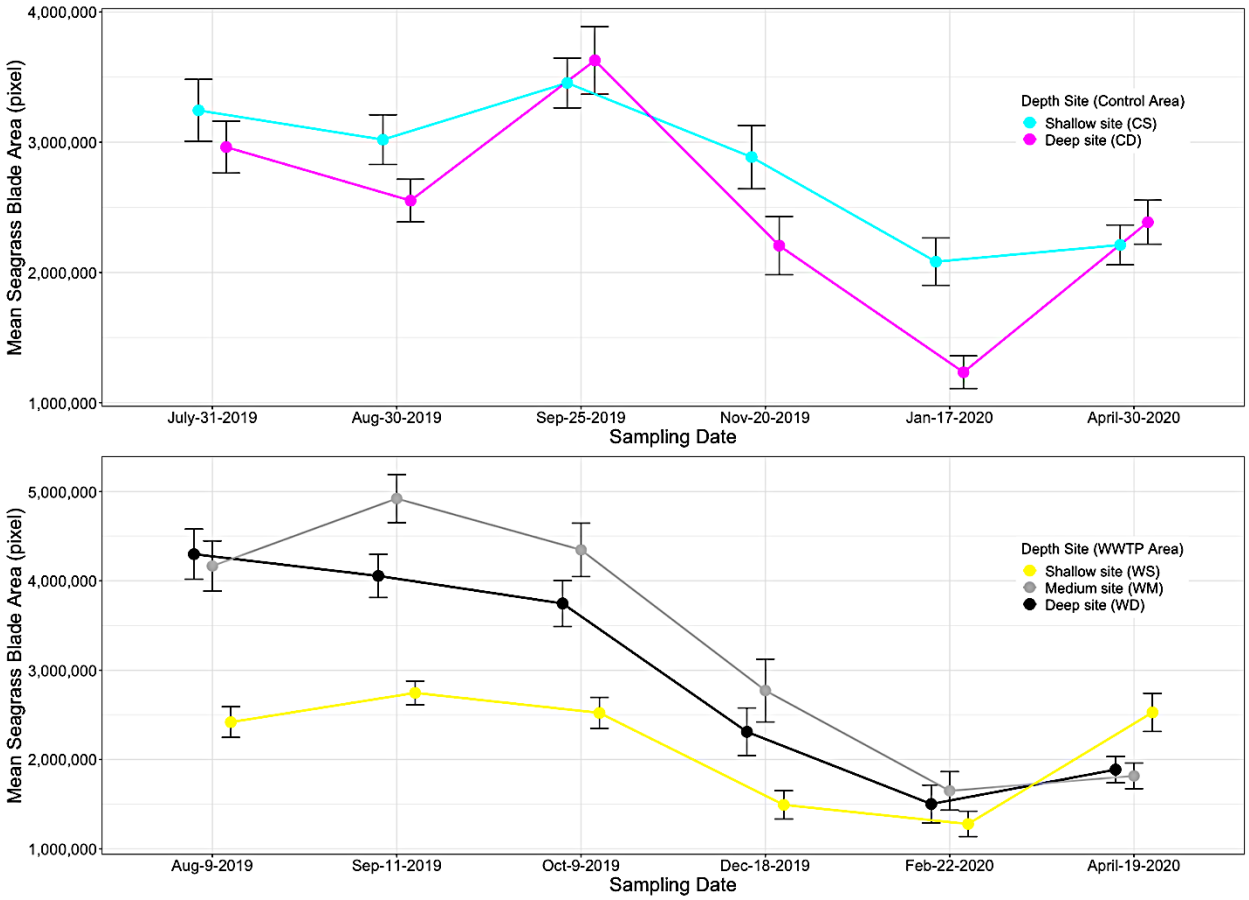

Figure 38. Changes in average seagrass blade area (±SE) among depth sites from the "Control" area (first panel, n = 675) and the "WWTP" area (second panel, n = 932) from July to April.

Epiphyte loads in the "Control" area showed a statistical difference with depth, but only in winter and spring, where CS site was significantly lower than at CD site (Figure 39; df = 1, F = 13.17, $P < 0.05$). On the contrary, the "WWTP" area did not show a significant depth difference in epiphyte load, except in February, when the WM site had a dramatically lower epiphyte load than WS and WD (Figure 39). Across the sampling period, imaged epiphyte coverage exhibited similar patterns from shallow to deep regions in either the "Control" area or the "WWTP" area (Figure 40). Epiphyte load and epiphyte coverage were not affected significantly by different water depths in the "WWTP" area.

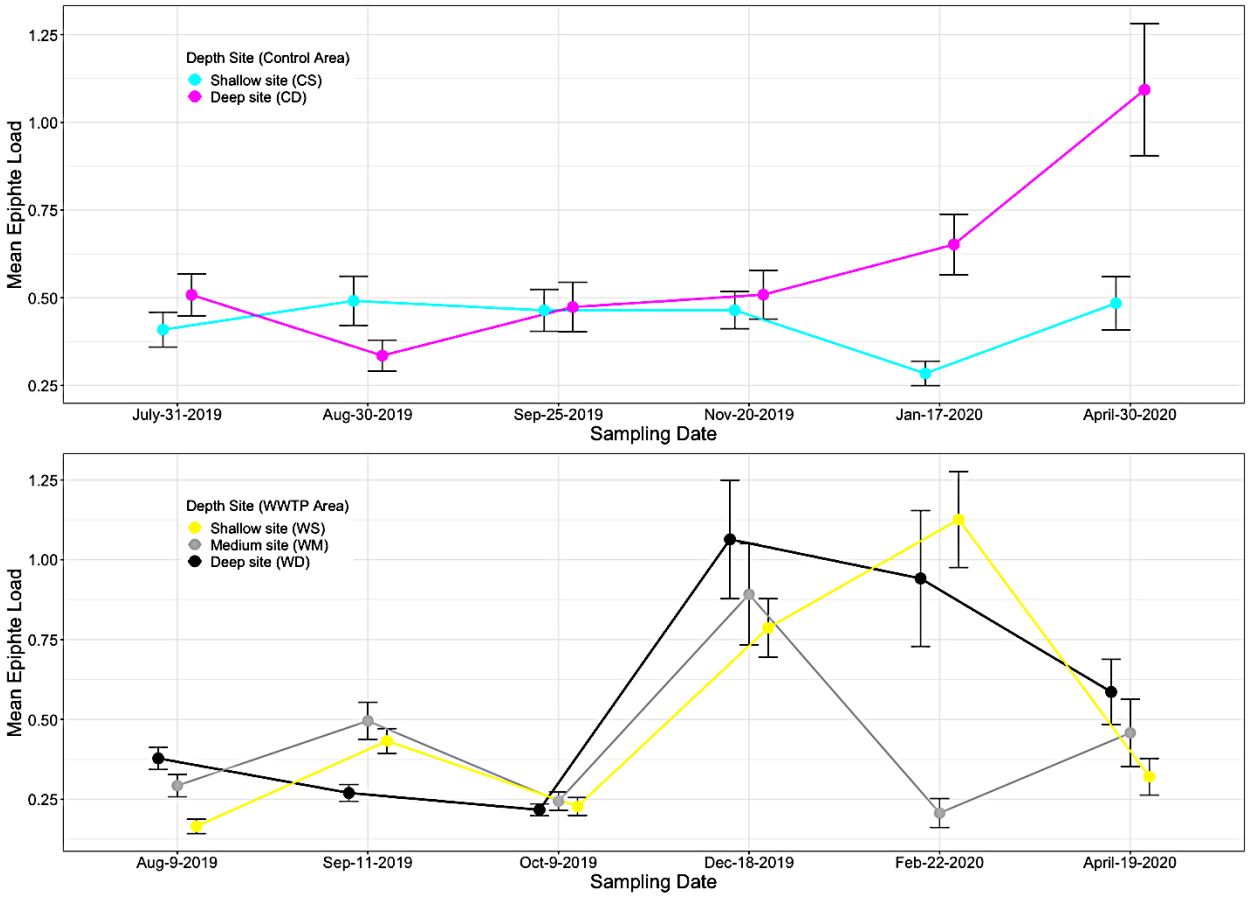

Figure 39. Changes in average epiphyte load (±SE) among depth sites from the "Control" area (first panel, n = 597) and the "WWTP" area (second panel, n = 835) from July to April.

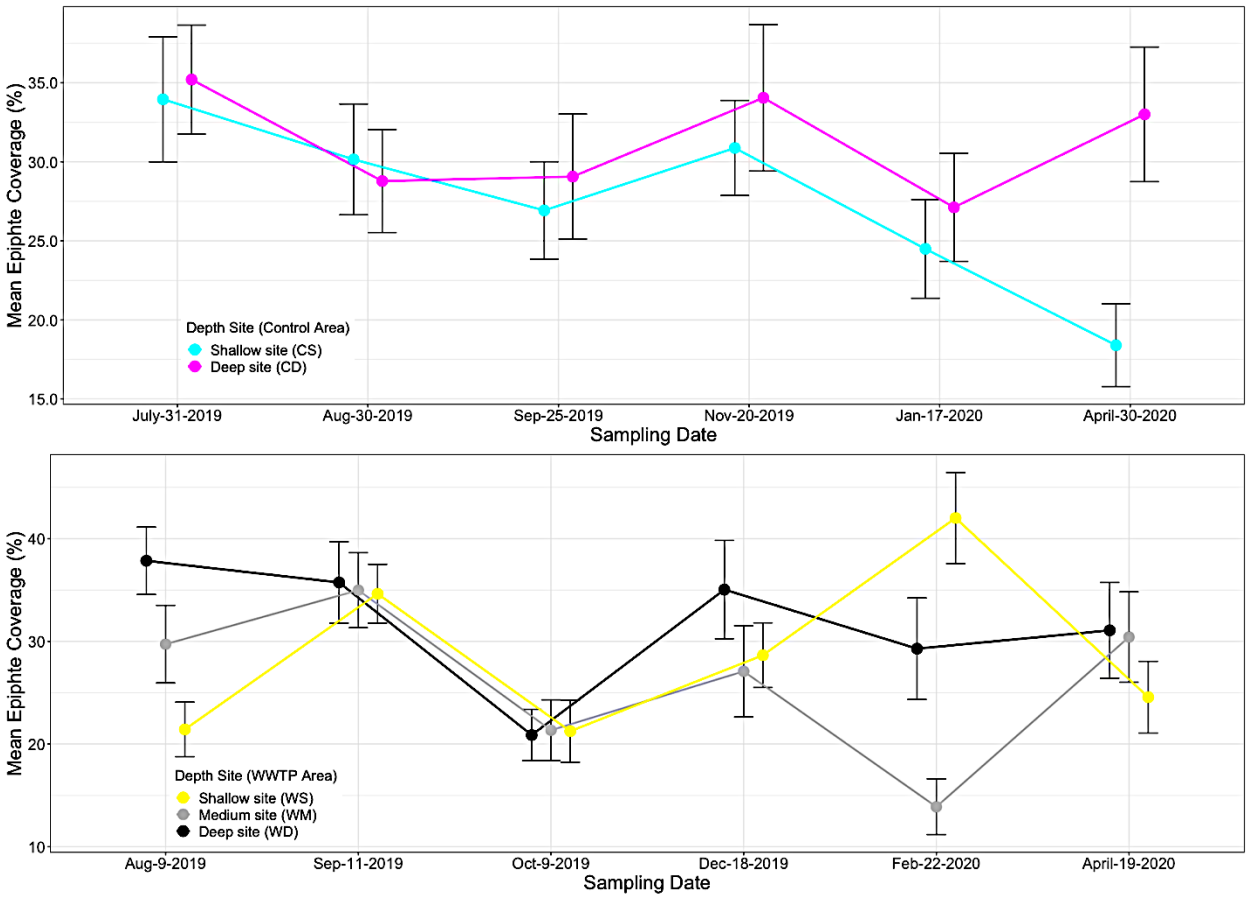

Figure 40. Changes in average epiphyte coverage (±SE) among depth sites from the "Control" area (first panel, n = 655) and the "WWTP" area (second panel, n = 909) from July to April.

3.4 Epiphyte dynamics in seagrass habitats

The observed spatiotemporal effects on seagrass and epiphyte growth prompted modeling attempts to explain the environmental factors affecting epiphyte-seagrass interactions. Multiple linear regression was used to derive a model to predict epiphyte biomass (*EB*) based on leaf biomass (*LB*) and other measured variables. Using selection for AICc values and adjusted R^2, the best model had four variables, which included seagrass leaf biomass (*LB*), associated seagrass shoot biomass (*SB*), $(NO_3^- + NH_4^+) : PO_4^-$ ratio of sediment porewater (*N*), and water temperatures (°C) (*T*). To correct for non-normality, epiphyte biomass and leaf biomass were ln(*X*) transformed. This model was expressed as:

$$\ln(EB) = 2.27 \ln(LB) - 1.79\times10^{-5} SB + 3.91\times10^{-2} N - 9.67\times10^{-2} T - 1.51\times10^{-7} (SB \times N) + 4.77\times10^{-7} (SB \times T) - 12.00$$

where the coefficients are statistically significant ($P < 0.05$). The four variables in the model explained 63% of the variation in the ln(epiphyte biomass) ($R^2 = 0.63$, n = 1002). The coefficients showed about 2.27% increase in epiphyte biomass per leaf for every 1% increase in leaf biomass. For every microgram increase in the shoot biomass, the epiphyte biomass decreases by about 1.79×10^{-3} %. This negative effect of increasing seagrass shoot biomass on epiphyte accumulation (Figure 41A) was similar to previous reports that epiphyte accumulation on older leaves might have reached a stable state and then decreased with leaf decline (Bulthuis & Woelkerling 1983, Borum 1987). Similarly, a high growth of seagrass (i.e., high shoot biomass) (Duarte & Sand-Jensen 1990) could increase leaf turnover and provide a more ephemeral substrate for epiphytes (Biber et al. 2004). There was a positive contribution of the $(NO_3^- + NH_4^+) : PO_4^-$ ratio of sediment pore water to epiphyte biomass. For every one-unit increase in the DIN:P ratio, the epiphyte biomass increases by about 3.95%. A warmer environment would limit the accumulation of epiphyte biomass per leaf. For every one-unit (°C) increase in the water temperature, the epiphyte biomass decreased by about 9.67%. However, the effects of water temperature and sediment nutrient level on epiphyte biomass per leaf also changed direction based on the seagrass shoot biomass. There was a negative relationship between water temperature and epiphyte biomass at lower shoot biomass, while for higher shoot biomass, it was a positive relationship (Figure 41B). On the contrary, the $(NO_3^- + NH_4^+) : PO_4^-$ ratio of sediment porewater facilitated epiphyte biomass at lower shoot biomass but contributed little to epiphyte biomass at higher shoot biomass (Figure 41C). The depth variable did not

contribute significantly to the prediction of ln(epiphyte biomass). This finding was consistent with the non-significant depth effect on seagrass and epiphyte growth in the "WWTP" area.

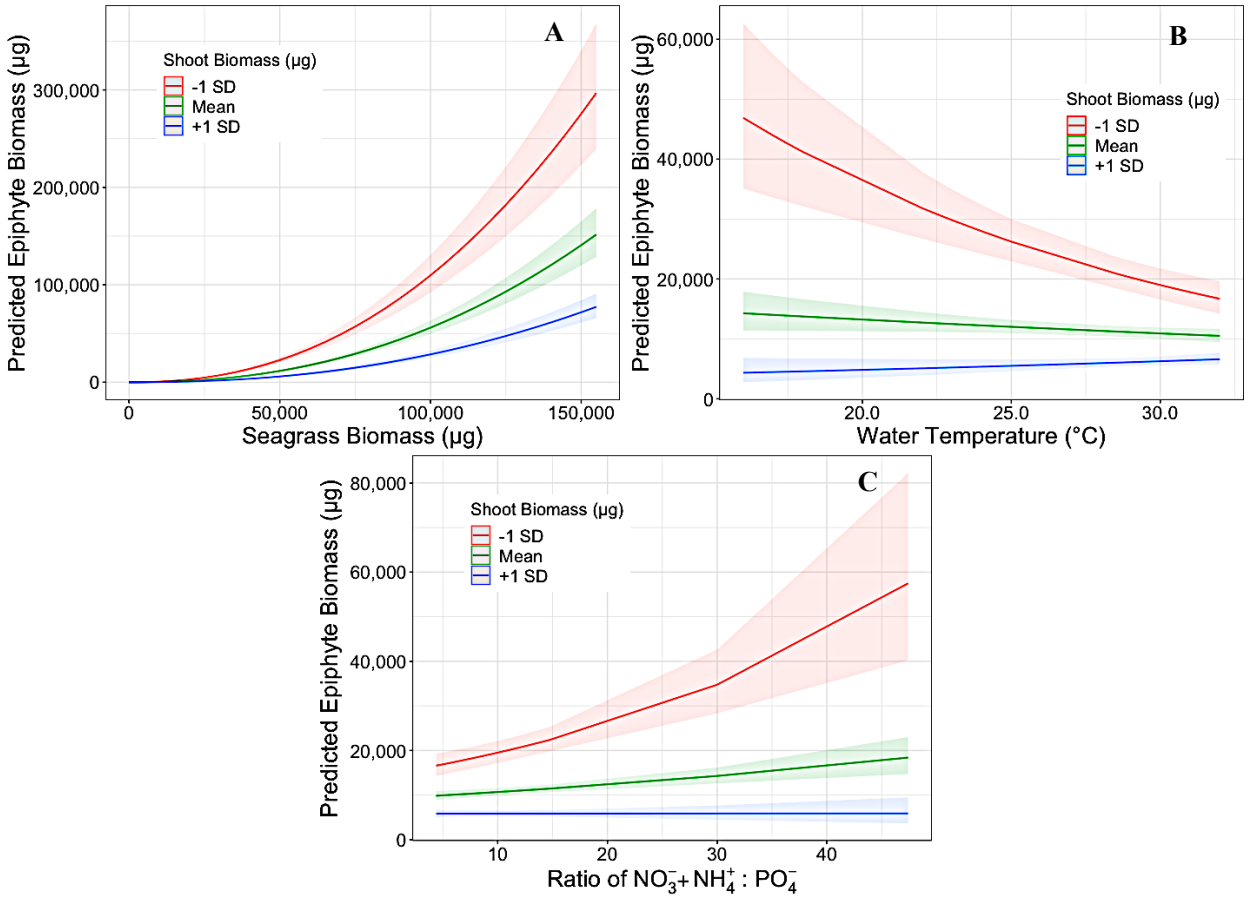

Figure 41. The effect of seagrass shoot biomass (A) water temperature (B) DIN:P ratio of sediment pore water (C) and interactions on the predicted values of epiphyte biomass relative to seagrass leaf biomass calculated by the multiple linear regression model. The shapes are the 95% confidence intervals of predicted epiphyte biomass. Red line: Mean + Standard Deviation shoot biomass; Green line: Mean shoot biomass; Blue line: Mean – Standard Deviation shoot biomass.

In the validation stage, the predictions of epiphyte biomass (Y) from epiphyte-seagrass model predictions (Y) were compared to additional observations of epiphyte (X), not used to formulate the model, from the "Control" area (n = 44) and the "WWTP" area (n = 56). The modeled data fitted the observed epiphyte biomass weakly for the "WWTP" area (R^2 = 0.13) (Figure 42A), but

better in the "Control" area (R^2 = 0.68) (Figure 42B). When simulated data from the two areas were compared with the observed data simultaneously, this regression had an R^2 = 0.56 (Figure 42C). The multiple linear regression underestimated 75.00% of the observed epiphyte biomass in the "Control" area with an average error of 26.24 × 10^3 (±5.39× 10^3) μg. The underestimated epiphyte biomass was possibly attributed to unobserved environmental factors such as water column nutrients. Conversely, the regression equation overestimated the epiphyte biomass for 68.97% of the observations in the "WWTP" area. The prediction error in the "WWTP" area averaged 3.03× 10^3 (±1.47× 10^3) μg. The overestimated epiphyte biomass might result from unobserved environmental factors such as epiphyte grazing by marine animals. Although the predicted epiphyte biomass fit the observed data poorly, the prediction error differed greatly within epiphyte accumulation. The prediction error was very great at a low epiphyte biomass level. It declined gradually as the epiphyte accumulation increased in both the "Control" and the "WWTP" areas (Figure 43). 60% of the predictions were underestimated at observed epiphyte biomass < 25 × $10^3\mu$g, but only 3.33% of the underestimated bias at epiphyte biomass > 25 × $10^3\mu$g.

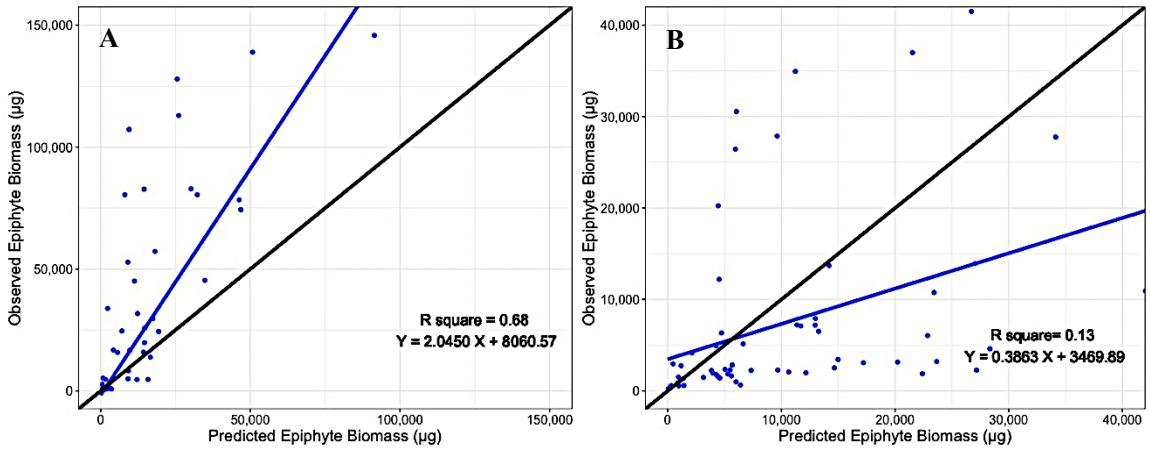

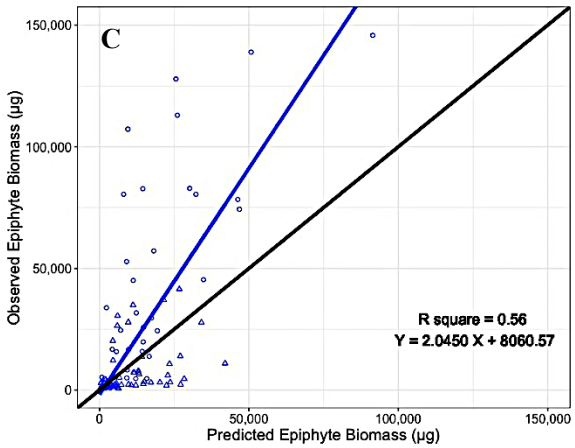

Figure 42. Observed *vs.* predicted plots of multiple linear regression output for the two locations. For reference, a perfect fit would show all the points falling on the black line (Y = X). Linear regressions showed the lines of best fit to the points. A) observed *vs.* predicted in the "Control" area; B) observed *vs.* predicted in the "WWTP" area; C) observed *vs.* predicted in the "Control" and "WWTP" areas, open circle: "Control" area; open triangles: "WWTP" area.

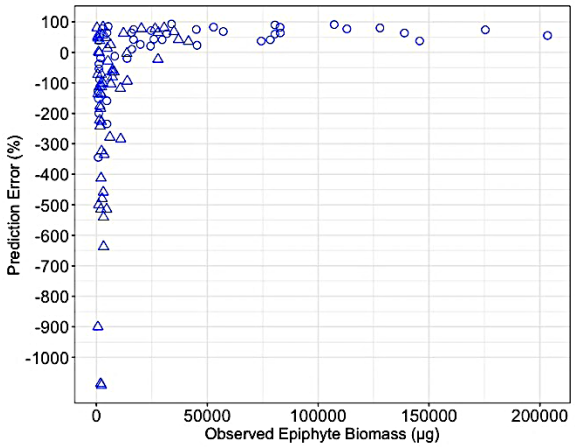

Figure 43. The relationship between the percent prediction error $[\frac{100\times(Observed\ Epiphyte\ Biomass - Predicted\ Epiphyte\ Biomass)}{Observed\ Epiphyte\ Biomass}]$ and observed epiphyte Biomass per leaf. Open circle: "Control" area; open triangles: "WWTP" area.

The variable epiphyte accumulations on seagrass suggest that multiple environmental factors contribute to this relationship. The prediction model qualified the role of water temperature and nutrient level from sediment pore water in the epiphyte-seagrass relationship. However, these results reveal that this epiphyte-seagrass model is not sufficiently comprehensive to fully explain

the epiphyte colonization relative to seagrass growth. The multiple regression model was not able to reliably predict the epiphyte biomass among unique environments.

CHAPTER IV: DISCUSSION

This study developed an efficient and informative epiphyte measurement to quantitatively distinguish the uncovered leaf areas from those colonized by diverse epiphytes. Seagrass and epiphyte indicators are usually determined using measurements based on biomass, chlorophyll *a* and *b* or other pigments, plant morphology, or visual determination of epiphyte coverage (Leuven et al. 1985, Porra er al. 1989, Armitage et al. 2005, Aumack et al. 2011, Brodersen et al. 2015, Ow et al. 2020). While those approaches demonstrate epiphyte loading and seagrass growth, only the pigment or visual inspection methods provide information about epiphyte communities. The image-based approach used here generated archivable color scan images that facilitate exploratory and iterative analyses, public accessibility and serve as a baseline for long term comparisons. A highly informative image analysis routine, once fully developed, could be largely automated to make this an efficient additional tool for monitoring seagrasses and their epiphytes. The image analysis method used different RGB properties of seagrass and epiphyte images to classify differently-pigmented areas of leaf surfaces in order to distinguish the patterns of seagrass morphology, epiphyte-covered area, and uncolonized leaf surfaces. Validation of the image-based metrics showed that they distinguished the uncovered seagrass from epiphyte-covered areas with approximately 90% effectiveness on 83% of the images. Imaging-derived seagrass and epiphyte metrics were correlated with biomass-based metrics and the two approaches exhibited similar, but not identical, spatiotemporal patterns across different environmental conditions. Multiple environmental variables control the seagrass-epiphyte relationship, with complex dynamics observed between epiphytes and seagrass in response to temperature, sediment porewater nutrients, depth and season. The seasonal shift in seagrass-

epiphyte dynamics is consistent with the previous studies in seagrass species, such as *Zostera marina* (Moore & Wetzel 2000, Hasegawa et al. 2007) and *Heterozostera tasmanica* (Bulthuis & Woelkerling 1983). The response of epiphyte load and epiphyte coverage under variable sediment porewater nutrient conditions suggested potential community changes. It is consistent with the changed epiphyte communities seen for experimental sediment nutrient enrichment (Armitage et al. 2005). The image analysis approach shows potential to be adapted to distinguish between different classes of epiphytic algae (e.g., green, red, etc) to extract structures of epiphytic communities and to detect their changes with environmental conditions.

4.1 Epiphyte and seagrass classification

The four dominant color groups classified on the images of *T. testudinum* leaves in the study area are a reddish-white group, a red group, a yellowish-brown group, and a green group. The four groups were classified by their RGB features in the current reference spectra of seagrass (482) and epiphyte (843) pixels. Based on Humm's description of algal epiphytes on *T. testudinum* in Florida (1964), the reddish-white group comprises white and pink pixels, which primarily contain small serpulid worms, coralline red algae, and several unidentified species (Figure 44a). The serpulid worms may be *Spirorbis spp* common on the basal growing *T. testudinum* leaves in the northwestern Gulf of Mexico (Dirnberger 1990). As the two most common coralline red algae on *T. testudinum, Melobesia spp* and *Hydrolithon farinosum* were possibly classified in this group (Willcocks 1982, Corlett & Jones 2007). These coralline algae produce calcified materials on the seagrass leaves, which has been used to estimate the longevity of *T. testudinum* and the production of calcium carbonate in seagrass habitat (Nelsen & Ginsburg 1986). The calcareous epiphytes are reddish, purple, or white and attach to seagrass leaves firmly by

secreting calcified substance (Borges et al. 2014). The red group perhaps combines pixels of several filamentous red algae and bryozoans (Figures 44b and 44c). The red algae species in this color group resembled the *Colaconemataceae*, *Rhodomelaceae*, and *Stylonemataceae* families, which have been recorded growing epiphytically on *T. testudinum* in Florida and the southwestern Caribbean (Humm 1964, Diaz-Pulido & Díaz-Ruíz 2003, Albis-Salas & Gavio 2011). The bryozoan species are commonly found on *T. testudinum* and easily mistaken for algae (Lewis & Hollingworth 1982, Barnes 1987, Frankovich & Fourqurean 1997). The yellowish-brown group includes pixels which can be recognized as yellowish or brownish filamentous *Chlorophyta* groups, as well as the yellowish tint of old chlorotic seagrass leaves (Figure 44d). A small number of unknown species are recognized in this group as well. Lastly, the green group contains RGB features of multiple green levels, which may identify as *Ulva spp*, and *Enteromorpha spp*. These epiphytic green algae are common on *Thalassia* and vary seasonally in the western Atlantic and southwestern Pacific (Humm 1964, Heijs 1985, Humm 1964, Thorhaug et al. 2007). Due to similar RGB characteristics, greenish epiphytes may be misclassified as bright green seagrass leaves in the image analysis (Figure 44e).

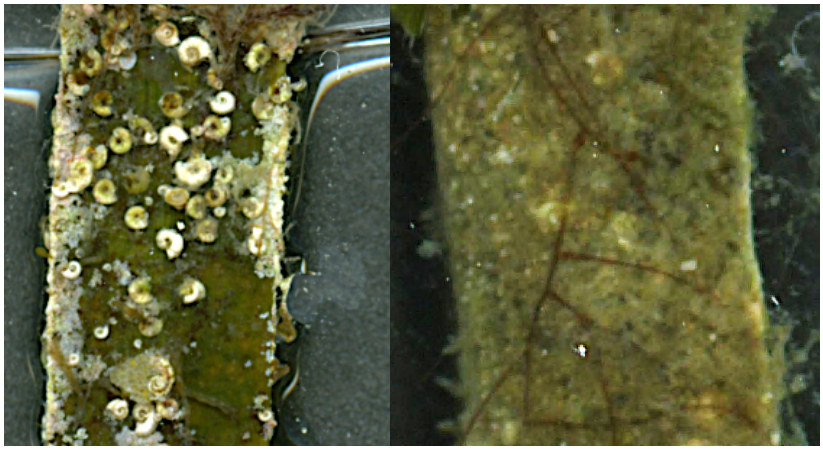

(a) (b)

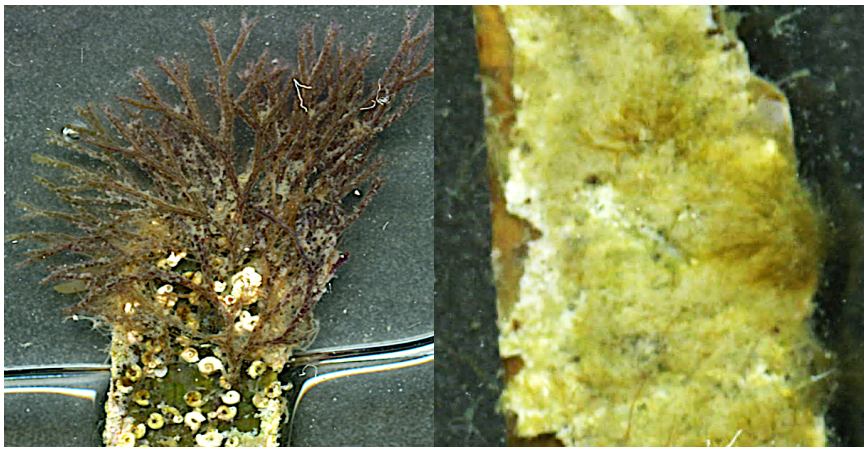

(c) (d)

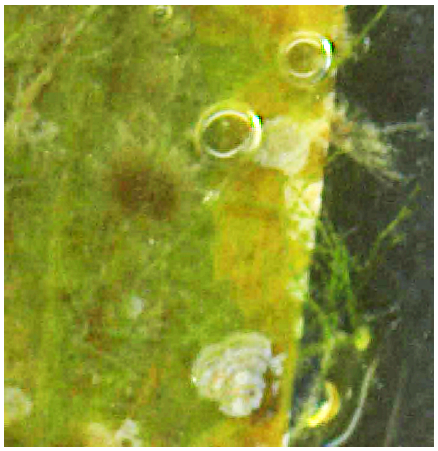

(e)

Figure 44. Four major color groups are distinguished by image analysis on seagrass leaf images. (a) Serpulid worms (center) vs. coralline red algae (edge, pink is living algae, and the white is dead) present on a seagrass blade (enhanced by 100% sharpness). (b) Filamentous red algae present on a coralline algae layer (enhanced by 50% sharpness and 30% brightness). (c) Epiphytic bryozoan can be mis-identified as filamentous algae (enhanced by 100% sharpness). (d) Clumps of yellowish green algae present on a senescent brownish-green seagrass blade (enhanced by 100% sharpness and 40% brightness). (e) Filamentous green algae present on the edge of a bright green seagrass blade (enhanced by 100% sharpness and 40% brightness).

4.2 "Intrinsic Validation" of image analysis

"Intrinsic Validation" (epiphyte classification vs. seagrass classification) and "Extrinsic Validation" (traditional metrics vs. imaging metrics) were used to assess the seagrass and epiphyte classification. Difference analysis, an "Intrinsic Validation" method reveals a low

discrepancy (< 10% differences in epiphyte coverage between epiphyte classification and seagrass classification) in 90% of the classification output, suggesting that the ENVI program can mostly distinguish the pixels of uncolonized seagrass and epiphytes through seagrass- and epiphyte- trained spectral libraries, respectively. The difference in percent cover of epiphyte between *Epi*- and *SG*- classified images presented both positive (overestimated epiphyte coverage) and negative (overestimated uncolonized seagrass) difference values that varied by season and site. Epiphyte coverage is overestimated if leaf pixels are misclassified as epiphyte by epiphyte spectral libraries or if seagrass is not classified by seagrass spectral libraries. Similarly, uncolonized seagrass is overestimated if epiphyte pixels are misclassified as seagrass by seagrass spectral libraries or if epiphytes are not classified by epiphyte spectral libraries. The image analysis likely mis-identified some greenish filamentous *Chlorophyta* groups as uncolonized seagrass leaves. Seagrass growth declined with cooler winter temperatures and the older senescing leaves presented more yellow color and brown broken edges that may have been mis-identified as yellowish green algae or brownish algae. This would explain the pronounced increase in overestimation of epiphyte classification observed in April samples. The effectiveness of classification also differed among sampling sites, with 87% of Control site images exhibiting < 5% discrepancy, compared to 76% and 78% at the WWTP and CI sites, respectively.

This suggests that epiphyte spectral libraries generated from one season or site cannot optimally identify the RGB features of multiple epiphytic components observed in another season or site. Seasonally variable algal epiphyte communities were previously observed on other aquatic plants, such as *Posidonia sinuosa*, *Amphibolis griffithii*, *Posidonia coriacea*, *Stratiotes aloides*,

and *Potamogeton lucens*, in both marine and lake ecosystems (Orth & Van Montfrans 1984, Kendrick & Burt 1997, Reyes & Sansón 1997, Lavery & Vanderklift 2002, Toporowska et al. 2008, Giovannetti et al. 2010). Kendrick and Burt (1997) showed that epiphytic *Chlorophyta* groups on leaves of *Posidonia sinuosa* only presented in winter and spring in western Australia. Separate epiphyte spectral libraries trained for different seasons and different sites would accommodate what appears to be changing epiphyte communities on *Thalassia.*

Unique environmental factors must underlie epiphyte community compositional differences, suggesting that imaging metrics could potentially be used as indicators of these factors. Previous studies have shown a variety of epiphytic algae were affected by hydrodynamics, light attenuation, water temperature, nutrient enrichment, salinity, or grazing effects (Borum 1985, Kendrick et al. 1988, Lavery & Vanderklift 2002, Biber et al. 2004, Heck & Valentine 2006, Frankovich et al. 2009, Aumack et al. 2011). Significant differences in sediment porewater nutrients were found among the three sampling locations in this study. Although hydrodynamic effects on epiphyte grazers were not measured, these may be important and unique at the CI site due to its proximity to the ICWW with its frequent boat and barge traffic. This site is further characterized by an adjacent subtidal oyster reef, which could be the source (Booth & Heck, 2009) of high levels of sediment porewater DIN observed in this study. Moreover, unpublished 18S rRNA sequencing observations from our laboratory found differences in both grazer and algal epiphyte communities from the “WWTP” and “Control” areas.

Overlap analysis, another method for “Intrinsic Validation”, was used to understand indeterminate pixels, those which could not be classified uniquely, as a combination of

overlapping pixels plus unaccounted pixels. It created three kinds of pixels, including correctly paired pixels (uniquely identified), overlapping pixels (misclassified in one or the other analyses), and unaccounted pixels (not identified in either analysis). Overlapping pixels reflect that the SAM algorithm did not distinguish epiphyte and seagrass pixels with similar RGB arrays based on current reference spectra and threshold angle. Unaccounted pixels are not identified by either reference library and may be largely attributed to inaccurate removal of the background which was done manually in this study. Underestimated epiphyte coverage can result from unaccounted pixels as well.

Expansion of the reference spectral libraries would reduce both misclassification and unidentified pixels. Additional work with other classification techniques using feature shape, texture and edge detection may also improve identification accuracy. For example, the Canny edge detector (Canny 1986) has been applied for plant leaf identification, description of leaf shape, and leaf disease pattern (Bankar et al. 2014, Codizar & Solano 2016, Salman et al. 2017).

4.3 "Extrinsic Validation" of image analysis

Image analysis-based metrics for seagrass and epiphytes were further evaluated by their correlation to traditional metrics. Strong linear relationships ($R^2 > 0.86$) were found between seagrass leaf pixels and seagrass leaf morphology (area, length, biomass). This result indicates that the pixel numbers of leaf derived from image analysis can substitute for manual morphology measurements and be suitable for leaf area index calculation in future seagrass investigations.

Correlations of epiphyte imaging metrics with biomass measures (Epiphyte pixels vs epiphyte biomass; $R^2 = 0.61$) were weaker than for the seagrass metrics when all project data were analyzed collectively. However, closer inspection reveals how image analysis provides new insights into epiphyte-seagrass dynamic relationships as they change across environmental conditions. The linear correlations greatly improved (R^2 ranged from 0.67 to 0.95) when the data was separately analyzed by sampling location, for each of the six sampling times. Most importantly, for all three sampling locations, the slopes of these linear regressions changed in a consistent seasonal pattern where the slope increased with progression from autumn through winter. The observation of increased epiphyte biomass per unit of epiphyte covered area is consistent with continued epiphyte growth despite observed decreases in seagrass leaf growth and production. Cooler water temperatures (and perhaps shorter days/lower light levels) may be critical environmental factors diminishing leaf growth (Zieman 1975, Marbà et al. 1994, Zieman et al. 1999, Koch & Erskine 2001). However, these observations could also be explained in part by changes in the nature of the epiphyte communities. In this work, the highest epiphyte biomass per epiphyte area (pixel) was observed at the CI site, which had unique influences from proximity to both oysters and hydrodynamic disturbance from boat traffic in the ICWW.

Studies have shown that algal epiphyte communities colonized *T. testudinum* leaves and other seagrass species in an orderly succession with three or more layers (Willcocks 1982, Bulthuis & Woelkerling 1983, Kitting et al. 1984, Zieman et al. 1999, Corlett & Jones 2007). Both diatoms and coralline red algae were reported on the tips and edges of young seagrass leaves as "pioneers", which then spread dominantly (Humm 1964, Jacobs et al. 1983, Fredriksen et al. 2005, Perry & Beavington-Penney 2005). Although the diatom community is reported as the

basal epiphytic layer and entirely covered by the coralline algae and other epiphyte groups (Edsbagge 1968, Corlett & Jones 2007), the scanned images in our study don't visualize microalgae. The upper layer is a diverse assemblage including macroalgae, dinoflagellates, foraminifera, bacteria, fungi, and invertebrates (e.g., sponge, gastropods, copepods, and serpulid worms) and their larvae, observed globally (Lethbridge 1989, Dirnberger 1990, Hall & Bell 1993, Kendrick & Burt 1997, Borowitzka et al. 2006, Michael et al. 2008, Mateu-Vicens et al. 2010). A community shift to a greater abundance of filamentous algae and/or heavier calcareous epiphytes, such as serpulid worm (Dirnberger 1990) would increase both biomass and biological diversity. Heavier and thicker epiphyte layers also have a greater light attenuation effect (Bulthuis & Woelkerling, 1983). While previous reports suggested a higher biomass accumulation rate of epiphytes on seagrass leaves in the summer (Bulthuis & Woelkerling 1983, Heijs 1984, Borum 1985), the apparent "thickness" of epiphyte accumulation presents a reverse seasonal pattern. Although the epiphyte mortality increased as the seagrass biomass and suitable blade substrate declined (Borum 1985, Fong & Harwell 1994), the serpulid worms and drift algae continuously attached on existing epiphyte layers because of polysaccharide production by diatoms (Corlett & Jones 2007, Saha et al. 2019). Armitage et al (2005) noted community changes for macro- and micro-algae in seagrass communities affected by experimental nutrient enrichment. Changes in the communities of epiphytes accumulating across different environmental contexts suggests that image analysis of the texture information of epiphyte biofilms could provide additional important insight into epiphyte-seagrass responses to the environment.

The described relationships between epiphyte load and epiphyte coverage of the leaf substrate indicated two likely epiphyte accumulation patterns on *T. testudinum* leaves. In the first accumulation scenario, a linear increase in epiphyte load with the spread of epiphyte coverage indicated sufficient leaf surface amenable for epiphyte colonization. In the second epiphytic accumulation phase, the epiphyte coverage of leaves becomes saturated as little surface remains to be colonized, yet the epiphytes continue to increase by growth in size, thickness and/or density. This phase was suggested by fitting exponential regressions of epiphyte load with epiphyte coverage for several specific sites and times. The exponential accumulation phase was observed in February and April at WWTP, in August at Control, and in August and April at CI (Figures 18, 19 and 20, Results). For the shift from the first to second phase, it is unclear if the leaf stops growing due to environmental factors, allowing epiphytes to accumulate exponentially, or if the epiphytes outgrow the seagrass and reduce light to the point of reducing seagrass leaf growth. But even with the heaviest epiphyte accumulations, coverage only rarely reaches 100%, and the basal 5 cm of leaves (near the leaf sheath) is usually not covered by visible epiphytes. This may represent a threshold point for the balance between leaf growth response to epiphyte shading versus leaf senescence. While an under-classification is likely the major source of epiphyte coverage interpretation error, it cannot account for either the incidence or occurrence pattern of exponential relationships.

The emerging interpretation from this study is that epiphyte community change impacts both biomass and imaging measures, and the epiphyte-seagrass dynamic relationship itself. Other factors to consider are impacts from animal grazing of epiphytes and plant host influences on epiphyte community structure. Diverse animal grazers can impact epiphyte accumulations

quantitatively and temporally (Orth & Van Montfrans 1984, Irlandi et al. 2004, Frankovich & Zieman 2005, Heck & Valentine 2006, Peterson et al. 2007, Whalen et al. 2013), and probably qualitatively as well. Grazing effects were not part of this study, so their impacts at our study sites are unknown. However, strong hydrodynamic forces can reduce grazing pressure (Schanz et al. 2002) and this could contribute to the high epiphyte accumulations at CI. In addition, our unpublished observations of 18S rRNA sequences revealed large differences in nematodes and other animals comparing the WWTP and Control areas. The seagrass host can also play a role in the epiphyte community composition. On the young leaf surface of *Zostera marina*, phenolic acid from *Zostera marina* inhibits the growth of several microalgae and marine bacteria and reduces photosynthesis of epiphytic diatoms, which probably maintains the low epiphyte biomass on young seagrass leaves (Harrison 1982, Harrison & Durance 1985). The bacterial community found on *Zostera marina* can produce agarases, which limit the growth of epiphytic algae (Crump et al. 2018).

4.4 Spatial and temporal patterns of seagrass growth

Seagrasses respond to numerous biotic and abiotic factors related to seasonal change and specific sites. Spatiotemporal variation was compared between imaging metrics and their biomass counterparts to vet the ability to detect change. The growth patterns of the seagrass host are important for understanding the seagrass-epiphyte dynamic relationship so leaf biomass and image-based leaf area were examined collectively to understand seagrass growth in the “Control” area, “WWTP” area and CI site across six sampling times. In the three sampling locations, the growth condition of *Thalassia testudinum* followed a seasonal pattern with the maximum in the summer and early autumn, followed by a decline through winter or early spring. Similar patterns

were observed in *T. testudinum* productivity in south Florida (Fourqurean et al. 2001) and the western Gulf of Mexico (Herzka & Dunton 1997). Decreasing temperature, light and/or salinity probably initiate the significant decline of leaf biomass and leaf area in winter. Zieman (1975) found that *T. testudinum* has an optimal temperature around 30°C and an optimal salinity around 30‰. Slow recovery of leaf area in April is consistent with a previous report that photosynthesis of *T. testudinum* increases gradually from winter to spring (Herzka & Dunton 1997). Numerous studies suggest water temperature is the primary influence on the seasonal pattern of seagrass growth (Lee & Dunton 1996, Campbell et al. 2006, Koch et al. 2007, Collier & Waycott, 2014). At salinity levels below optimum, photosynthesis of *T. testudinum* was suggested to be limited by reduced chlorophyll content (Doering & Chamberlain 2000, Thorhaug et al. 2006). The temporal influence of nutrient and light availability create variable conditions for seagrass growth (Pérez-Lloréns & Niell 1993, Herzka & Dunton 1997, Lee et al. 2007). *T. testudinum* in Corpus Christi Bay showed higher ammonium acquisition in summer and autumn than in the winter (Lee & Dunton 1999). For our study, given that seagrasses obtain most of their nutrients from the sediments, sediment porewater nutrients were measured (once) under the assumption that the porewater would reflect the long-term average status of water column nutrients. The DIN/phosphate ratio was highest at CI and lowest at WWTP, with the highest DIN at CI and the highest phosphate at WWTP, but that did not translate into *significantly* higher seagrass biomass or leaf area consistently, on an average *per leaf* basis. For this study, potential light effects were gauged by comparing seagrasses from different depths. Two significant seagrass differences were 1) a lower (1/2 X) biomass and leaf area observed at the WWTP Shallow site compared to the two deeper sites, which was only apparent in summer and autumn; and 2) a lower biomass and leaf area at the Control Deep site compared to Control Shallow, only observed in January.

The low seagrass biomass and leaf area at the shallow site in the "WWTP" area may be due to photoinhibition at high light intensities, which could occur at low summer water levels (Ralph & Burchett 1995, Ralph 1999, Hanelt & Roleda 2009). Excessive light stress in tidally exposed seagrass can also limit biomass (Stapel et al. 1997). However, the similarly low leaf biomass and leaf area demonstrated across the depth gradient in the winter and spring may be related to decreased incident light and increased light attenuation from higher seasonal epiphyte accumulation. In Fong and Harwell's seagrass communities model (1994), drift macroalgae and epiphytic algae limited photosynthetic performance of seagrass. Opposite depth effects at the "Control" and "WWTP" areas implies that variability of available light caused by water depth is probably not an important factor in this study. Several studies reported that seasonal changes in grazing density in the coastal ecosystem possibly contribute to the variation of seagrass biomass (de Iongh et al. 1995, Thom et al. 1995, Tomas et al. 2005, Heck & Valentine 2006). While light, water column nutrients and grazing were not part of this study, their seasonal variation likely contributed to the measured seagrass parameters that are also tied to the seagrass-epiphyte dynamic relationships observed at the three unique sampling locations.

4.5 Spatial and temporal patterns of epiphyte accumulation on seagrass

Spatiotemporal variation of the different epiphyte metrics were also examined to further evaluate the reproducibility of imaging approaches in detecting epiphyte accumulation. Unlike the seasonal pattern of seagrass growth, the epiphyte load, which is relative to the seagrass host, presents an opposite pattern across the sampling periods among three locations. The epiphyte load in the "WWTP" area and the CI site follow a similar seasonal pattern with the maximum in winter and low relative epiphyte accumulation in summer. The increased epiphyte load from

summer to winter is consistent with the previous reports of epiphyte accumulation on *Cymodocea nodosa* in the Canary Islands off the northwestern African coast (Reyes & Sansón 2001) and epiphyte biomass on *Zostera marina* in the San Juan Islands, US (Nelson & Waaland 1997). In the "Control" area, epiphyte load was intermediate between that of CI and WWTP for 3 of the 4 seasons, with a maximum level in spring that implies either unique controlling factors or timing of their interaction. *T. testudinum* in the Caribbean showed highest epiphyte abundance and diversity per unit of leaf surface in a warmer season and declines in a colder season due to the inflow of nutrients during the warm season (Richardson 2004). Several studies have suggested that the available seagrass substrate primarily influenced the seasonal variability of epiphyte colonization, which was secondarily controlled by other extrinsic environmental conditions (Alcoverro et al. 1997, Biber et al. 2004). A faster leaf turnover rate probably drives a lower epiphyte load in the summer than in the winter (Duarte & Sand-Jensen 1990, Biber et al. 2004, Peterson et al. 2007), which causes a shorter period for epiphyte accumulation on the available leaf surface. On the contrary, the highest epiphyte load in the winter or spring among three sampling locations may result from slower growth of the seagrass host, and/or different epiphyte community succession patterns (Corlett & Jones 2007) in winter vs summer, as discussed previously. Biber er al. (2004) have reported that epiphytic algae on the *T. testudiunm* have a high tolerance of low temperature and the optimal temperature is 20~28℃, but decline rapidly over 30℃. The elevated temperature possibly drives the relatively lower proportions of diatoms in summer compared to winter and spring (Snoeijs 1994). Despite the acute seagrass leaf biomass and area declines in the winter and spring, diverse epiphytic species, such as diatoms, sponges, filamentous algae, and invertebrates, may continuously colonize on the basal and middle layer of diatoms and coralline red algae, to increase epiphyte biomass relative to

covered leaf area. This means that the epiphyte biofilms continue their growth in biomass in the cool season whereas the seagrass does not to the same extent. These observations are consistent with the secondary colonization by diverse groups of organisms and the seasonally distinct slopes of epiphyte biomass to epiphyte pixels plots discussed above. It is significant to note that the average % epiphyte coverage metric showed relatively little seasonal fluctuation compared to the epiphyte load metric. Although the seasonal variation in epiphyte coverage is not significant, the remarkably decreased leaf area from summer to winter indicates a sharp reduction of the uncovered leaf area for available photosynthesis, which probably further inhibits the growth of *T. testudinum* (Harlin 1975, Bulthuis & Woelkerling, 1983, Fitzpatrick & Kirkman 1995, Drake1 et al. 2003, Ruiz & Romero 2001, Ow et al. 2020). The lower seagrass growth would provide less new colonization surface so the increased epiphyte biomass would result from growth of existing epiphytes, additional layers of epiphytes colonizing secondarily, or else a shift towards a denser (calcareous) community. A lower leaf turnover rate, however, would facilitate all of these mechanisms of epiphyte accumulation.

While the seasonal seagrass growth condition has been suggested as the major factor controlling the temporal epiphyte accumulation pattern (Alcoverro et al. 1997), additional biotic and abiotic factors also vary temporally to affect epiphyte accumulation. Although a statistically significant decrease in salinity from summer to winter for our study probably inhibits the growth of several coralline red algae and diatoms (Walker & Woelkerling 1988, Snoeijs 1994), the increase in epiphyte load during winter may suggest that decreased leaf turnover is a primary factor driving the epiphyte accumulation and the variability of epiphyte on seagrass was not significantly impacted by salinity level (Biber et al. 2004, Fernández-Torquemada & Sánchez-Lizaso 2005).

Seasonal changes in water column nutrient concentration (Alcoverro et al. 1997, Moore & Wetzel 2000, Ruesink 2016) and grazer densities (Thom et al. 1995, Nelson & Waaland 1997, Frankovich & Zieman 2005, Heck & Valentine 2006) also play essential roles in the epiphyte accumulation in seagrass habitats. The temporal shift in invertebrate herbivores may control the spatial variability of epiphyte accumulation in our study as well (Peterson et al. 2007b, Whalen et al. 2013). A seasonal pattern of major mesograzers' biomass in *Zostera marina* habitat in Willapa Bay reported low mesograzer biomass in winter (Ruesink 2016). Conversely, the highest abundance and species diversity of harpacticoid copepod was reported in *Posidonia oceanica* habitat in the Mediterranean Sea during late spring and summer (Mascart et al. 2015).

The significant difference in epiphyte accumulation patterns among three sampling locations demonstrated the impact of the spatially unique environmental conditions. The ranking of sampling locations from highest (CI site) to lowest ("Control" and "WWTP" areas) epiphyte accumulation was the same for epiphyte load (biomass metric) and epiphyte coverage (imaged based metric). If the light attenuation effects of epiphytes significantly impact the seagrass host, then the image-derived coverage metric is informative. The seagrass biomass was highest at WWTP in summer and autumn (only), when that area also had the lowest epiphyte accumulation, which would be consistent with a shading effect from epiphytes. There was no significant and consistent depth effect on epiphyte accumulation by any measure for the "Control" and "WWTP" area. Within the "Control" area, only the April sampling showed a significant lower accumulation for both epiphyte load and epiphyte coverage. It suggests that the influence of light availability caused by depth variation is probably not a major factor controlling the epiphyte accumulation in this study.

Nutrient effects on epiphytes have been explored extensively (Borum 1985, Frankovich & Fourqurean 1997, Frankovich & Zieman 2005, Johnson et al. 2006, Frankovich et al. 2009, Nelson 2017b). Some indicate that water column nutrients are the only source, whereas others weakly correlated sediment ammonia and epiphyte biomass (Ruckelshaus 1993, Biber et al. 2004) or indirect uptake through seagrass blades (Penhale & Thayer, 1980), which uptake dissolved inorganic nitrogen (DIN) from both sediment porewater and the water column (Iizumi & Hattori 1982, Stapel et al. 1996, Cornelisen & Thomas 2004). In this study, the highest DIN:P was found at CI due primarily to high DIN, whereas WWTP had the lowest DIN:P ratio due primarily to high P. Correspondingly, in summer and autumn, CI had the highest epiphyte and lowest seagrass biomass; while WWTP had the lowest epiphyte and highest seagrass biomass. This would be consistent with some role of DIN in the seagrass and epiphyte growth during summer and autumn in Texas (Lee & Dunton, 2000). Given the similarity of seagrass growth pattern among the three locations, the high epiphyte load at CI is probably not primarily driven by a decreased leaf turnover rate due to phosphorus limitation in the porewater (Fourqurean et al. 1992, Lavery & Vanderklift 2002, Biber et al. 2004). The highest observed epiphyte load and coverage at the CI site then seems likely due to either a high DIN in summer and/or a change in epiphyte community composition. A decreased grazer density at CI is possible and also consistent with the high epiphyte accumulation, especially given the likely hydrodynamic effects from proximity to the ICWW (Schanz et al. 2002).

The dynamic seagrass-epiphyte interactions can present various patterns driven by combinations of factors mentioned above and these were used to develop models (Fong & Harwell 1994, Biber

et al. 2004). In this work, MODREG was used to assess the spatial variability of epiphyte accumulation on individual leaves. This approach indicated the pattern of epiphyte accumulation on *young* seagrass leaves did not vary significantly among sampling locations. This likely corresponds to a linear colonization phase based on available leaf surface, but could also reflect inhibitory substances from bacteria or the seagrass host. MODREG analysis indicated a divergence of epiphyte accumulation patterns occurring above different leaf biomass thresholds across environmental contexts (Table 7, Results). The highest epiphyte accumulation simulated at the CI site was highest across six sampling times above leaf biomass threshold: (summer: 50×10^3 µg; autumn: 40×10^3 µg; winter: 28×10^3 µg; spring: 38×10^3 µg). The "Control" area showed a higher epiphyte accumulation than the "WWTP" area above leaf biomass threshold: (summer: 28×10^3 µg; winter: 62×10^3 µg; spring: 38×10^3 µg), except in autumn. This simulation might correspond to the spatiotemporal patterns of epiphyte load discussed above. It may also represent the initiation of exponential accumulation observed for some samples. As discussed above, there seems to be spatial variation in epiphyte composition and/or growth. It might be attributed to the spatial variance in grazing due to changes in species composition and consumption strategies (Jernakoff et al. 1996, Nelson & Waaland 1997, Schanz et al. 2002). If nutrients are responsible, it would likely be changes in water column N availability. While nutrient enrichment at the "WWTP" area was expected to promote seagrass and epiphyte growth (Borum 1985, Lee et al. 2007, Baggett et al. 2010), such effects were not observed on any consistent basis, with the exception of elevated seagrass biomass and leaf area in autumn at WWTP. There was no corresponding increase in epiphytes. Unless there was a corresponding increase in herbivory (Heck & Valentine 2006, Peterson et al. 2007, Heck et al. 2015), there does not appear to be significant differences between Control and WWTP. Alcoverro et al. (1997) and

Baggett et al. (2010) have suggested that the grazing effect on epiphyte accumulation is more significant than the nutrient level in the water column and even the primary environmental factor. However, the epiphyte accumulation pattern is perhaps primarily driven by the bottom-up impact in the marine ecosystem shifting with the season (Whalen et al. 2013). Future studies should include monitoring of grazing effects and epiphyte community change, in addition to water column nutrient levels, to improve understanding of the seagrass-epiphyte relationship.

4.6 Modeling dynamics of epiphytes on *Thalassia testudinum* leaves

The epiphyte-seagrass dynamics model is initiated from Fong and Harwell's seagrass conceptual model (1994) and Biber et al.'s epiphyte conceptual model (2004). Numerous factors, including water temperature, DIN : P in the sediment porewater, salinity, light condition caused by water depth, seagrass leaf biomass, and seagrass shoot biomass, are employed in multiple linear regression analysis in an attempt to explain the variation of epiphyte biomass per leaf across environmental context. Several essential factors in this multiple linear regression model are lacking, such as the light condition caused by seasonal weather and water clarity, grazing impact, and influence of hydrodynamic factors.

According to the equation, seagrass leaf biomass has a strongly positive impact on epiphyte biomass. Epiphyte biomass is primarily driven by the seagrass growth condition (Alcoverro et al. 1997) with more availability of seagrass leaf surface for colonization. Several studies have observed an exponential increase in epiphyte biomass with elongation of seagrass leaves, but the epiphyte biomass stopped accumulating or decreased at a specific seagrass "growth state" (Bulthuis & Woelkerling 1983, Borum 1985). Biber et al.'s model (2004) estimated the epiphyte

accumulation pattern under the assumption that the epiphyte biomass is reduced due to leaf senescence. However, diverse epiphytes have been shown to continue to colonize on the upper epiphytic layer and increase biomass even on the broken and declining seagrass leaves (Humm 1964, Corlett & Jones 2007, Michael et al. 2008, Frankovich et al. 2009, Giovannetti et al. 2010).

A major intrinsic factor controlling epiphyte accumulation is the seagrass leaf turnover rate (Fong & Harwell 1994, Biber et al. 2004). Epiphyte biomass declined as seagrass leaf biomass decreased by senescence. However, increased leaf turnover within flourishing seagrass growth may also contribute to epiphyte mortality because of a shorter period for epiphyte colonizing on a seagrass leaf than a leaf with a slower turnover rate. Although we did not measure leaf turnover, seagrass shoot biomass was positively correlated to the growth status of seagrass (Duarte & Sand-Jensen 1990, Duarte & Chiscano 1999). A small negative coefficient term for seagrass shoot biomass reveals that the epiphyte biomass probably accumulates more on growing leaves that replace older ones when total shoot biomass declines.

As indicated by the multiple linear regression, temperature contributes to the epiphyte biomass accumulation negatively, explaining the higher epiphyte biomass in winter or spring. Epiphytes on *T. testudinum* have been suggested to have a growth optimum below 30℃ (Harlin 1975, Biber et al. 2004). However, epiphytes are diverse and probably exhibit a range of temperature optimums, which could encourage changing species dominance (Frankovich et al. 2009, Giovannetti et al. 2010). The positive coefficient of the Seagrass Shoot Biomass × Temperature interaction term implies that *Thalassia* biomass decreases with lower temperatures from summer to winter. The leaf turnover rate of seagrass probably decreases due to the decline of seagrass

growth at a low temperature (Biber et al. 2004, Lee et al. 2007, Peterson et al. 2007b). Although some epiphytes are lost from senescence, the low leaf turnover rate provides less ephemeral substrates and thus increase the proportion of successional colonization and thickening growth.

Conversely, the DIN : P ratio in sediment porewater shows a significantly positive impact on epiphyte biomass in the equation. While several studies have reported that the nutrient source of epiphyte is not directly from sediment (Williams & Ruckelshaus 1993, Biber et al. 2004), epiphytes can uptake carbon and phosphorus from sediment transferred through the seagrass blade (Penhale & Thayer 1980). Our results are not consistent with a previous report that long-term phosphorus enrichment in the sediment was associated with an increase in abundance of epiphytic red and green algae (Frankovich et al. 2009). However, elevated DIN : P ratio in sediment porewater may possibly promote epiphyte accumulation by limiting the seagrass growth/turnover due to phosphorus limitation (Fourqurean et al. 1992, Gras et al. 2003) and offers relatively "long-lived" seagrass substrates for more epiphyte accumulation.

The salinity level did not contribute significantly to the variation of epiphyte biomass per leaf in this multiple regression analysis, although several studies suggested considerable effects of salinity level on specific epiphytic species and seagrass growth (Kendrick et al. 1988, Snoeijs 1994, Fernández-Torquemada & Sánchez-Lizaso 2005, Thorhaug et al. 2006). The epiphyte community probably has a high tolerance to variable salinity because of species diversity (Humm 1964, Thorhaug et al. 2006, Michael et al. 2008). The variable light conditions caused by water depth differences in this study did not contribute significantly to the epiphyte

accumulation, despite light being critical in determining the productivity of seagrass and epiphytic algae.

Error estimation from this regression model demonstrated the lack of sufficient information for accurately describing the epiphyte-seagrass dynamics, particularly factors of grazing effect in seagrass habitats and water column nutrient levels, which is the primary nutrient source for epiphytes. Several studies have addressed the positive impact of grazer reduction on epiphyte accumulation (Jernakoff et al. 1996, Frankovich & Zieman, 2005, Heck & Valentine 2006, Aumack et al. 2011, Whalen et al. 2013). Our overestimated epiphyte biomass is probably attributed to a lack of the grazer-limiting effect on epiphyte growth in the regression model. The underestimates of epiphyte biomass are probably due to lack of water column nutrient data. Epiphyte recruitment and community composition within a water column nutrient gradient can be driven by nitrogen or phosphorus limitation (Borum 1985, Tomasko & Lapointe 1991, Frankovich & Fourqurean 1997, Johnson et al. 2006, Nelson 2017). Future studies will need to fill in these gaps in our knowledge of this study area.

These results suggest that the image analysis approach is a promising tool to aid in efficiently understanding the epiphyte-seagrass dynamic relationship, and the impact of environmental stressors on this relationship. However, evaluation of the image analysis method shows that classification discrepancies still exist and the major challenge is related to misclassification and omission of green algal epiphyte groups that resemble the seagrass leaf spectrally. The image-analysis tool should be able to define the spatiotemporal changes in epiphyte communities, but

refinement and expansion of epiphyte and seagrass reference spectra will be required. More advanced analyses, such as deep learning with neural networks, may prove fruitful.

CHAPTER V: CONCLUSION

The influence of unique environmental conditions on epiphyte accumulation on *T. testudinum* leaves in the study area has been observed through image analysis and biomass measurement. The development of image analysis in this study presented a high accuracy (< 10% discrepancy) of seagrass and epiphytes classification in 83% of the images. The validation output indicates that image analysis will improve with expanded spectral libraries, automated segmentation of leaves from the background, and capturing information beyond just an RGB signature. The spatiotemporal variability of seagrass and epiphyte growth presented mostly similar patterns through biomass and image-based metrics, but the epiphyte coverage metric did not show the degree of temporal variability observed for the epiphyte load metric. Nonetheless, the ranking of study sites by degree of epiphyte loading was consistently similar for the epiphyte coverage and epiphyte loading metrics across the study period. The observation that the mean epiphyte coverage stayed relatively constant (maximum range of variation was about 15%) across seasons, but differed by site, suggests that leaf growth may be regulated to maintain the proportion of uncolonized leaf surface. The relationship between epiphyte biomass accumulation and leaf coverage spread provides insight into the morphology of the epiphyte biofilm and is worth examining more closely for understanding the significance of the epiphyte colonization pattern. The current multiple linear regression model could not accurately predict the contribution of various internal and external factors and their interactions comprehensively. However, several available data, including water temperature, nutrient levels of sediment porewater, and seagrass growth state, were important contributory factors and consistent with previous models. Future work will involve the contribution of grazing effect and water column nutrient levels to epiphyte-seagrass dynamics. Detailed validation output of image analysis

through ENVI and response of epiphyte and seagrass growth to spatiotemporal variability have yielded the following conclusions:

(1) The image analysis presented here effectively distinguished four major color groups on a seagrass blade image, including the red groups of filamentous red algae and bryozoan; reddish-white groups of coralline red algae and serpulid worms; brownish-yellow groups of older seagrass leaves and green algae which have a brownish-green appearance; green groups of younger seagrass leaves and filamentous green algae;

(2) Image-based metrics for seagrass growth and morphology were well correlated with traditional biomass or manual measures of seagrass shoots;

(3) Average seagrass leaf growth (leaf biomass and pixel numbers of leaves) was 2-fold higher in summer and autumn months than in winter and spring months across different environmental conditions within the study area, but there were no significant spatial differences among the three locations across the study period. The similarities of spatiotemporal observations for the different seagrass measures further validate the utility of the image analysis approach in seagrass investigations;

(4) Image analysis of epiphytes revealed complicated accumulation patterns and correlations to biomass measures. Epiphyte loading, relative to seagrass, was 2-fold higher in winter and spring months than in summer and autumn months across different environmental conditions, but the % leaf coverage within a given site was relatively constant across seasons;

(5) Despite the wide range of discrepancy of epiphyte and seagrass classification for individual images, (0.1% to 30.0%), 83% of the blade images had <10% discrepancy.

The epiphyte and seagrass spectral libraries should be expanded to encompass more diverse epiphyte groups represented by seasonal changes. Misclassifications, especially between green pixels of seagrass and filamentous algae, could also be reduced by edge detection to filter out less relevant information and find boundaries of different objects by detecting discontinuities in brightness.

(6) The two modes of correlation (linear vs exponential) between the epiphyte biomass metric and image-based metrics demonstrated that epiphytes continue to accumulate on epiphyte-covered seagrass blades and can be explained by successional growth (new layers), filamentous growth, and/or community compositional changes towards denser (calcareous) epiphytes. Elucidation of epiphyte colonization patterns, variable thickness of epiphyte accumulation and light attenuation will reveal insight into epiphyte-seagrass dynamic relationships and environmental effects;

(7) The epiphyte accumulation relative to seagrass presented significant spatial variability with seasonal change. The epiphyte accumulation is highest near the ICWW and lowest adjacent to the wastewater treatment plant for most sampling times. The temporal variability of epiphyte/seagrass biomass ratio but consistent epiphyte coverage implies seasonal community composition changes. The image analysis will improve from using multi-season epiphyte spectral libraries to identify the major epiphyte groups and explore environmental influences based on various components of epiphyte groups;

(8) The prediction model qualified the negative impact of water temperature and intrinsic seagrass leaf turnover, and a positive impact of nutrient level from sediment porewater on the epiphyte-seagrass relationship. However, this model did not predict the epiphyte

accumulation accurately due to lacking environmental information. Key missing data include grazing effects and water column nutrient levels.

REFERENCES

Abal EG, Loneragan N, Bowen P, Perry CJ, Udy JW, Dennison WC (1994) Physiological and morphological responses of the seagrass *Zostera capricorni* Aschers, to light intensity. Journal of Experimental Marine Biology and Ecology 178:113–129.

Albis-Salas MR, Gavio B (2011) Notes on marine algae in the International Biosphere Reserve Seaflower, Caribbean Colombian I: new records of macroalgal epiphytes on the seagrass *Thalassia testudinum*. Botanica Marina 54:537–543.

Alcoverro T, Duarte CM, Romero J (1997a) The influence of herbivores on *Posidonia oceanica* epiphytes. Aquatic Botany 56:93–104.

Alcoverro T, Romero J, Duarte C, López N (1997b) Spatial and temporal variations in nutrient limitation of seagrass *Posidonia oceanica* growth in the NW Mediterranean. Marine Ecology Progress Series 146:155–161.

Aloi JE (1990) A critical review of recent freshwater periphyton field methods. Canadian Journal of Fisheries and Aquatic Sciences 47:656–670.

Armitage AR, Frankovich TA, Heck KL, Fourqurean JW (2005) Experimental nutrient enrichment causes complex changes in seagrass, microalgae, and macroalgae community structure in Florida Bay. Estuaries 28:422–434.

Aumack CF, Amsler CD, McClintock JB, Baker BJ (2011) Impacts of mesograzers on epiphyte and endophyte growth associated with chemically defended macroalge from the Western Antarctic Peninsula: A mesocosm experiment. Journal of Phycology 47:36–41.

Bader M, Dunné HJF van, Stuiver HJ (2000) Epiphyte distribution in a secondary cloud forest vegetation; a case study of the application of GIS in epiphyte ecology. Ecotropica 6:181–195.

Baggett LP, Jr KLH, Frankovich TA, Armitage AR, Fourqurean JW (2010) Nutrient enrichment, grazer identity, and their effects on epiphytic algal assemblages: field experiments in subtropical turtlegrass *Thalassia testudinum* meadows. Marine Ecology Progress Series 406:33–45.

Bankar S, Dube A, Kadam P, Deokule S (2014) Plant Disease Detection Techniques Using Canny Edge Detection & Color Histogram in Image Processing. 5:4.

Barnes RD (1987) Invertebrate Zoology. W.B. Saunders Company, Eastbourne, East Sussex, UK, p 142

Baumstark R, Dixon B, Carlson P, Palandro D, Kolasa K (2013) Alternative spatially enhanced integrative techniques for mapping seagrass in Florida's marine ecosystem. International Journal of Remote Sensing 34:1248–1264.

Bell SS, Fonseca MS, Kenworthy WJ (2008) Dynamics of a subtropical seagrass landscape: links between disturbance and mobile seed banks. Landscape Ecology 23:67–74.

Bell SS, Middlebrooks ML, Hall MO (2014) The value of long-term assessment of restoration: support from a seagrass investigation. Restoration Ecology 22:304–310.

Biber PD, Harwell MA, Cropper WP (2004) Modeling the dynamics of three functional groups of macroalgae in tropical seagrass habitats. Ecological Modelling 175:25–54.

Boese BL, Clinton PJ, Dennis D, Golden RC, Kim B (2008) Digital image analysis of *Zostera marina* leaf injury. Aquatic Botany 88:87–90.

Booth D, Heck K Jr (2009) Effects of the American oyster *Crassostrea virginica* on growth rates of the seagrass *Halodule wrightii*. Marine Ecology Progress Series 389:117–126.

Borges VP, Bastos E, Batista MB, Bouzon Z, Lhullier C, Schmidt EC, Sissini MN, Horta PA (2014) The genus Melobesia (Corallinales, Rhodophyta) from the subtropical South Atlantic, with the addition of *M. rosanoffii* (Foslie) Lemoine. Phytotaxa 190:268–276.

Borowitzka MA, Lavery PS, van Keulen M (2006) Epiphytes of Seagrasses. In: *Seagrasses: Biology, Ecology and Conservation*. Larkum AWD, Orth RJ, Duarte CM (eds) Springer Netherlands, Dordrecht, p 441–461

Borum J (1985) Development of epiphytic communities on eelgrass (*Zostera marina*) along a nutrient gradient in a Danish estuary. Mar Biol 87:211–218.

Borum J (1987) Dynamics of epiphyton on eelgrass (*Zostera marina* L.) leaves: Relative roles of algal growth, herbivory, and substratum turnover. Limnology and Oceanography 32:986–992.

Bretz F, Hothorn T, Westfall P (2016) Multiple Comparisons Using R. Chapman and Hall/CRC., New York, p 70-108

Brodersen KE, Lichtenberg M, Paz L-C, Kühl M (2015) Epiphyte-cover on seagrass (*Zostera marina* L.) leaves impedes plant performance and radial O_2 loss from the below-ground tissue. Frontiers in Marine Science 2: 58.

Brush MJ, Nixon SW (2002) Direct measurements of light attenuation by epiphytes on eelgrass Zostera marina. Marine Ecology Progress Series 238:73–79.

Bulthuis DA, Woelkerling WmJ (1983) Biomass accumulation and shading effects of epiphytes on leaves of the seagrass, *Heterozostera tasmanica*, in Victoria, Australia. Aquatic Botany 16:137–148.

Burkholder JM, Tomasko DA, Touchette BW (2007) Seagrasses and eutrophication. Journal of Experimental Marine Biology and Ecology 350:46–72.

Buschmann AH, Gómez P (1993) Interaction mechanisms between *Gracilaria chilensis* (Rhodophyta) and epiphytes. Hydrobiologia 260:345–351.

Callaway RM, Reinhart KO, Moore GW, Moore DJ, Pennings SC (2002) Epiphyte host preferences and host traits: mechanisms for species-specific interactions. Oecologia 132:221–230.

Campbell SJ, McKenzie LJ, Kerville SP (2006) Photosynthetic responses of seven tropical seagrasses to elevated seawater temperature. Journal of Experimental Marine Biology and Ecology 330:455–468.

Campbell SJ, McKenzie LJ, Kerville SP, Bité JS (2007) Patterns in tropical seagrass photosynthesis in relation to light, depth and habitat. Estuarine, Coastal and Shelf Science 73:551–562.

Canny J (1986) A computational approach to edge detection. IEEE Transactions on Pattern Analysis and Machine Intelligence PAMI-8:679–698.

Canty MJ (2014) Image Analysis, Classification and Change Detection in Remote Sensing: with Algorithms for ENVI/IDL and Python, Third Edition. CRC Press.

Claydon J, Calosso M, Traiger S (2012) Progression of invasive lionfish in seagrass, mangrove and reef habitats. Marine Ecology Progress Series 448:119–129.

Clesceri, L. S, Greenberg, A. E, Eaton, A. D (1988) Standard Methods for the Examination of Water and Wastewater, 20th Edition. American Public Health Association., Washington DC. p 15-50

Codizar AL, Solano G (2016) Plant Leaf Recognition by Venation and Shape Using Artificial Neural Networks. In: *2016 7th International Conference on Information, Intelligence, Systems Applications (IISA)*. p 1–4

Collier CJ, Waycott M (2014) Temperature extremes reduce seagrass growth and induce mortality. Marine Pollution Bulletin 83:483–490.

Congdon VM, Dunton KH (2016) A Long-Term Seagrass Monitoring Program for Corpus Christi Bay and Upper Laguna Madre. Coastal Bend Bays & Estuaries Program, Corpus Christi, Texas. p 1-27

Contreras C, Whisenant A, Bronson J, Radloff P (2011) Final Report for Seagrass Response to Wastewater Inputs: Implementation of A Seagrass Monitoring Program in Two Texas estuaries. Water Resources Branch, Texas Parks and Wildlife Department, Austin, Texas, p 26-37

Corlett H, Jones B (2007) Epiphyte communities on *Thalassia testudinum* from Grand Cayman, British West Indies: Their composition, structure, and contribution to lagoonal sediments. Sedimentary Geology 194:245–262.

Cornelisen CD, Thomas FIM (2004) Ammonium and nitrate uptake by leaves of the seagrass *Thalassia testudinum*: impact of hydrodynamic regime and epiphyte cover on uptake rates. Journal of Marine Systems 49:177–194.

Costanza R, d'Arge R, Groot R de, Farber S, Grasso M, Hannon B, Limburg K, Naeem S, O'Neill RV, Paruelo J, Raskin RG, Sutton P, Belt M van den (1997) The value of the world's ecosystem services and natural capital. Nature 387:253.

Crump BC, Wojahn JM, Tomas F, Mueller RS (2018) Metatranscriptomics and Amplicon Sequencing Reveal Mutualisms in Seagrass Microbiomes. Frontiers in Microbiology 9: 388.

Dennison WC, Alberte RS (1982) Photosynthetic responses of *Zostera marina* L. (Eelgrass) to in situ manipulations of light intensity. Oecologia 55:137–144.

Dennison WC, Alberte RS (1985) Role of daily light period in the depth distribution of *Zostera marina* (eelgrass). Marine Ecology Progress Series 25: 51-61.

Diaz-Pulido G, Díaz-Ruíz M (2003) Diversity of benthic marine algae of the Colombian Atlantic. Biota Colombiana:4: 203-246.

Dirnberger J (1990) Benthic determinants of settlement for planktonic larvae: availability of settlement sites for the tube-building polychaete *Spirorbis spirillum* (Linnaeus) settling onto seagrass blades. Journal of Experimental Marine Biology and Ecology 140:89–105.

Doering PH, Chamberlain RH (2000) Experimental Studies in the Salinity Tolerance of Turtlegrass *Thalassia testudinum*. CRC Marine Science Series. In: *Seagrasses: monitoring, ecology, physiology, and management*, Bortone, SA (eds) CRC Press, Cleveland, Ohio, p 81-98

Drake LA, Dobbs FC, Zimmerman RC (2003) Effects of epiphyte load on optical properties and photosynthetic potential of the seagrasses *Thalassia testudinum* Banks ex König and Zostera marina L. Limnology and Oceanography 48:456–463.

Duarte C, Sand-Jensen K (1990) Seagrass colonization: biomass development and shoot demography in *Cymodocea nodosa* patches. Marine Ecology Progress Series 67:97–103.

Duarte CM (1995) Submerged aquatic vegetation in relation to different nutrient regimes. Ophelia 41:87–112.

Duarte CM (2002) The future of seagrass meadows. Environmental Conservation 29:192–206.

Duarte CM, Chiscano CL (1999) Seagrass biomass and production: a reassessment. Aquatic Botany 65:159–174.

Dunton K, Pulich W, Mutchler T (2010) A Seagrass Mntoring Program for Texas Coasta Waters. Coastal Bend Bays & Estuaries Program, Corpus Christi, Texas, p 2-39.

Dunton KH (1994) Seasonal growth and biomass of the subtropical seagrass *Halodule wrightii* in relation to continuous measurements of underwater irradiance. Marine Biology 120:479–489.

Edsbagge H (1968) Some problems in the relationship between diatoms and seaweeds. Botanica Marina 11:64–67.

Enríquez S, Borowitzka MA (2010) The Use of the Fluorescence Signal in Studies of Seagrasses and Macroalgae. In: *Chlorophyll a Fluorescence in Aquatic Sciences: Methods and Applications*. Developments in Applied Phycology, Suggett DJ, Prášil O, Borowitzka MA (eds) Springer Netherlands, Dordrecht, p 187–208

Fernández-Torquemada Y, Sánchez-Lizaso JL (2005) Effects of salinity on leaf growth and survival of the Mediterranean seagrass *Posidonia oceanica* (L.) Delile. Journal of Experimental Marine Biology and Ecology 320:57–63.

Fikes RL, Lehman RL (2008) Small-Scale Recruitment of Flora to a Newly Developed Tidal Inlet in the Northwest Gulf of Mexico. Gulf of Mexico Science 26: 5.

Fitzpatrick J, Kirkman H (1995) Effects of prolonged shading stress on growth and survival of seagrass *Posidonia australis* in Jervis Bay, New South Wales, Australia. Marine Ecology Progress Series 127:279–289.

Fong P, Harwell MA (1994) Modeling seagrass communities in tropical and subtropical bays and estuaries: A mathematical model synthesis of current hypotheses. Bulletin of Marine Science 54:757–781.

Fourqurean JW, Muth MF, Boyer JN (2010) Epiphyte loads on seagrasses and microphytobenthos abundance are not reliable indicators of nutrient availability in oligotrophic coastal ecosystems. Marine Pollution Bulletin 60:971–983.

Fourqurean JW, Willsie A, Rose CD, Rutten LM (2001) Spatial and temporal pattern in seagrass community composition and productivity in south Florida. Marine Biology 138:341–354.

Fourqurean JW, Zieman JC, Powell GVN (1992a) Phosphorus limitation of primary production in Florida Bay: Evidence from C:N:P ratios of the dominant seagrass *Thalassia testudinum*. Limnology and Oceanography 37:162–171.

Fourqurean JW, Zieman JC, Powell GVN (1992b) Relationships between porewater nutrients and seagrasses in a subtropical carbonate environment. Marine Biology 114:57–65.

Frankovich TA, Armitage AR, Wachnicka AH, Gaiser EE, Fourqurean JW (2009) Nutrient effects on seagrass epiphyte community structure in Florida Bay. Journal of Phycology 45:1010–1020.

Frankovich TA, Fourqurean JW (1997) Seagrass epiphyte loads along a nutrient availability gradient, Florida Bay, USA. Marine Ecology Progress Series 159:37–50.

Frankovich TA, Zieman JC (2005) A temporal investigation of grazer dynamics, nutrients, seagrass leaf productivity, and epiphyte standing stock. Estuaries 28:41–52.

Fredriksen S, Christie H, Sæthre BA (2005) Species richness in macroalgae and macrofauna assemblages on *Fucus serratus* L. (Phaeophyceae) and *Zostera marina* L. (Angiospermae) in Skagerrak, Norway. Marine Biology Research 1:2–19.

Fry B, Parker PL (1979) Animal diet in Texas seagrass meadows: δ13C evidence for the importance of benthic plants. Estuarine and Coastal Marine Science 8:499–509.

Gallegos M, Merino-Ibarra M, Marba N, Duarte C (1993) Biomass and dynamics of *Thalassia testudinum* in the Mexican Caribbean: elucidating rhizome growth. Marine Ecology Progress Series 95:185–192.

Giovannetti E, Montefalcone M, Morri C, Bianchi CN, Albertelli G (2010) Early warning response of *Posidonia oceanica* epiphyte community to environmental alterations (Ligurian Sea, NW Mediterranean). Marine Pollution Bulletin 60:1031–1039.

Golzarian MR, Frick RA, Rajendran K, Berger B, Roy S, Tester M, Lun DS (2011) Accurate inference of shoot biomass from high-throughput images of cereal plants. Plant Methods 7:2.

Gras AF, Koch MS, Madden CJ (2003) Phosphorus uptake kinetics of a dominant tropical seagrass *Thalassia testudinum*. Aquatic Botany 76:299–315.

Green EP, Short FT, Short FT (2003) World Atlas of Seagrasses. University of California Press, Berkeley, California, p 48-75.

Greening HS, Cross LM, Sherwood ET (2011) A multiscale approach to seagrass recovery in Tampa Bay, Florida. Ecological Rest 29:82–93.

Grice AM, Loneragan NR, Dennison WC (1996) Light intensity and the interactions between physiology, morphology and stable isotope ratios in five species of seagrass. Journal of Experimental Marine Biology and Ecology 195:91–110.

Hall MO, Bell SS (1993) Meiofauna on the seagrass *Thalassia testudinum*: population characteristics of harpacticoid copepods and associations with algal epiphytes. Marine Biology 116:137–146.

Hanelt D, Roleda MY (2009) UVB radiation may ameliorate photoinhibition in specific shallow-water tropical marine macrophytes. Aquatic Botany 91:6–12.

Harlin MM (1975) Epiphyte—host relations in seagrass communities. Aquatic Botany 1:125–131.

Harlin MM (1973) Transfer of products between epiphytic marine algae and host plants. Journal of Phycology 9:243–248.

Harrison PG (1982) Control of microbial growth and of amphipod grazing by water-soluble compounds from leaves of *Zostera marina*. Marine Biology 67:225–230.

Harrison PG, Durance CD (1985) Reductions in photosynthetic carbon uptake in epiphytic diatoms by water-soluble extracts of leaves of Zostera marina. Marine Biology (Berl.) 90:117–119.

Hasegawa N, Hori M, Mukai H (2007) Seasonal shifts in seagrass bed primary producers in a cold-temperate estuary: Dynamics of eelgrass Zostera marina and associated epiphytic algae. Aquatic Botany 86:337–345.

Hays CG (2005) Effect of nutrient availability, grazer assemblage and seagrass source population on the interaction between *Thalassia testudinum* (turtle grass) and its algal epiphytes. Journal of Experimental Marine Biology and Ecology 314:53–68.

Heck KL, Fodrie FJ, Madsen S, Baillie CJ, Byron DA (2015) Seagrass consumption by native and a tropically associated fish species: potential impacts of the tropicalization of the northern Gulf of Mexico. Marine Ecology Progress Series 520:165–173.

Heck KL, Nadeau DA, Thomas R (1997) The nursery role of seagrass beds. Gulf of Mexico Science 15:8.

Heck KL, Valentine JF (2006a) Plant–herbivore interactions in seagrass meadows. Journal of Experimental Marine Biology and Ecology 330:420–436.

Heck KL, Valentine JF (2007) The primacy of top-down effects in shallow benthic ecosystems. Estuaries and Coasts 30:371–381.

Heijs FML (1984) Annual biomass and production of epiphytes in three monospecific seagrass communities of *Thalassia hemprichii* (Ehrenb.) Aschers. Aquatic Botany 20:195–218.

Heijs FML (1985) The seasonal distribution and community structure of the epiphytic algae on *Thalassia hemprichii* (Ehrenb.) Aschers. from Papua New Guinea. Aquatic Botany 21:295–324.

Hemminga MA (1998) The root/rhizome system of seagrasses: an asset and a burden. Journal of Sea Research 39:183–196.

Hemminga MA, Duarte CM (2000) Seagrass Ecology. Cambridge University Press, Cambridge, England, p 146-248.

Herzka S, Dunton K (1997) Seasonal photosynthetic patterns of the seagrass *Thalassia testudinum* in the western Gulf of Mexico. Marine Ecology Progress Series 152:103–117.

Hickman M (1971) The standing crop and primary productivity of the epiphyton attached to Equisetum fluviatile L. in Priddy Pool, North Somerset. British Phycological Journal 6:51–59.

Hobson C, Whisenant A (2018) Seagrass monitoring in San Antonio Bay, Texas with implications for management. Texas Journal of Science 70:1.

Holz I, Gradstein RS (2005) Cryptogamic epiphytes in primary and recovering upper montane oak forests of Costa Rica – species richness, community composition and ecology. Plant Ecology 178:89–109.

Hughes AR, Stachowicz JJ (2004) Genetic diversity enhances the resistance of a seagrass ecosystem to disturbance. PNAS 101:8998–9002.

Humm HJ (1964) Epiphytes of the Sea Grass, *Thalassia Testudinum*, in Florida. Bulletin of Marine Science 14:306–341.

Iizumi H, Hattori A (1982) Growth and organic production of eelgrass (Zostera marina L.) in temperate waters of the Pacific coast of Japan. III. The kinetics of nitrogen uptake. Aquatic Botany 12:245–256.

de Iongh HH, Wenno BJ, Meelis E (1995) Seagrass distribution and seasonal biomass changes in relation to dugong grazing in the Moluccas, East Indonesia. Aquatic Botany 50:1–19.

Irlandi E, Orlando B, Biber P (2004) Drift algae-epiphyte-seagrass interactions in a subtropical Thalassia testudinum meadow. Marine Ecology Progress Series 279:81–91.

Jacobs RPWM, Hermelink PM, Van Geel G (1983) Epiphytic algae on eelgrass at Roscoff, France. Aquatic Botany 15:157–173.

Jaschinski S, Sommer U (2008) Functional diversity of mesograzers in an eelgrass–epiphyte system. Mar Biol 154:475–482.

Jernakoff P, Brearley A, Nielsen J (1996) Factors affecting grazer-epiphyte interactions in temperate seagrass meadows. Oceanography and Marine Biology: An Annual Review 34: 109-162.

Johnson JB, Omland KS (2004) Model selection in ecology and evolution. Trends in Ecology & Evolution 19:101–108.

Johnson MW, Heck KL, Fourqurean JW (2006) Nutrient content of seagrasses and epiphytes in the northern Gulf of Mexico: Evidence of phosphorus and nitrogen limitation. Aquatic Botany 85:103–111.

Kaldy J (2011) Using a macroalgal δ15N bioassay to detect cruise ship wastewater effluent inputs. Marine Pollution Bulletin 62:1762–1771.

Katwijk MM van, Thorhaug A, Marbà N, Orth RJ, Duarte CM, Kendrick GA, Althuizen IHJ, Balestri E, Bernard G, Cambridge ML, Cunha A, Durance C, Giesen W, Han Q,

Hosokawa S, Kiswara W, Komatsu T, Lardicci C, Lee K-S, Meinesz A, Nakaoka M, O'Brien KR, Paling EI, Pickerell C, Ransijn AMA, Verduin JJ (2016) Global analysis of seagrass restoration: the importance of large-scale planting. Journal of Applied Ecology 53:567–578.

Kendrick G, Duarte C, Marbà N (2005) Clonality in seagrasses, emergent properties and seagrass landscapes. Marine Ecology Progress Series 290:291–296.

Kendrick GA, Burt JS (1997) Seasonal changes in epiphytic macro-algae assemblages between offshore exposed and inshore protected *Posidonia sinuosa* Cambridge et Kuo seagrass meadows, Western Australia. Botanica Marina 40:77–86.

Kendrick GA, Walker DI, McComb AJ (1988) Changes in distribution of macro-algal epiphytes on stems of the seagrass *Amphibolis antarctica* along a salinity gradient in Shark Bay, Western Australia. Phycologia 27:201–208.

Kitting CL, Fry B, Morgan MD (1984) Detection of inconspicuous epiphytic algae supporting food webs in seagrass meadows. Oecologia 62:145–149.

Koch M, Bowes G, Ross C, Zhang X-H (2013) Climate change and ocean acidification effects on seagrasses and marine macroalgae. Global Change Biology 19:103–132.

Koch MS, Erskine JM (2001) Sulfide as a phytotoxin to the tropical seagrass *Thalassia testudinum*: interactions with light, salinity and temperature. Journal of Experimental Marine Biology and Ecology 266:81–95.

Koch MS, Schopmeyer S, Kyhn-Hansen C, Madden CJ (2007) Synergistic effects of high temperature and sulfide on tropical seagrass. Journal of Experimental Marine Biology and Ecology 341:91–101.

Kohler KE, Gill SM (2006) Coral Point Count with Excel extensions (CPCe): A visual basic program for the determination of coral and substrate coverage using random point count methodology. Computers & Geosciences 32:1259–1269.

Kornicker LS (no date) A seasonal study of living *Ostracoda* in a Texas bay (Redfish Bay) adjoining the Gulf of Mexico. Pubblicazione della Stazione Zoologica di Napoli 33: 45-60.

Kowalski JL, DeYoe HR, Krull CP, Allison TC (2009) Comparison of leaf-clipping and leaf-piercing techniques as applied to the seagrass *Syringodium filiforme*. Bulletin of Marine Science 14: 159-172.

Kruse FA, Lefkoff AB, Boardman JW, Heidebrecht KB, Shapiro AT, Barloon PJ, Goetz AFH (1993) The spectral image processing system (SIPS)—interactive visualization and analysis of imaging spectrometer data. Remote Sensing of Environment 44:145–163.

Landsberg JH, Flewelling LJ, Naar J (2009) Karenia brevis red tides, brevetoxins in the food web, and impacts on natural resources: Decadal advancements. Harmful Algae 8:598–607.

Larkin PD, Maloney TJ, Rubiano-Rincon S, Barrett MM (2017) A map-based approach to assessing genetic diversity, structure, and connectivity in the seagrass *Halodule wrightii*. Marine Ecology Progress Series 567:95–107.

Lavery P, Vanderklift M (2002) A comparison of spatial and temporal patterns in epiphytic macroalgal assemblages of the seagrasses *Amphibolis griffithii* and *Posidonia coriacea*. Marine Ecology Progress Series 236:99–112.

Lee K-S, Dunton KH (1997) Effect of in situ light reduction on the maintenance, growth and partitioning of carbon resources in *Thalassia testudinum* banks ex König. Journal of Experimental Marine Biology and Ecology 210:53–73.

Lee K-S, Dunton KH (2000) Effects of nitrogen enrichment on biomass allocation, growth, and leaf morphology of the seagrass *Thalassia testudinum*. Marine Ecology Progress Series 196:39–48.

Lee K-S, Dunton KH (1999) Inorganic nitrogen acquisition in the seagrass *Thalassia testudinum*: Development of a whole-plant nitrogen budget. Limnology and Oceanography 44:1204–1215.

Lee K-S, Dunton KH (1996) Production and carbon reserve dynamics of the seagrass *Thalassia testudinum* in Corpus Christi Bay, Texas, USA. Marine Ecology Progress Series 143:201–210.

Lee K-S, Park SR, Kim YK (2007) Effects of irradiance, temperature, and nutrients on growth dynamics of seagrasses: A review. Journal of Experimental Marine Biology and Ecology 350:144–175.

Leppink J (2018) Analysis of Covariance (ANCOVA) vs. Moderated Regression (MODREG): Why the interaction matters. Health Professions Education 4:225–232.

Leuven RSEW, Brock TCM, van Druten HAM (1985) Effects of preservation on dry- and ash-free dry weight biomass of some common aquatic macro-invertebrates. Hydrobiologia 127:151–159.

Lewis JB, Hollingworth CE (1982) Leaf epifauna of the seagrass *Thalassia testudinum*. Marine Biology 71:41–49.

Libes M (1986) Productivity-irradiance relationship of *Posidonia oceanica* and its epiphytes. Aquatic Botany 26:285–306.

Lotze HK, Lenihan HS, Bourque BJ, Bradbury RH, Cooke RG, Kay MC, Kidwell SM, Kirby MX, Peterson CH, Jackson JBC (2006) Depletion, degradation, and recovery potential of estuaries and coastal seas. Science 312:1806–1809.

Marbà N, Gallegos ME, Merino M, Duarte CM (1994) Vertical growth of *Thalassia testudinum*: seasonal and interannual variability. Aquatic Botany 47:1–11.

Martin S, Rodolfo-Metalpa R, Ransome E, Rowley S, Buia M-C, Gattuso J-P, Hall-Spencer J (2008) Effects of naturally acidified seawater on seagrass calcareous epibionts. Biology Letters 4:689–692.

Mascart T, Lepoint G, Deschoemaeker S, Binard M, Remy F, De Troch M (2015) Seasonal variability of meiofauna, especially harpacticoid copepods, in *Posidonia oceanica* macrophytodetritus accumulations. Journal of Sea Research 95:149–160.

Mateu-Vicens G, Box A, Deudero S, Rodríguez B (2010) Comparative analysis of epiphytic foraminifera in sediments colonized by seagrass *Posidonia oceanica* and invasive macroalgae Caulerpa spp. Journal of Foraminiferal Research 40:134–147.

McCune B (1993) Gradients in epiphyte biomass in three Pseudotsuga-Tsuga Forests of different ages in Western Oregon and Washington. The Bryologist 96:405–411.

McGlathery KJ (2001) Macroalgal blooms contribute to the decline of seagrass in nutrient-enriched coastal waters. Journal of Phycology 37:453–456.

McKenna S, Rasheed M, Sankey T (2007) Long term seagrass monitoring in the Port of Mourilyan: November 2006. Department of Primary Industries and Fisheries (DPI&F), Cairns, QLD, Australia, p 1-3

Michael TS, Shin HW, Hanna R, Spafford DC (2008) A review of epiphyte community development: Surface interactions and settlement on seagrass. Journal of Environmental Biology 29:629–638.

Moncreiff C, Sullivan M, Daehnick A (1992) Primary production dynamics in seagrass beds of Mississippi Sound: the contributions of seagrass epiphytic algae, sand microflora, and phytoplankton. Marine Ecology Progress Series 87:161–171.

Monier J-M, Lindow SE (2004) Frequency, size, and localization of bacterial aggregates on bean leaf surfaces. Appl Environ Microbiol 70:346–355.

Moore KA, Wetzel RL (2000) Seasonal variations in eelgrass (*Zostera marina* L.) responses to nutrient enrichment and reduced light availability in experimental ecosystems. Journal of Experimental Marine Biology and Ecology 244:1–28.

Nagelkerken I, Connell SD (2015) Global alteration of ocean ecosystem functioning due to increasing human CO_2 emissions. PNAS 112:13272–13277.

Neckles HA, Kopp BS, Peterson BJ, Pooler PS (2012) Integrating scales of seagrass monitoring to meet conservation needs. Estuaries and Coasts 35:23–46.

Neckles HA, Wetzel RL, Orth RJ (1993) Relative effects of nutrient enrichment and grazing on epiphyte-macrophyte (*Zostera marina* L.) dynamics. Oecologia 93:285–295.

Nelsen JE, Ginsburg RN (1986) Calcium carbonate production by epibionts on *Thalassia* in Florida Bay. Journal of Sedimentary Research 56:622–628.

Nelson TA, Waaland JR (1997) Seasonality of eelgrass, epiphyte, and grazer biomass and productivity in subtidal eelgrass meadows subjected to moderate tidal amplitude. Aquatic Botany 56:51–74.

Nelson WG (2017a) Development of an epiphyte indicator of nutrient enrichment: Threshold values for seagrass epiphyte load. Ecological Indicators 74:343–356.

Nelson WG (2017b) Patterns of shading tolerance determined from experimental light reduction studies of seagrasses. Aquatic botany 141:39–46.

Nielsen J, Lethbridge R (1989) Feeding and the epiphyte food resources of gastropods living on leaves of the Seagrass *Amphibolis griffithii* in south-western Australia. Journal of the Malacological Society of Australia 10:47–58.

Nieuwenhuize J, Erftemeijer PLA, Maas YEM, Verwaal M, Nienhuis PH (1994) Pretreatment artefacts associated with the removal of calcareous epiphytes from seagrass leaves. Aquatic Botany 48:355–361.

Novak R (1982) Spatial and seasonal distribution of the meiofauna in the seagrass *Posidonia oceanica*. Netherlands Journal of Sea Research 16:380–388.

Olesen B, Enríquez S, Duarte C, Sand-Jensen K (2002) Depth-acclimation of photosynthesis, morphology and demography of *Posidonia oceanica* and *Cymodocea nodosa* in the Spanish Mediterranean Sea. Marine Ecology Progress Series 236:89–97.

Orth RJ, Carruthers TJB, Dennison WC, Duarte CM, Fourqurean JW, Heck KL, Hughes AR, Kendrick GA, Kenworthy WJ, Olyarnik S, Short FT, Waycott M, Williams SL (2006a) A global crisis for seagrass ecosystems. BioScience 56:987–996.

Orth RJ, Luckenbach ML, Marion SR, Moore KA, Wilcox DJ (2006b) Seagrass recovery in the Delmarva Coastal Bays, USA. Aquatic Botany 84:26–36.

Orth RJ, Van Montfrans J (1984) Epiphyte-seagrass relationships with an emphasis on the role of micrograzing: A review. Aquatic Botany 18:43–69.

Ow YX, Ng KJ, Lai S, Yaakub SM, Todd P (2020) Contribution of epiphyte load to light attenuation on seagrass leaves is small but critical in turbid waters. Mar Freshwater Res 71:929–934.

Pasqualini V, Pergent-Martini C, Pergent G, Agreil M, Skoufas G, Sourbes L, Tsirika A (2005) Use of SPOT 5 for mapping seagrasses: An application to *Posidonia oceanica*. Remote Sensing of Environment 94:39–45.

Penhale PA (1977) Macrophyte-epiphyte biomass and productivity in an eelgrass (*Zostera marina* L.) community. Journal of Experimental Marine Biology and Ecology 26:211–224.

Penhale PA, Thayer GW (1980) Uptake and transfer of carbon and phosphorus by eelgrass (*Zostera marina* L.) and its epiphytes. Journal of Experimental Marine Biology and Ecology 42:113–123.

Pérez-Lloréns JL, Niell FX (1993) Seasonal dynamics of biomass and nutrient content in the intertidal seagrass *Zostera noltii* Hornem. from Palmones River estuary, Spain. Aquatic Botany 46:49–66.

Perry CT, Beavington-Penney SJ (2005) Epiphytic calcium carbonate production and facies development within sub-tropical seagrass beds, Inhaca Island, Mozambique. Sedimentary Geology 174:161–176.

Peterson BJ, Frankovich TA, Zieman JC (2007) Response of seagrass epiphyte loading to field manipulations of fertilization, gastropod grazing and leaf turnover rates. Journal of Experimental Marine Biology and Ecology 349:61–72.

Pinckney JL, Micheli F (1998) Microalgae on seagrass mimics: Does epiphyte community structure differ from live seagrasses? Journal of Experimental Marine Biology and Ecology 221:59–70.

Porra RJ, Thompson WA, Kriedemann PE (1989) Determination of accurate extinction coefficients and simultaneous equations for assaying chlorophylls a and b extracted with four different solvents: verification of the concentration of chlorophyll standards by atomic absorption spectroscopy. Biochimica et Biophysica Acta (BBA) - Bioenergetics 975:384–394.

Posey MH (1988) Community Changes associated with the spread of an introduced seagrass, *Zostera Japonica*. Ecology 69:974–983.

Ralph PJ (1999) Light-induced photoinhibitory stress reponses of laboratory-cultured *Halophila ovalis*. Botanica Marina 42:11–22.

Ralph PJ, Burchett MD (1995) Photosynthetic responses of the seagrass *Halophila ovalis* (R. Br.) Hook. f. to high irradiance stress, using chlorophyll a fluorescence. Aquatic Botany 51:55–66.

Ralph PJ, Durako MJ, Enríquez S, Collier CJ, Doblin MA (2007) Impact of light limitation on seagrasses. Journal of Experimental Marine Biology and Ecology 350:176–193.

Ralph PJ, Macinnis-Ng CMO, Frankart C (2005) Fluorescence imaging application: effect of leaf age on seagrass photokinetics. Aquatic Botany 81:69–84.

Ray BR, Johnson MW, Cammarata K, Smee DL (2014) Changes in seagrass species composition in northwestern gulf of Mexico estuaries: effects on associated seagrass fauna. PLOS ONE 9: e107751.

Reyes J, Sansón M (2001) Biomass and production of the epiphytes on the leaves of *Cymodocea nodosa* in the Canary Islands. Botanica Marina 44:307–313.

Reyes J, Sansón M (1997) Temporal distribution and reproductive phenology of the epiphytes on *Cymodocea nodosa* leaves in the Canary Islands. Botanica Marina 40:193–202.

Richardson SL (2004) Seasonal Variation in Epiphytic Foraminiferal Biotas from *Thalassia* Seagrass Habitats, Twin Cays, Belize. Smithsonian Institution, National Museum of Natural History, Washington D. C, p 2-38.

Ruesink JL (2016) Epiphyte load and seagrass performance are decoupled in an estuary with low eutrophication risk. Journal of Experimental Marine Biology and Ecology 481:1–8.

Ruiz JM, Romero J (2001) Effects of in situ experimental shading on the Mediterranean seagrass *Posidonia oceanica.* Marine Ecology Progress Series 215:107–120.

Saha M, Berdalet E, Carotenuto Y, Fink P, Harder T, John U, Not F, Pohnert G, Potin P, Selander E, Vyverman W, Wichard T, Zupo V, Steinke M (2019) Using chemical language to shape future marine health. Frontiers in Ecology and the Environment 17:530–537.

Salman A, Semwal A, Bhatt U, Thakkar VM (2017) Leaf Classification and Identification Using Canny Edge Detector and SVM classifier. In: *2017 International Conference on Inventive Systems and Control (ICISC)*. p 1–4

Sand-Jensen K (1975) Biomass, net production and growth dynamics in an eelgrass (*Zostera marina* L.) population in Vellerup Vig, Denmark. Ophelia 14:185–201.

Sand-Jensen K (1977) Effect of epiphytes on eelgrass photosynthesis. Aquatic Botany 3:55–63.

Schanz A, Polte P, Asmus H (2002) Cascading effects of hydrodynamics on an epiphyte–grazer system in intertidal seagrass beds of the Wadden Sea. Marine Biology 141:287–297.

Shafer DJ, Kaldy JE, Sherman TD, Marko KM (2011) Effects of salinity on photosynthesis and respiration of the seagrass Zostera japonica: A comparison of two established populations in North America. Aquatic Botany 95:214–220.

Shamir L, Delaney JD, Orlov N, Eckley DM, Goldberg IG (2010) Pattern recognition software and techniques for biological image analysis. PLOS Computational Biology 6: e1000974.

Sherwood ET, Greening HS, Johansson JOR, Kaufman K, Raulerson GE (2017) Tampa Bay (Florida, USA): Documenting seagrass recovery since the 1980's and reviewing the benefits. Southeastern Geographer 57:294–319.

Snoeijs P (1994) Distribution of epiphytic diatom species composition, diversity and biomass on different macroalgal hosts along seasonal and salinity gradients in the Baltic Sea. Diatom Research 9:189–211.

Stapel J, Aarts TL, van Duynhoven BHM, de Groot JD, van den Hoogen PHW, Hemminga MA (1996) Nutrient uptake by leaves and roots of the seagrass *Thalassia hemprichii* in the Spermonde Archipelago, Indonesia. Marine Ecology Progress Series 134:195–206.

Stapel J, Manuntun R, Hemminga M (1997) Biomass loss and nutrient redistribution in an Indonesian *Thalassia hemprichii* seagrass bed following seasonal low tide exposure during daylight. Marine Ecology Progress Series 148:251–262.

Su L, Huang Y (2019) Seagrass resource asessment using worldview-2 imagery in the Redfish Bay, Texas. Journal of Marine Science and Engineering 7:98.

Suchanek TH, Williams SL, Ogden JC, Hubbard DK, Gill IP (1985) Utilization of shallow-water seagrass detritus by Carribbean deep-sea macrofauna: δ13C evidence. Deep Sea Research Part A Oceanographic Research Papers 32:201–214.

Texas Sunset Advisory Commision (1997) Status, trends, and changes in freshwater inflows to bay systems in the Corpus Christi Bay National Estuary Program study area. Texas Natural Resource Conservation Commission, Austin, Texas. (Report No. CCBNEP–17)

Thom R, Miller B, Kennedy M (1995) Temporal patterns of grazers and vegetation in a temperate seagrass system. Aquatic Botany 50:201–205.

Thorhaug A, Richardson AD, Berlyn GP (2006) Spectral reflectance of *Thalassia testudinum* (Hydrocharitaceae) seagrass: low salinity effects. American Journal of Botany 93:110–117.

Thorhaug A, Richardson AD, Berlyn GP (2007) Spectral reflectance of the seagrasses: *Thalassia testudinum*, *Halodule wrightii*, *Syringodium filiforme* and five marine algae. International Journal of Remote Sensing 28:1487–1501.

Tomas F, Turon X, Romero J (2005) Seasonal and small-scale spatial variability of herbivory pressure on the temperate seagrass *Posidonia oceanica*. Marine Ecology Progress Series 301:95–107.

Tomasko DA, Dawes CJ (1989) Evidence for physiological integration between shaded and unshaded short shoots of *Thalassia testudinum*. Marine Ecology Progress Series 54:299–305.

Tomasko DA, Lapointe BE (1991) Productivity and biomass of *Thalassia testudinum* as related to water column nutrient availability and epiphyte levels: field observations and experimental studies. Marine Ecology Progress Series 75:9–17.

Toporowska M, Pawlik-Skowrońska B, Wojtal A (2008) Epiphytic algae on *Stratiotes aloides* L., Potamogeton lucens L., Ceratophyllum demersum L. and Chara spp. in a macrophyte-dominated lake. Oceanological and Hydrobiological Studies 37:51–63.

Walker DI, Woelkerling WmJ (1988) Quantitative study of sediment contribution by epiphytic coralline red algae in seagrass meadows in Shark Bay, Western Australia. Marine Ecology Progress Series 43:71–77.

Waycott M, Duarte CM, Carruthers TJB, Orth RJ, Dennison WC, Olyarnik S, Calladine A, Fourqurean JW, Heck KL, Hughes AR, Kendrick GA, Kenworthy WJ, Short FT, Williams SL (2009) Accelerating loss of seagrasses across the globe threatens coastal ecosystems. PNAS 106:12377–12381.

Whalen MA, Duffy JE, Grace JB (2013) Temporal shifts in top-down vs. bottom-up control of epiphytic algae in a seagrass ecosystem. Ecology 94:510–520.

Willcocks PA (1982) Colonization and distribution of the red algal epiphytes *Melobesia mediocris* and *Smithora naiadum* on the seagrass *Phyllospadix torreyi.* Aquatic Botany 12:365–373.

Williams SL, Ruckelshaus MH (1993) Effects of nitrogen availability and herbivory on eelgrass (*Zostera Marina*) and epiphytes. Ecology 74:904–918.

Wolaver TG, Wetzel RL, Zieman JC, Webb KL (1980) Nutrient Interactions Between Salt marsh, Mudflats, and Estuarine Water. In: *Estuarine Perspectives*. Kennedy VS (ed) Academic Press, p 123–133

Worm B, Sommer U (2000) Rapid direct and indirect effects of a single nutrient pulse in a seaweed-epiphyte-grazer system. Marine Ecology Progress Series 202:283–288.

Wright A, Bohrer T, Hauxwell J, Valiela I (1995) Growth of epiphytes on *Zostera marina* in estuaries subject to different nutrient loading. The Biological Bulletin 189:261–261.

Yang X, Zhang P, Li W, Hu C, Zhang X, He P (2018) Evaluation of four seagrass species as early warning indicators for nitrogen overloading: Implications for eutrophic evaluation and ecosystem management. Science of The Total Environment 635:1132–1143.

Zieman JC (1975) Seasonal variation of turtle grass, *Thalassia testudinum* König, with reference to temperature and salinity effects. Aquatic Botany 1:107–123.

Zieman JC, Fourqurean JW, Frankovich TA (1999) Seagrass die-off in Florida Bay: Long-term trends in abundance and growth of turtle grass, *Thalassia testudinum*. Estuaries 22:460–470.

Zimba PV, Hopson MS (1997) Quantification of epiphyte removal efficiency from submersed aquatic plants. Aquatic Botany 58:173–179.